

The Monitoring of Linear Profiles and the Inertial Properties of Control Charts

Mahmoud A. Mahmoud

Dissertation submitted to the faculty of the
Virginia Polytechnic Institute and State University
in partial fulfillment of the requirements for the degree of

Doctor of Philosophy
in
Statistics

William H. Woodall, Chairman

Marion R. Reynolds, Jr.

G. Geoffrey Vining

Jeffrey B. Birch

Eric P. Smith

November 10, 2004

Blacksburg, Virginia

Key Words: Calibration; Functional data; Likelihood ratio; Multivariate charts;
Segmented regression; Statistical process control.

Copyright 2004, Mahmoud A. Mahmoud

The Monitoring of Linear Profiles and the Inertial Properties of Control Charts

Mahmoud A. Mahmoud

(ABSTRACT)

The Phase I analysis of data when the quality of a process or product is characterized by a linear function is studied in this dissertation. It is assumed that each sample collected over time in the historical data set consists of several bivariate observations for which a simple linear regression model is appropriate, a situation common in calibration applications. Using a simulation study, the researcher compares the performance of some of the recommended approaches used to assess the stability of the process. Also in this dissertation, a method based on using indicator variables in a multiple regression model is proposed.

This dissertation also proposes a change point approach based on the segmented regression technique for testing the constancy of the regression parameters in a linear profile data set. The performance of the proposed change point method is compared to that of the most effective Phase I linear profile control chart approaches using a simulation study. The advantage of the proposed change point method over the existing methods is greatly improved detection of sustained step changes in the process parameters.

Any control chart that combines sample information over time, e.g., the cumulative sum (CUSUM) chart and the exponentially weighted moving average (EWMA) chart, has an ability to detect process changes that varies over time depending on the past data observed. The chart statistics can take values such that some shifts in the parameters of the underlying probability distribution of the quality characteristic are more difficult to detect. This is referred to as the “inertia problem” in the literature. This

dissertation shows under realistic assumptions that the worst-case run length performance of control charts becomes as informative as the steady-state performance. Also this study proposes a simple new measure of the inertial properties of control charts, namely *the signal resistance*. The conclusions of this study support the recommendation that Shewhart limits should be used with EWMA charts, especially when the smoothing parameter is small. This study also shows that some charts proposed by Pignatiello and Runger (1990) and Domangue and Patch (1991) have serious disadvantages with respect to inertial properties.

Dedication

*To my parents,
and
to my wife, Rehab*

Acknowledgments

This dissertation is the result of a great deal of struggle, persistence, and dedication. It would not have been possible without the financial, intellectual, and emotional support from others. I would like to thank all of those who taught me, inspired me, and supported me during my Ph.D. program at Virginia Tech.

My first debt of gratitude must go to my advisor and chair professor William H. Woodall for his constant guidance and encouragement throughout the course of this work. I have benefited enormously from his moral support, insightful suggestions, and deepest experience in the field of statistical process control. My debt to him is enormous.

The members of my dissertation committee, Marion R. Reynolds, Jr., G. Geoffrey Veining, Jeffery B. Birch, and Eric P. Smith, were truly remarkable. Their opinions based upon a wealth of knowledge and experience have contributed substantively in the evolution of this work. I have greatly benefited from them both in the classroom and during the preparation of this dissertation. I would especially like to extend my deepest appreciation to my initial advisor, Professor Marion R. Reynolds, Jr., for his great help during the first years of my Ph.D. program at Virginia Tech.

I also would like to extend my deepest appreciation to Professor Douglas M. Hawkins of the School of Statistics at the University of Minnesota, for his insightful suggestions for the change point approach presented in Chapter 4.

It has been a great pleasure working with the faculty, staff, and students in the Department of Statistics at Virginia Tech during my Ph.D. program of study. I gratefully acknowledge all of them for their great support and encouragement. Special thanks to my colleagues James D. Williams and Peter A. Parker for their invaluable help and discussions.

During this work, I was financially supported from the Faculty of Economics and Political Sciences; Cairo University. Without this generous support this work would not have been done.

Finally, I would like to give special thanks to my parents. Their support and prayers at all times were particularly important to me and provided a constant source of inspiration. I would also like to dedicate this dissertation to my greatest blessing, my wife Rehab Mostafa. I am greatly indebted to her generous love, enthusiasm, and support at all times.

Table of Contents

	page #
List of Figures	x
List of Tables	xiii
Chapter 1	
Introduction	1
1.A	The Monitoring of Linear Profiles 1
1.B	A Change Point Approach for Linear Profile Data Sets 3
1.C	The Inertial Properties of Quality Control Charts 7
Chapter 2	
Linear Profile Models and Approaches	10
2.A	Phase I Monitoring of Linear Profiles 10
2.A.1	T^2 Control Chart Approaches 12
2.A.2	Kim et al.'s (2003) Shewhart-Type Control Charts Approach 15
2.A.3	Principal Component Approaches 19
2.A.4	An Alternative Approach 20
2.B	Phase II Monitoring of Linear Profiles 22
2.B.1	Kang and Albin's (2000) Phase II Approaches 22
2.B.2	Kim et al.'s (2003) Phase II Approach 25
2.C	Model Assumptions 27
Chapter 3	
Performance Comparisons for Some Phase I Approaches	28
3.A	Performance Comparisons 28
3.A.1	Estimation of False Alarm Probabilities 29
3.A.2	Estimation of Out-of-Control Probabilities of a Signal 34
3.A.3	Violations of the Normality Assumption 56
3.B	Calibration Example 58
3.C	Summary 66

Chapter 4	A Change Point Method Based on Linear Profile	
	Data	68
4.A	A Change Point Approach	69
4.A.1	Factoring the lrt_{m_1} Statistic into Different Sources of Variability	71
4.A.2	Expectation of the lrt_{m_1} Statistic	72
4.B	Performance Comparisons	75
4.C	Approximate Test Statistics	96
4.C.1	Approximate Thresholds	96
4.C.2	Approximate Normalizing Factor	99
4.C.3	Using Approximate Statistics to Estimate Probabilities of Type I Error	99
Appendix 4.A	Factoring the lrt_{m_1} Statistic into the Three Different Sources of Variability.	102
Appendix 4.B	Derivation of the Approximate Expected Value of the lrt_{m_1} Statistic	103
Chapter 5	Examples	105
5.A	Examples with Simulated Data Sets	106
5.B	A Calibration Application at NASA	110
Chapter 6	The Inertial Properties of Quality Control Charts	115
6.A	Some Control Charting Methods for Monitoring the Process Mean	115
6.B	Limitations of Steady-State Analysis	117
6.C	Signal Resistance of Univariate Control Charts	119
6.D	Signal Resistance of Multivariate Control Charts	123
6.E	Performance Comparisons	130
6.E.1	Univariate Control Charts	130

6.E.2	Multivariate Control Charts	135
Appendix 6.A	Derivation of Signal Resistance for MEWMA Chart	140
Chapter 7	Summary, Conclusions, and Future Work	141
References		

List of Figures

Figure		page #
Figure 1.1	The framework of a linear profile data set	6
Figure 1.2	EWMA chart with downward undetected sustained shift	7
Figure 3.1	Probability of out-of-control signal under intercept shifts from A_0 to $A_0 + 1 s / \sqrt{n}$ ($m=20$ and $X=0(0.2)1.8$)	39
Figure 3.2	Probability of out-of-control signal under slope shifts from A_1 to $A_1 + b s / \sqrt{S_{xx}}$ ($m=20$ and $X=0(0.2)1.8$)	40
Figure 3.3	Probability of out-of-control signal under slope shifts from B_1 to $B_1 + d s / \sqrt{S_{xx}}$ ($m=20$ and $X=0(0.2)1.8$)	41
Figure 3.4	Probability of out-of-control signal under standard deviation shifts from s to gs ($m=20$ and $X=0(0.2)1.8$)	42
Figure 3.5	Probability of out-of-control signal under intercept shifts from A_0 to $A_0 + 1 s / \sqrt{n}$ ($m=60$ and $X=0(0.2)1.8$)	44
Figure 3.6	Probability of out-of-control signal under slope shifts from A_1 to $A_1 + b s / \sqrt{S_{xx}}$ ($m=60$ and $X=0(0.2)1.8$)	45
Figure 3.7	Probability of out-of-control signal under slope shifts from B_1 to $B_1 + d s / \sqrt{S_{xx}}$ ($m=60$ and $X=0(0.2)1.8$)	46
Figure 3.8	Probability of out-of-control signal under standard deviation shifts from s to gs ($m=60$ and $X=0(0.2)1.8$)	47
Figure 3.9	Probability of out-of-control signal under intercept shifts from A_0 to $A_0 + 1 s / \sqrt{n}$ ($m=20$ and $X=0(0.2)1.8$ are used twice)	48
Figure 3.10	Probability of out-of-control signal under slope shifts from A_1 to $A_1 + b s / \sqrt{S_{xx}}$ ($m=20$ and $X=0(0.2)1.8$ are used twice)	49
Figure 3.11	Probability of out-of-control signal under slope shifts from B_1 to $B_1 + d s / \sqrt{S_{xx}}$ ($m=20$ and $X=0(0.2)1.8$ are used twice)	50
Figure 3.12	Probability of out-of-control signal under standard deviation shifts from s to gs ($m=20$ and $X=0(0.2)1.8$ are used twice)	51
Figure 3.13	Probability of out-of-control signal under intercept shifts from A_0 to $A_0 + 1 s / \sqrt{n}$ ($m=20$ and $X=-30, -23, -12, -4, 0, 3, 10, 20, 25,$ and 35)	52
Figure 3.14	Probability of out-of-control signal under slope shifts from A_1 to $A_1 + b s / \sqrt{S_{xx}}$ ($m=20$ and $X=-30, -23, -12, -4, 0, 3, 10, 20, 25,$ and 35)	53
Figure 3.15	Probability of out-of-control signal under slope shifts from B_1 to $B_1 + d s / \sqrt{S_{xx}}$ ($m=20$ and $X=-30, -23, -12, -4, 0, 3, 10, 20, 25,$ and 35)	54
Figure 3.16	Probability of out-of-control signal under standard deviation shifts from s to gs ($m=20$ and $X=-30, -23, -12, -4, 0, 3, 10, 20, 25,$ and 35)	55

Figure 3.17	Calibration curves corresponding to the minimum, median, and maximum first principal component scores	61
Figure 3.18	Control chart for Method A	61
Figure 3.19	Control chart for Method B	62
Figure 3.20	Method C control chart for the error term variance	63
Figure 3.21	Method C control chart for the intercept	63
Figure 3.22	Method C control chart for the slope	63
Figure 3.23	Control chart using Mestek et al.'s (1994) T^2 approach	65
Figure 3.24	Control chart for the T^2 statistics in Equation (3.1)	66
Figure 4.1	Probability of out-of-control signal under intercept shifts from A_0 to $A_0 + 1 s / \sqrt{n}$ ($m=20$ and $X=0(0.2)1.8$)	78
Figure 4.2	Probability of out-of-control signal under slope shifts from A_1 to $A_1 + b s / \sqrt{S_{xx}}$ ($m=20$ and $X=0(0.2)1.8$)	79
Figure 4.3	Probability of out-of-control signal under slope shifts from B_1 to $B_1 + d s / \sqrt{S_{xx}}$ ($m=20$ and $X=0(0.2)1.8$)	80
Figure 4.4	Probability of out-of-control signal under standard deviation shifts from s to gs ($m=20$ and $X=0(0.2)1.8$)	81
Figure 4.5	Probability of out-of-control signal under intercept shifts from A_0 to $A_0 + 1 s / \sqrt{n}$ ($m=60$ and $X=0(0.2)1.8$)	82
Figure 4.6	Probability of out-of-control signal under slope shifts from A_1 to $A_1 + b s / \sqrt{S_{xx}}$ ($m=60$ and $X=0(0.2)1.8$)	83
Figure 4.7	Probability of out-of-control signal under slope shifts from B_1 to $B_1 + d s / \sqrt{S_{xx}}$ ($m=60$ and $X=0(0.2)1.8$)	84
Figure 4.8	Probability of out-of-control signal under standard deviation shifts from s to gs ($m=60$ and $X=0(0.2)1.8$)	85
Figure 4.9	Probability of out-of-control signal under intercept shifts from A_0 to $A_0 + 1 s / \sqrt{n}$ ($m=20$ and $X=0(0.2)1.8$ are used twice)	86
Figure 4.10	Probability of out-of-control signal under slope shifts from A_1 to $A_1 + b s / \sqrt{S_{xx}}$ ($m=20$ and $X=0(0.2)1.8$ are used twice)	87
Figure 4.11	Probability of out-of-control signal under slope shifts from B_1 to $B_1 + d s / \sqrt{S_{xx}}$ ($m=20$ and $X=0(0.2)1.8$ are used twice)	88
Figure 4.12	Probability of out-of-control signal under standard deviation shifts from s to gs ($m=20$ and $X=0(0.2)1.8$ are used twice)	89
Figure 4.13	Probability of out-of-control signal under intercept shifts from A_0 to $A_0 + 1 s / \sqrt{n}$ ($m=20$ and $X=-30, -23, -12, -4, 0, 3, 10, 20, 25,$ and 35)	90
Figure 4.14	Probability of out-of-control signal under slope shifts from A_1 to $A_1 + b s / \sqrt{S_{xx}}$ ($m=20$ and $X=-30, -23, -12, -4, 0, 3, 10, 20, 25,$ and 35)	91
Figure 4.15	Probability of out-of-control signal under slope shifts from B_1 to $B_1 + d s / \sqrt{S_{xx}}$ ($m=20$ and $X=-30, -23, -12, -4, 0, 3, 10, 20, 25,$ and 35)	92

Figure 4.16	Probability of out-of-control signal under standard deviation shifts from s to gs ($m=20$ and $X=-30, -23, -12, -4, 0, 3, 10, 20, 25,$ and 35)	93
Figure 4.17	Probability of out-of-control signal under randomly occurring unsustained intercept shifts from A_0 to $A_0 + I s / \sqrt{n}$	94
Figure 4.18	Probability of out-of-control signal under randomly occurring unsustained slope shifts from A_1 to $A_1 + b s / \sqrt{S_{xx}}$	94
Figure 4.19	Probability of out-of-control signal under randomly occurring unsustained slope shifts from B_1 to $B_1 + d s / \sqrt{S_{xx}}$	95
Figure 4.20	Probability of out-of-control signal under randomly occurring unsustained slope shifts from s to gs	95
Figure 5.1	Control chart for the variance (Example 1)	107
Figure 5.2	Control chart for the intercept (Example 1)	107
Figure 5.3	Control chart for the slope (Example 1)	108
Figure 5.4	Control chart for the variance (Example 2)	109
Figure 5.5	Control chart for the intercept (Example 2)	109
Figure 5.6	Control chart for the slope (Example 2)	110
Figure 5.7	Calibration curves corresponding to the minimum, median, and maximum first principal component scores	113
Figure 5.8	A chart for the intercept estimates for the NASA data set	113
Figure 6.1	The steady state distribution and the distributions of the EWMA statistic when there is undetected sustained shift with size d_1 for $I = .15$ and $L_2 = 3.0$	118
Figure 6.2	The signal resistance for the EWMA control chart with $I = .15$ and $L_2 = 2.801$	131
Figure 6.3	The signal resistance for the CUSUM control chart with $k = 0.5$ and $h_1 = 4.775$	131
Figure 6.4	The signal resistance for the EWMA control chart with $I = .05$ and $L_2 = 2.492$ used alone and used in conjunction with a 4.5-sigma Shewhart limit	132
Figure 6.5	The signal resistance for the AEWMA control chart with $\lambda = 0.1354, h_3 = 0.7931,$ and $k=3.2587$	133
Figure 6.6	The signal resistance for the omnibus EWMA control chart for $\alpha=0.5,$ with $I = .025$ and $L_4=1.815$	134
Figure 6.7	The worst-case signal resistance values for some univariate control charts corresponding to different in-control ARL values	135
Figure 6.8	The signal resistance for the MEWMA control chart with $I = .15, p=2,$ and $h_6 = 10.7$	136
Figure 6.9	The signal resistance for the MEWMA control chart with $I = .02, p=2,$ and $h_6 = 6.92$ used alone and used in conjunction with a χ^2 -chart with control limit $h_5 = 20.25$	138
Figure 6.10	The worst-case signal resistance values for some multivariate control charts corresponding to different in-control ARL values	138
Figure 6.11	The signal resistance values for some multivariate charts, calculated for the example with simulated data	139

List of Tables

Table		page #
Table 1.1	A comparison between Phase I and Phase II of the monitoring of profiles	3
Table 3.1	Overall false alarm probabilities: Nominal vs. Simulated ($m=5, n=10$)	30
Table 3.2	Overall false alarm probabilities: Nominal vs. Simulated ($m=20, n=10$)	31
Table 3.3	Overall false alarm probabilities: Nominal vs. Simulated ($m=40, n=10$)	31
Table 3.4	Overall false alarm probabilities: Nominal vs. Simulated ($m=60, n=10$)	32
Table 3.5	Overall false alarm probabilities: Nominal vs. Simulated ($m=20, n=20$)	32
Table 3.6	Overall false alarm probabilities: Nominal vs. Simulated ($m=20, n=30$)	33
Table 3.7	Overall false alarm probabilities: Nominal vs. Simulated ($m=20, X=-30, -23, -12, -4, 0, 3, 10, 20, 25, \text{ and } 35$)	33
Table 3.8	Overall false alarm Probabilities: Nominal vs. Simulated ($m=20, X=-600, -450, -380, -260, -100, 0, 90, 210, 400, \text{ and } 500$)	34
Table 3.9	False alarm probabilities, percentiles, and control limits used for the different cases considered in the performance comparisons	36
Table 3.10	Overall false alarm probabilities when the e_{ij} 's are i.i.d. double exponential random variables with mean 0 and variance 1	56
Table 3.11	Overall false alarm probabilities when the e_{ij} 's are i.i.d. double exponential random variables with mean 0 and variance 2	57
Table 3.12	Overall false alarm probabilities when the e_{ij} 's are i.i.d. exponential random variables with mean 1	57
Table 3.13	Overall false alarm probabilities when the e_{ij} 's are i.i.d. t -random variables with 3 degrees of freedom	57
Table 3.14	Overall false alarm probabilities when the e_{ij} 's are i.i.d. t -random variables with 5 degrees of freedom	58
Table 3.15	Example Data with the response measured according to each Fe^{3+} level (from Mestek et al. (1994))	59
Table 3.16	The linear regression results for the 22 samples	60
Table 4.1	The simulated and approximate in-control expected values for the lrt_{m_1} statistic for $m=5$ and $X=0(0.2)1.8$	73
Table 4.2	The simulated and approximate in-control expected values for the lrt_{m_1} statistic for $m=20$ and $X=0(0.2)1.8$	73
Table 4.3	The simulated and approximate in-control expected values for the lrt_{m_1} statistic for $m=60$ and $X=0(0.2)1.8$	74
Table 4.4	The simulated and approximate in-control expected values for the lrt_{m_1} statistic for $m=20$ and $X=0(0.2)1.8$ are used twice	74
Table 4.5	The simulated and approximate in-control expected values for the lrt_{m_1} statistic for $m=20$ and $X=-30, -23, -12, -4, 0, 3, 10, 20, 25, \text{ and } 3573$	75

Table 4.6	The overall probabilities of a Type error using the conservative Bonferroni's inequality	97
Table 4.7	Best and approximate values of r	98
Table 4.8	Overall probabilities of a Type I error: nominal vs. simulated	100
Table 4.9	The overall probabilities of a Type error using the approximation of Csörgo and Horvath (1997)	101

Chapter 1: Introduction

The current study addresses two main subjects, the monitoring of linear profiles and the inertial properties of control charts. The following sections introduce both subjects and present related literature reviews.

1.A The Monitoring of Linear Profiles

In most statistical process control (SPC) applications it is assumed that the quality of a process or product can be adequately represented by the distribution of a univariate quality characteristic or by the general multivariate distribution of a vector consisting of several quality characteristics. In many practical situations, however, the quality of a process or product is characterized and summarized better by a relationship between a response variable and one or more explanatory variables. This relationship is referred to as a *profile*. In particular, there has been recent interest in monitoring processes characterized by simple linear regression profiles.

The monitoring of linear profiles is a relatively new quality control application, with most of the work done in this application having appeared in the last few years. Woodall et al. (2004) gave a review of the literature on this topic and presented a general framework for process monitoring using profile data. Most of the studies conducted have been motivated by calibration applications. For example, Mestek et al. (1994) considered the stability of linear calibration curves in the photometric determination of Fe^{3+} with sulfosalicylic acid. Stover and Brill (1998) studied the multilevel ion chromatography linear calibrations to determine instrument response stability and the proper calibration frequency. Lawless et al. (1999) discussed a pair of examples in automotive engineering for which the relationship between the input and output dimensions of a part could be represented by a straight line for each stage of the manufacturing process. Their emphasis was in understanding how the variation is transmitted through the stages of the manufacturing process. Kang and Albin (2000) presented two examples of process profiles; one of them is a semiconductor manufacturing application in which the process

is represented by a linear calibration function. Ajmani (2003) presented an Intel Corporation semiconductor manufacturing application not involving calibration. Other researchers have considered more complicated models than the simple linear regression model. For instance, the other example presented in Kang and Albin (2000) involved a non-linear relationship between the amount of dissolved artificial sweetener aspartame and the temperature levels. The non-linear profile applications were also studied by Jin and Shi (1999); Walker and Wright (2002); and Williams et al. (2003).

The analysis of linear profiles includes two phases, Phase I and Phase II. The purpose of the analysis in Phase I is to analyze a historical set of a fixed number of process samples collected over time to understand the process variation, determine the stability of the process, and remove samples associated with any assignable causes. Having removed those samples, one estimates the in-control values of the process parameters to be used in designing control charts for the Phase II analysis. The performance of a Phase I control chart method is usually measured in terms of the probability of signal; this is the probability of obtaining at least one charted statistic outside the control limits. On the other hand, the main interest in Phase II monitoring of linear profiles is to quickly detect parameter changes from the in-control parameter values. The performance of control chart methods in Phase II is usually measured in terms of the average run length (*ARL*), where the run length is the number of samples taken until the chart gives an out-of-control signal. Table 1.1 shows a comparison between the two phases of the monitoring of profiles.

The vast majority of the research on control charting is on Phase II methods and their performance. In most of this study, the focus is on Phase I. The current study investigates the performance of some of the recommended approaches for Phase I monitoring of linear profiles used to assess the stability of the process. Also in the current study, the researcher proposes a method for Phase I monitoring of linear profiles based on using indicator variables in a multiple regression model.

Table 1.1: A comparison between Phase I and Phase II of the monitoring of profiles

	Phase I analysis	Phase II analysis
Data	m samples of historical data.	On-line data.
Regression parameters	The parameters are unknown and to be estimated.	The parameters are assumed to be either <ul style="list-style-type: none"> • known or • estimated from a data set in Phase I.
Goals	<ul style="list-style-type: none"> • Determine the stability of the process. • Remove samples associated with any assignable causes. • Estimate the in-control values of the process parameters. 	Signal as quickly as possible when the process parameters change from the in-control parameters.
Criteria to compare competing methods	The probability of obtaining at least one charted statistic outside the control limits.	The run length distribution parameters (usually the <i>ARL</i>).

1.B A Change Point Approach for Linear Profile Data Sets

There are many practical applications in which a researcher may wish to test the constancy of the regression parameters in m samples of profile data. For example, a medical researcher may wish to test the constancy of the mean reaction time of a manufactured drug when applied to two or more groups of patients, using the age of the patient as the explanatory variable; see Kulasekera (1995). The Phase I monitoring of profiles described in Section 1.A is another practical application in the area of SPC. The main concern in these applications is to test the hypothesis that all of the profiles follow a single regression model against the hypothesis that a change occurred in one or more model parameters after sample m_1 , $m_1 = 1, 2, \dots, m-1$. For this purpose, the current study proposes a change point method based on using a likelihood ratio test (LRT) in a segmented simple linear regression model. This method can be used to assess the stability of and to detect change points in a Phase I simple linear profile data set.

Many authors have studied the change point problem in regression models, such as simple linear regression, multiple linear regression, polynomial regression and non-linear regression, but under a different sampling framework from that of the linear profile data. These authors assumed that either there is a possible change point after any single observation or that data are obtained sequentially one observation at a time. Using this sampling approach, Quandt (1958, 1960) proposed a likelihood ratio approach to detect a change point in a simple linear regression model. His main concern was to estimate the position of the point in time at which the regression model changed and to estimate the regression parameters in the models prior to and following the change point. In the literature of regression analysis this is usually referred to as two-phase regression, switching regression, or segmented regression. Brown et al. (1975) proposed tests based on recursive residuals to check for the stability over time in multiple regression models. MacNeill (1978) presented tests for changes in a polynomial regression model at unknown times based on raw regression residuals. In addition, Chen (1998) proposed the Schwarz Information Criterion (SIC) to locate a change point in both simple and multiple linear regression models. Also, Krieger et al. (2003) considered detection of a gradual change in the slope in a simple linear regression model. Jandhyala and Al-Saleh (1999) considered the change point problem in non-linear regression models. Many other authors have studied the change point problem in regression models in this sampling framework, including, e.g., Farley and Hinich (1970); Esterby and El-Shaarawi (1981); Worsley (1983); Kim and Siegmund (1989); Jandhyala and MacNeill (1991); Kim and Cai (1993); Kim (1994); Chang and Huang (1997); and Yakir et al. (1999).

In a segmented simple linear regression model we assume that the data set consists of a single sample in the form $\{(X_1, Y_1), (X_2, Y_2), \dots, (X_N, Y_N)\}$. The s -segment regression model with an explanatory variable X and a response Y is assumed to be

$$Y_i = A_{0j} + A_{1j}X_i + \varepsilon_i, \quad \theta_{j-1} < i \leq \theta_j, j=1, \dots, s, \quad i=1, 2, \dots, N, \quad (1.1)$$

where the θ_j 's are the change points between segments (usually $\theta_0 = 0$ and $\theta_s = N$) and the ε_i 's are the error terms. Most work on segmented regression has been based on the

assumption that the ε_i 's were independent, identically distributed (i.i.d.) normal random variables with mean zero. The segment error term variance, σ_j^2 , can be considered to be either constant (homoscedastic model) or non-constant (heteroscedastic model). In some articles the authors have assumed the continuity of the model at the change points; see Gallant and Fuller (1973), for example. In this study, no assumption of continuity is made. The models without continuity requirements have been studied by several authors; see Quandt (1958) and Hawkins (1976), for example. Segmented linear regression methods can be used to detect changes in the regression parameters within the given sample, to estimate the locations of the change points (θ_j 's), and to determine the appropriate number of change points. Hawkins (1976) gave formulas for the likelihood of the general segmented multiple regression model, along with a dynamic programming algorithm (DP) to determine the exact maximum likelihood statistics for a multiple segmented model, both for the homoscedastic and heteroscedastic models. Hawkins (2001) gave formulas for the LRT for testing the null hypothesis of a single segment against the alternative of s segments ($s > 1$).

In a profile data set with a single explanatory variable X and a response Y , the data are m samples in the form $\{(X_{i1}, Y_{i1}), i=1, 2, \dots, n_1\}, \{(X_{i2}, Y_{i2}), i=1, 2, \dots, n_2\}, \dots, \{(X_{im}, Y_{im}), i=1, 2, \dots, n_m\}$ with $n_j > 2$, $j = 1, 2, \dots, m$. The model that relates the explanatory variable X to the response Y in this case is

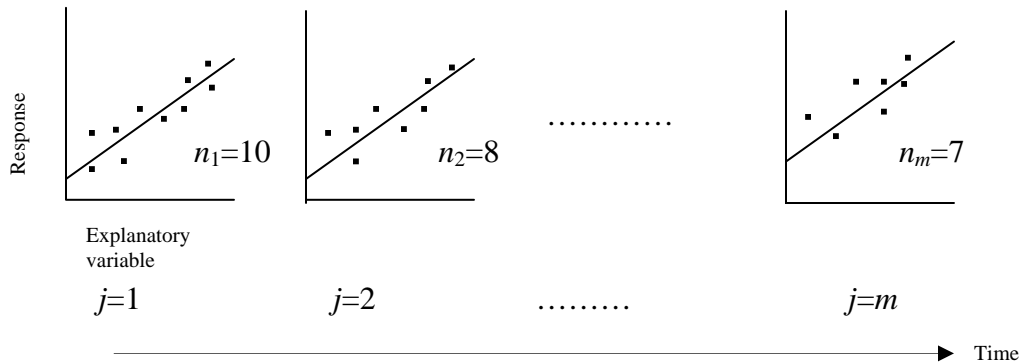
$$Y_{ij} = A_{0j} + A_{1j}X_{ij} + \varepsilon_{ij}, \quad i = 1, 2, \dots, n_j, \text{ and } j=1, 2, \dots, m. \quad (1.2)$$

The emphasis in this situation is to detect changes in the regression parameters from sample to sample, assuming that no parameter change has occurred within each sample.

Figure 1.1 shows graphically the framework of a linear profile data set. This sampling framework is identical to that of panel data in econometrics. Only a very few econometricians, however, have proposed methods to detect structural changes in the context of panel data. Han and Park (1989) proposed an extension of the method of Brown et al. (1975) to panel data. Hansen (1999) and Emerson and Kao (2001, 2002)

proposed methods more similar to the proposed change point method discussed in Chapter 4, but considered only the detection of shifts in the slope. Using a sampling framework similar to the profile data, Gulliksen and Wilks (1950) proposed a likelihood ratio method to test for the equality of the regression parameters in several samples. This approach, however, is not a change point method.

Figure 1.1: The framework of a linear profile data set.

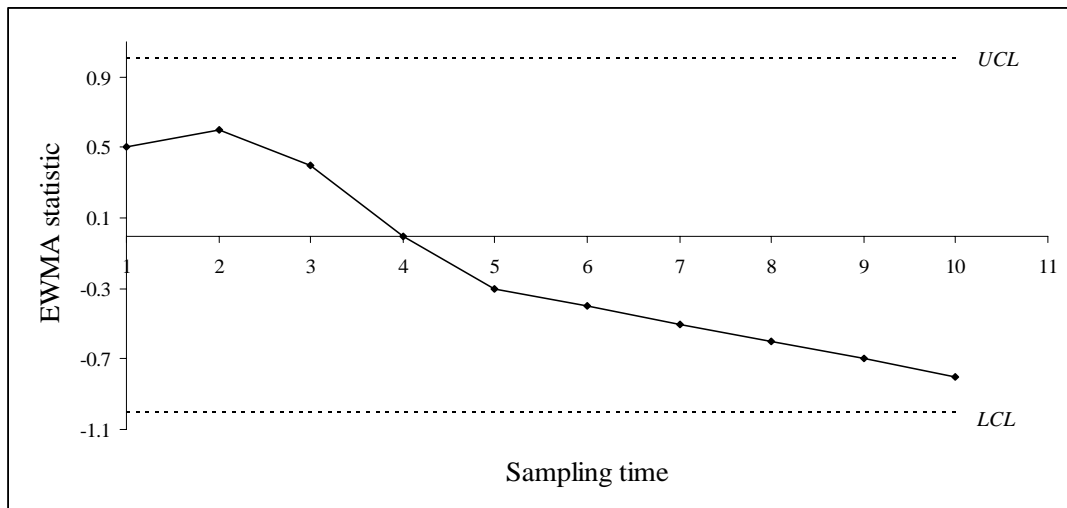


To detect parameter changes in a profile data set, this study proposes an approach based on the segmented regression model in Equation (1.1). In this approach one pools all the profile samples into one sample of size $N = \sum_{j=1}^m n_j$. Then, for the pooled sample, one applies the segmented regression model in Equation (1.1). As mentioned above, in the linear profile model we assume that no parameter changes occur within each sample. Thus, in the proposed approach for profile data, the θ_j 's in Equation (1.1) are restricted to the indices i corresponding to the ends of the profile samples. To test for a change in one or more of the regression parameters, one applies the LRT of Hawkins (2001). This method can be applied recursively to identify multiple change points in the data set. Moreover, the LRT statistic can be partitioned into 3 terms indicating to a large extent the relative contribution of the Y -intercept, slope, and variance shifts to an out-of-control signal.

1.C The Inertial Properties of Quality Control Charts

When a control chart that combines information over time is being used, e. g, the cumulative sum (CUSUM) chart or the exponentially weighted moving average (EWMA) chart, then it is possible that the chart statistic is in a somewhat disadvantageous position immediately before a process parameter change. For example the univariate EWMA chart statistic based on sample means may be close to the lower control limit when an upward shift in the process mean occurs. Being near the lower control limit causes the time required to reach the upper control limit, producing an out-of-control signal, to be longer than if the EWMA statistic were close to the centerline or close to the upper control limit when the shift occurred. An illustrative example is shown in Figure 1.2. This figure shows an EWMA chart with a trend in the process mean in the lower direction of the centerline occurs after sampling time 2. If a shift in the process mean in the upper direction of the centerline occurs at sampling time 10, the EWMA chart may not pick up this shift immediately.

Figure 1.2: EWMA chart with downward undetected sustained shift.



Yashchin (1987, 1993) recommended the consideration of such “worst-case scenarios” in the selection of a control chart. Others, such as Lowry et al. (1992), Lowry

and Montgomery (1995), and Woodall and Adams (1998), refer to the potential delay in signaling as resulting in an “inertia problem.”

In physics, “inertia” refers to the resistance an object has to a change in its state of motion. Similarly, in statistical process control “inertia” can be used to refer to a measure of the resistance that a chart has to signaling a particular process shift. The amount of inertia depends on the value of the chart statistic. The measure of inertia could be low if the charting statistic is near the appropriate boundary when a shift occurs, so there is not always an inertia *problem*, as it is usually phrased in the literature. The author refers instead to the inertial properties of control charts.

Yashchin (1993) gave a table that showed a comparison of the EWMA chart and the CUSUM chart on the basis of steady-state and worst-case *ARLs*. The worst-case scenario is that the control chart statistic is at the value that maximizes the out-of-control *ARL*. The steady-state *ARL* is based on averaging the out-of-control *ARL* values over the possible values of the control chart statistic under the assumptions that the process has been operating for a while and that the process mean stays on target until the specified shift in the mean occurs. Yashchin’s conclusion was that the EWMA and CUSUM charts have roughly equivalent steady-state *ARL* performance, but in the worst-case scenarios the EWMA *ARLs* are higher. Yashchin (1987) stated that in most cases one will be more interested in control schemes with better worst-case sensitivity. Thus, Yashchin (1987, 1993) argued that the possibility of an EWMA statistic being in a disadvantageous position is a serious disadvantage for the EWMA chart compared to other charts, such as the CUSUM chart, that use resets and do not have such a significant inertia problem. For this reason, he concluded that the use of the CUSUM chart should be preferred over the use of the EWMA chart.

Moustakides (1986) showed that the one-sided CUSUM chart is optimal in the sense that among all control charts with at least a specified in-control *ARL*, the out-of-control *ARL* for a specified out-of-control distribution is minimized by the CUSUM chart

when considering each competing chart under its corresponding worst-case scenario. Lucas and Saccucci (1990) also showed some worst-case *ARLs* for EWMA charts, but they downplayed the importance of the inertia issue, saying it only takes a few observations after the shift for the EWMA chart to overcome its initial inertia.

This study shows under realistic assumptions that the worst-case run length performance of control charts becomes as informative as steady-state performance. Also, the current study proposes a simple new measure of the inertial properties of control charts, defining the *signal resistance* of a chart to be the largest standardized shift from target not leading to an immediate out-of-control signal. The signal resistance from the worst-case to the best-case scenario is calculated for several types of univariate and multivariate control charts, including some charts augmented with Shewhart limits. This study considers only control charts for monitoring the process mean or mean vector, although the ideas can be easily extended to other types of charts.

Chapter 2: Linear Profile Models and Approaches

As mentioned in Chapter 1, the monitoring of linear profiles includes two phases, Phase I and Phase II. In this chapter, the Phase I and Phase II models and approaches for monitoring a simple linear profile data set are presented.

2.A Phase I Monitoring of Simple Linear Profiles

The setting of a Phase I simple linear profile data set can be described as follows. The observed data collected over time are m random samples, with each sample consisting of a sequence of n_j pairs of observations (X_{ij}, Y_{ij}) , $i=1, 2, \dots, n_j$, $j=1, 2, \dots, m$. For each sample it is assumed that the model relating the independent variable X to the response Y is

$$Y_{ij} = A_{0j} + A_{1j}X_{ij} + \varepsilon_{ij}, \quad i = 1, 2, \dots, n_j, \text{ and } j=1, 2, \dots, m, \quad (2.1)$$

where the ε_{ij} 's are assumed to be independent, identically distributed (i.i.d.) $N(0, \sigma_j^2)$ random variables. The X -values in each sample are assumed to be known constants; [Neter et al. (1990, pp. 86-87) discussed the regression analysis when the X -values are random]. In many of the Phase I linear profile applications the X -values are known constants and take the same values in all samples. The in-control values of the parameters A_0 , A_1 , and σ^2 in Equation (2.1) are unknown. If $A_{0j} = A_0$, $A_{1j} = A_1$, and $\sigma_j^2 = \sigma^2$, $j = 1, 2, \dots, m$, then the process is considered to be stable in Phase I.

Our main objective in the Phase I analysis is to evaluate the stability of the process and to estimate the in-control parameters. Obtaining a data set reflecting expected in-control performance is usually accomplished by discarding samples associated with assignable causes from the data set, assuming that the associated assignable causes can be identified and removed.

In the SPC literature, usually the statistical performance of a Phase I method is

measured in terms of the probability of a signal. As defined in Chapter 1, the probability of a signal is the probability of obtaining at least one charted statistic outside the control limits.

It is well-known that the least squares estimates of A_0 and A_1 for sample j are

$$a_{0j} = \bar{Y}_j - a_{1j}\bar{X}_j \quad \text{and} \quad a_{1j} = S_{XY(j)} / S_{XX(j)}, \quad (2.2)$$

where $\bar{Y}_j = \sum_{i=1}^{n_j} Y_{ij} / n_j$, $\bar{X}_j = \sum_{i=1}^{n_j} X_{ij} / n_j$, $S_{XY(j)} = \sum_{i=1}^{n_j} (X_{ij} - \bar{X}_j)Y_{ij}$, and $S_{XX(j)} = \sum_{i=1}^{n_j} (X_{ij} - \bar{X}_j)^2$, [see, e.g., Myers (1990, chap. 2)]. Furthermore, σ_j^2 is estimated by the j^{th} mean square error MSE_j , where $MSE_j = SSE_j / (n_j - 2)$. Here $SSE_j = \sum_{i=1}^{n_j} e_{ij}^2$ is the residual sum of squares, where $e_{ij} = Y_{ij} - a_{0j} - a_{1j}X_{ij}$, $i = 1, 2, \dots, n_j$. It is also well-known that the least squares estimators a_{0j} and a_{1j} are distributed as a bivariate normal distribution with the mean vector

$$\boldsymbol{\mu} = (A_0, A_1)^T$$

and the variance-covariance matrix

$$\boldsymbol{\Sigma} = \begin{pmatrix} \sigma_0^2 & \sigma_{01}^2 \\ \sigma_{01}^2 & \sigma_1^2 \end{pmatrix}, \quad (2.3)$$

where $\sigma_0^2 = \sigma^2(1/n_j + \bar{X}_j^2 / S_{XX(j)})$, $\sigma_1^2 = \sigma^2 / S_{XX(j)}$ and $\sigma_{01}^2 = -\sigma^2 \bar{X}_j / S_{XX(j)}$ are the variance of a_{0j} , the variance of a_{1j} , and the covariance between a_{0j} and a_{1j} , respectively. Also the quantity $(n_j - 2)MSE_j / \sigma^2$ is distributed as a chi-square distribution with $(n_j - 2)$ degrees of freedom independently of a_{0j} and a_{1j} , $j=1, 2, \dots, m$.

Once a set of data reflecting in-control performance is obtained, one estimates the in-control process parameters, the Y -intercept, the slope, and the variance by the intercept average $\bar{a}_0 = \sum_{j=1}^m a_{0j} / m$, the slope average $\bar{a}_1 = \sum_{j=1}^m a_{1j} / m$, and the mean square error average

$$MSE = \sum_{j=1}^m MSE_j / m, \quad (2.4)$$

respectively. In the following subsections the recommended approaches for monitoring Phase I linear profile data sets are presented.

2.A.1 T^2 Control Chart Approaches

The SPC literature includes three T^2 control chart approaches for analyzing linear profile data sets in Phase I. These are Mestek et al.'s (1994) T^2 chart, Stover and Brill's (1998) T^2 chart, and Kang and Albin's (2000) T^2 chart.

Mestek et al. (1994) proposed a T^2 control chart to check for the stability of the linear calibration curve in the photometric determination of Fe^{3+} with sulfosalicylic acid. Their T^2 approach is based on successive vectors containing the absorbances of the calibration curve, i.e., the response Y -values. In this approach one must assume that the X -values are fixed and take the same set of values for each sample (i.e. $X_{ij}=X_i, j=1, 2, \dots, m$). The T^2 statistics for this method are

$$T_j^2 = (\mathbf{y}_j - \bar{\mathbf{y}})^T \mathbf{S}^{-1} (\mathbf{y}_j - \bar{\mathbf{y}}) \quad j=1, 2, \dots, m, \quad (2.5)$$

where $\mathbf{y}_j = (y_{1j}, y_{2j}, \dots, y_{nj})$ is a vector containing the response values of the j^{th} sample, and $\bar{\mathbf{y}} = (\bar{y}_1, \bar{y}_2, \dots, \bar{y}_n)$ is a vector of the response averages, where $\bar{y}_i = \sum_{j=1}^m y_{ij} / m$. Also,

$$\mathbf{S} = \begin{bmatrix} s_1^2 & s_{21} & \dots & s_{n1} \\ s_{12} & s_2^2 & \dots & s_{n2} \\ \cdot & \cdot & \dots & \cdot \\ s_{1n} & s_{2n} & \dots & s_n^2 \end{bmatrix}$$

is the pooled sample covariance matrix, where $s_i^2 = \sum_{j=1}^m (y_{ij} - \bar{y}_i)^2 / (m-1)$, ($i=1, 2, \dots, n$) and $s_{il} = \sum_{j=1}^m (y_{ij} - \bar{y}_i)(y_{lj} - \bar{y}_l) / (m-1)$, [$i, l=1, 2, \dots, n (i \neq l)$]. Mestek et al. (1994) used a T^2 -distribution with n and m degrees of freedom to determine the upper control limit of their T^2 chart. Using the relationship between the T^2 - and F -distributions, they calculated

the upper control limit as $UCL = n(m-1)F_{n,m-n,\alpha} / (m-n)$, where $F_{n,m-n,\alpha}$ is the $100(1-\alpha)$ percentile of the F -distribution with n and $m-n$ degrees of freedom. However, as mentioned in Tracy et al. (1992) and Sullivan and Woodall (1996a), the T^2 -distribution can be used to determine the UCL of the conventional T^2 control chart for individual multivariate observations when estimating the population covariance matrix Σ with \mathbf{S} only for future observations, i.e., only in Phase II. In Phase I, if the population covariance matrix Σ is estimated by \mathbf{S} , then the T^2 statistic in Equation (2.5) follows a beta distribution. The proof can be found in Gnanadesikan and Kettenring (1972). Thus, as pointed out by Tracy et al. (1992), a more appropriate UCL for the chart is

$$UCL = (m-1)^2 B_{n/2, m-n-1/2, \alpha} / m, \quad (2.6)$$

where $B_{n/2, m-n-1/2, \alpha}$ is the $100(1-\alpha)$ percentile of the beta distribution with parameters $n/2$ and $(m-n-1)/2$. Note that values of the T^2 statistics in Equation (2.5) are not independent because each of the m charted T^2 statistics is calculated based on the same sample estimators.

The use of this T^2 control chart for monitoring linear profile data sets in Phase I is not recommended for four reasons. First, this chart can be applied directly only when the X -values are fixed and constant from sample to sample. Second, the T^2 control chart for individual multivariate observations when estimating the population covariance matrix Σ with \mathbf{S} can have very poor statistical performance in terms of the probability of an out-of-control signal. This was demonstrated by Sullivan and Woodall (1996a), Vargas (2003), and by the simulation study described in Chapter 3 of this dissertation. Third, when $m \leq n$ the sample covariance matrix \mathbf{S} is singular and the beta distribution cannot be used. Finally, with a simple profile relationship, use of a T^2 chart based on the n Y -values leads to overparameterization.

Stover and Brill (1998) proposed two methods for a Phase I linear profile calibration process. The first method is a T^2 approach based on vectors containing estimators of the Y -intercept and slope. The T^2 statistics of this method are

$$T_j^2 = (\mathbf{z}_j - \bar{\mathbf{z}})^T \mathbf{S}_1^{-1} (\mathbf{z}_j - \bar{\mathbf{z}}), \quad j=1, 2, \dots, m, \quad (2.7)$$

where $\mathbf{z}_j = (a_{0j}, a_{1j})^T$, $\bar{\mathbf{z}} = (\bar{a}_0, \bar{a}_1)^T$, and $\mathbf{S}_1 = \begin{pmatrix} S_0^2 & S_{01} \\ S_{01} & S_1^2 \end{pmatrix}$. Here a_{0j} and a_{1j} are as defined in Equation (2.2), and $S_0^2 = \sum_{j=1}^m (a_{0j} - \bar{a}_0)^2 / (m-1)$, $S_1^2 = \sum_{j=1}^m (a_{1j} - \bar{a}_1)^2 / (m-1)$, and $S_{01} = \sum_{j=1}^m (a_{1j} - \bar{a}_1)(a_{0j} - \bar{a}_0) / (m-1)$ are the sample variance of a_{0j} , the sample variance of a_{1j} , and the sample covariance between a_{0j} and a_{1j} , respectively. The upper control limit for this chart used by Stover and Brill (1998) is obtained from the T^2 -distribution. Using the relationship between the T^2 - and F -distributions, they calculated the upper control limit of this chart to be $UCL = 2(m+1)(m-1)F_{2,m-2,\alpha} / m(m-2)$. However, as mentioned previously in the context of the method proposed by Mestek et al. (1994), the T^2 distribution is not the appropriate marginal distribution for the T^2 statistic when estimating the population covariance matrix using the pooled sample covariance matrix in Phase I. A more appropriate upper control limit in this case is

$$UCL = (m-1)^2 B_{1,(m-3)/2,\alpha} / m. \quad (2.8)$$

Even though the values of the T^2 statistics in Equation (2.7) are dependent, the simulation study described in Chapter 3 shows that the overall false alarm probabilities produced by this chart can be approximated closely using this marginal beta distribution.

The T^2 control chart of Kang and Albin (2000) is based on successive vectors of the least squares estimators of the Y -intercept and slope. The T^2 statistics in this method are

$$T_j^2 = m (\mathbf{z}_j - \bar{\mathbf{z}})^T \mathbf{S}_2^{-1} (\mathbf{z}_j - \bar{\mathbf{z}}) / (m-1), \quad j=1, 2, \dots, m, \quad (2.9)$$

where \mathbf{z}_j and $\bar{\mathbf{z}}$ are as defined for Equation (2.7), and $\mathbf{S}_2 = \begin{pmatrix} \hat{\sigma}_0^2 & \hat{\sigma}_{01} \\ \hat{\sigma}_{01} & \hat{\sigma}_1^2 \end{pmatrix}$, where $\hat{\sigma}_0^2$, $\hat{\sigma}_1^2$ and $\hat{\sigma}_{01}$ are the estimators of the variance of a_{0j} , the variance of a_{1j} and the covariance

between a_{0j} and a_{1j} defined in Equation (2.3), respectively. These estimators are obtained by replacing σ^2 in Equation (2.3) by MSE , where MSE is as defined in Equation (2.4). The upper control limit of this chart used by Kang and Albin (2000) is

$$UCL = 2F_{2,m(n-2),\alpha} \cdot \quad (2.10)$$

Obviously, this method is similar to the T^2 method of Stover and Brill (1998), although the marginal distributions of the control statistic used differ because of different estimators for the covariance matrix.

One should note that the values of the T^2 statistics in Equation (2.9) are also dependent, as was the case for those in Equations (2.5) and (2.7), but again the simulation study in Chapter 3 shows that the marginal F -distribution can lead to a close approximation of the overall probability of a false alarm.

2.A.2 Kim et al.'s (2003) Shewhart-Type Control Charts Approach

Kim, Mahmoud, and Woodall (2003) proposed another approach for Phase I analysis of linear profiles. They recommended coding the X -values within each sample so that the estimators of the Y -intercept and slope are independent. Using their coding recommendation and the fact that the estimator of the variance is independent of the estimators of the Y -intercept and slope, one can monitor each of the three regression parameters using a separate Shewhart-type control chart. If one codes the X -values within each sample so that the average coded value is zero, then the resulting linear regression model is in the form

$$Y_{ij} = B_{0j} + B_{1j}X'_{ij} + \varepsilon_{ij}, \quad i = 1, 2, \dots, n_j, \quad j=1, 2, \dots, m, \quad (2.11)$$

where $B_{0j} = A_{0j} + A_{1j}\bar{X}_j$, $B_{1j} = A_{1j}$, and $X'_{ij} = (X_{ij} - \bar{X}_j)$. In this case, the least squares estimators for the regression parameters for sample j are $b_{0j} = \bar{y}_j$, and $b_{1j} = a_{1j} = S_{XY(j)} / S_{XX(j)}$. It is very well-known that for an in-control process, b_{0j} and b_{1j}

are mutually independent normally distributed random variables with means B_0 and B_1 and variances σ^2/n_j and $\sigma^2/S_{xx(j)}$, respectively.

Notice that a shift in the Y -intercept in Equation (2.1) from A_{0j} to $A_{0j} + \Delta A_0$ is equivalent to a shift in the Y -intercept in Equation (2.11) from B_{0j} to $B_{0j} + \Delta A_0$. A shift in the slope of the regression model in Equation (2.1) from A_{1j} to $A_{1j} + \Delta A_1$, however, leads to shifts in both the Y -intercept and slope in Equation (2.11). In this case, the Y -intercept shifts from B_{0j} to $B_{0j} + \bar{X}_j \Delta A_1$, while the slope shifts from B_{1j} to $B_{1j} + \Delta A_1$. In the special case when $\bar{X}_j = \bar{X}$, $j=1, 2, \dots, m$, if the Y -intercept in equation (2.1) shifts from A_{0j} to $A_{0j} + \Delta A_0$ and simultaneously the slope in Equation (2.1) shifts from A_{1j} to $A_{1j} + \Delta A_1$ so that $\Delta A_0 + \bar{X}_j \Delta A_1 = 0$, then only the slope in Equation (2.11) shifts from B_{1j} to $B_{1j} + \Delta A_1$. However, if \bar{X}_j varies from sample to sample, the shifts in the parameters in Equation (2.11) corresponding to this type of shift is not clearly interpretable. Finally, it is obvious that shifts in the variances of both models in Equations (2.1) and (2.11) would be equivalent.

Assuming that the X -values are the same in all samples and that the process is in control, it can be shown that the quantity $b_{0j} - \bar{b}_0$, where $\bar{b}_0 = \sum_{j=1}^m b_{0j} / m$, has a normal distribution with mean of 0 and variance of $\frac{m-1}{nm} \sigma^2$. It also can be shown that the quantity $\frac{m(n-2)MSE}{\sigma^2}$ has a chi-square distribution with $m(n-2)$ degrees of freedom.

Since these two variables are independent, the quantity $(b_{0j} - \bar{b}_0) / \sqrt{MSE \frac{m-1}{nm}}$ follows a t -distribution with $m(n-2)$ degrees of freedom. Thus, it seems reasonable as an approximation to use a Shewhart-type control chart for monitoring the intercept B_0 with the following lower and upper control limits:

$$LCL = \bar{b}_0 - t_{m(n-2), \frac{\alpha}{2}} \sqrt{\frac{(m-1)MSE}{nm}} \quad \text{and} \quad UCL = \bar{b}_0 + t_{m(n-2), \frac{\alpha}{2}} \sqrt{\frac{(m-1)MSE}{nm}}, \quad (2.12)$$

where $t_{m(n-2), \alpha/2}$ is the $100(1 - \alpha/2)$ percentile of the t -distribution with $m(n - 2)$ degrees of freedom.

Also assuming that the process is in control, it can be shown that $b_{1j} - \bar{b}_1$, where $\bar{b}_1 = \sum_{j=1}^m b_{1j} / m$, has a normal distribution with mean of 0 and variance of $\frac{m-1}{mS_{XX}} \sigma^2$.

Hence, the quantity $(b_{1j} - \bar{b}_1) / \sqrt{MSE \frac{m-1}{mS_{XX}}}$ follows a t -distribution with $m(n - 2)$ degrees of freedom. Therefore, approximate upper and lower control limits for a Shewhart control chart for monitoring B_1 can be set at

$$LCL = \bar{b}_1 - t_{m(n-2), \frac{\alpha}{2}} \sqrt{\frac{(m-1)MSE}{mS_{XX}}} \quad \text{and} \quad UCL = \bar{b}_1 + t_{m(n-2), \frac{\alpha}{2}} \sqrt{\frac{(m-1)MSE}{mS_{XX}}}. \quad (2.13)$$

Assuming in-control process, it can be shown that the quantity

$$F_j = MSE_j / MSE_{-j} \quad (2.14)$$

has an F -distribution with $n-2$ and $(m-1)(n-2)$ degrees of freedom, where $MSE_{-j} = \sum_{i \neq j}^m MSE_i / (m-1)$. Therefore, a Shewhart control chart for monitoring the process variance σ^2 requires plotting the quantity F_j on a chart with the following control limits

$$LCL = F_{(n-2), (m-1)(n-2), \alpha/2} \quad \text{and} \quad UCL = F_{(n-2), (m-1)(n-2), (1-\alpha/2)}. \quad (2.15)$$

A mathematically equivalent control chart for monitoring the process variance can be obtained by plotting MSE_j on a chart with the following lower and upper control limits:

$$LCL = \frac{mF_{(n-2),(m-1)(n-2),\frac{\alpha}{2}}}{m-1 + F_{(n-2),(m-1)(n-2),\frac{\alpha}{2}}} MSE \quad \text{and} \quad UCL = \frac{mF_{(n-2),(m-1)(n-2),1-\frac{\alpha}{2}}}{m-1 + F_{(n-2),(m-1)(n-2),1-\frac{\alpha}{2}}} MSE. \quad (2.16)$$

If the X -values vary from sample to sample, one can obtain the control limits of the process parameters corresponding to a specified false alarm probability using simulation.

Since the accuracy of the estimators of the in-control regression coefficients relies heavily on the stability of the process variance, it is recommended that one apply a control chart for the variance before applying the control charts for the Y -intercept and slope.

This method is also based on the plotting of dependent statistics in each one of the three charts for monitoring the three process parameters. For example, if E_i represents the event that the i^{th} mean square error exceeds the control limits in Equation (2.16), then E_i and E_j ($i \neq j$) are not independent. This is also the case using the control limits of the Y -intercept and slope in Equation (2.12) and Equation (2.13), respectively. However, the simulation study presented in Chapter 3 shows that these dependencies do not prevent good approximations of the overall false alarm probabilities.

As an alternative, one can consider these charting methods for the Y -intercept and slope under the framework of the analysis of means (ANOM). The charts can be constructed such that joint distribution of the plotted statistics within each chart is a multivariate t -distribution with a correlation between each pair of variables of $\rho = -1/(m-1)$. See, for example, Nelson (1982). Also as an alternative for the control chart for monitoring the process variance in Kim et al.'s (2003) method, one can consider the analysis of means-type test for the equality of variances, denoted by ANOMV, proposed by Wludyka and Nelson (1997). However, the simpler approach taken above is shown to be quite accurate in the simulation study presented in Chapter 3.

2.A.3 Principal Component Approaches

Control chart methods for monitoring Phase I linear profiles based on principal components technique were suggested by Mestek et al. (1994) and Stover and Brill (1998). The principal component method of Mestek et al. (1994) employs a Shewhart-type control chart for the first principal component corresponding to vectors of the Y -values, assuming that the X -values are fixed from sample to sample. The principal components approach of Stover and Brill (1998) is based on control charting the first principal component corresponding to vectors containing the estimates of the regression parameters for each sample. These principal component methods, however, are not recommended because they will not be able to detect some out-of-control conditions. The first principal component explains in-control variation in the direction of the major axis corresponding to the first principal component. Therefore, one will not be able to detect combinations of shifts in the Y -intercept and the slope in the direction perpendicular to the major axis corresponding to the first principal component.

On the other hand, the principal components approach of Jones and Rice (1992) is a very useful tool to identify and understand the nature of the variability among the profiles in a Phase I profile data set with equal, equally spaced X -values for each profile. This approach has become a fundamental part of functional data analysis. See, for example, Ramsay and Silverman (2002). In this principal component approach, one determines the first few principal components that account for most of the profile variation. Then, for each principal component, one plots the average profile and the profiles corresponding to the minimum and maximum principal component scores. This approach is strongly recommended for use in Phase I analysis of profile data. If the X -values are not equally spaced and/or equal for each profile, one can fit a regression model for each sample and obtain fitted response values for a set of equally spaced values. The approach, however, is not a control chart-based method.

2.A.4 An Alternative Approach

The problem of monitoring linear profiles in Phase I can be expressed in terms of a problem of comparing several regression lines. The literature of regression analysis includes an F -test approach based on using indicator variables (dummy variables) in a multiple regression model to compare two or more regression lines. The use of indicator variables in comparing several regression lines is described in many references; see, for example, Myers (1990, p. 135), Neter et al. (1990, chap. 10), and Kleinbaum and Kupper (1978, chap. 13).

Suppose that we have m samples of bivariate observations and we need to test the equivalence (coincidence) of the regression lines of all samples. The first step in the indicator variables technique is to pool all the m samples into one sample of size $N = \sum_{j=1}^m n_j$. Then we create $m-1$ indicator variables such that

$$Z_{ji} = \begin{cases} 1 & \text{if observation } i \text{ is from sample } j \\ 0 & \text{otherwise} \end{cases}, \quad i = 1, 2, \dots, N, \quad j = 1, 2, \dots, m'.$$

where $m' = m - 1$. Finally, we fit to the pooled data the following multiple regression model:

$$y_i = A_0 + A_1 x_i + \beta_{01} Z_{1i} + \beta_{02} Z_{2i} + \dots + \beta_{0m'} Z_{m'i} + \beta_{11} Z_{1i} x_i + \beta_{12} Z_{2i} x_i + \dots + \beta_{1m'} Z_{m'i} x_i + \varepsilon_i, \quad i = 1, 2, \dots, N, \quad (2.17)$$

where the ε_i 's are assumed to be i.i.d. $N(0, \sigma^2)$ random variables and (x_i, y_i) , $i=1, 2, \dots, N$, are N bivariate observations resulting from pooling the m samples into one sample of size N . To test for the equality of the m regression lines we test the hypotheses $H_0 : \beta_{01} = \beta_{02} = \dots = \beta_{0m'} = \beta_{11} = \beta_{12} = \dots = \beta_{1m'} = 0$ versus $H_1 : H_0$ is not true. Under the null hypothesis we have the following reduced model:

$$y_i = A_0 + A_1 x_i + \varepsilon_i, \quad i = 1, 2, \dots, N. \quad (2.18)$$

The usual test statistic for testing H_0 is

$$F = \frac{\{SSE(reduced) - SSE(full)\} / 2(m-1)}{MSE(full)}, \quad (2.19)$$

where $SSE(full)$ and $SSE(reduced)$ are the residual sum of squares resulting from fitting the regression models in Equations (2.17) and (2.18), respectively, and $MSE(full)$ is the mean square error of the full model in Equation (2.17). This test statistic follows an F distribution with $2(m-1)$ and $N-2m$ degrees of freedom under the null hypothesis.

In this alternative approach for Phase I analysis of linear profiles, one applies the global F -test based on the statistic in Equation (2.19) in conjunction with a univariate control chart to check for the stability of the variation about the regression line. For this purpose, the third control chart of Kim et al. (2003) that is based on control limits in Equation (2.15) [or Equation (2.16)] is recommended. Again, since the accuracy of the estimators of the in-control regression coefficients relies on the stability of the process variance, it is recommended that one check for the stability of the error variance before performing the F -test.

If an out-of-control signal is obtained from the global F -test (i.e., we reject H_0), one follows by coding the X -values such that the average coded value within each sample is zero and applying 3-sigma control charts for the Y -intercept and slope separately. If the X -values are the same in all samples, the 3-sigma control chart for monitoring the intercept is based on plotting the quantity $t_{0j} = (b_{0j} - \bar{b}_0) / \sqrt{MSE/n}$ on a chart with control limits ± 3 . Also, the 3-sigma control chart for monitoring the slope is based on plotting the quantity $t_{1j} = (b_{1j} - \bar{b}_1) / \sqrt{MSE/S_{xx}}$ on a chart with control limits ± 3 . These two charts are used for diagnostic purposes. Alternately, one could perform tests of hypotheses to test the equality of the intercepts and slopes in the m samples. If assignable causes can be identified, the corresponding samples are removed from the data and the method reapplied. Once one has a set of data reflecting expected in-control performance, the regression parameters can be estimated for use in Phase II monitoring. Jensen et al.

(1984) proposed a Phase II method (for multiple linear regression models) similar in several respects to this Phase I method.

2.B Phase II Monitoring of Simple Linear Profiles

The Phase II simple linear profile model is in the form

$$Y_{ij} = A_0 + A_1 X_{ij} + \varepsilon_{ij}, \quad i = 1, 2, \dots, n_j, \text{ and } j=1, 2, \dots \quad (2.20)$$

Again, the ε_{ij} 's are assumed to be i.i.d. $N(0, \sigma^2)$ random variables and the X -values in each sample are assumed to be known constants. Here, the in-control values of the parameters A_0 , A_1 , and σ^2 are assumed to be known or estimated from a data set reflecting expected in-control performance.

The performance of a Phase II control charting method is usually measured by some parameter of the run length distribution. As mentioned in Chapter 1, the run length is the number of samples taken until the chart produces an out-of-control signal. In the literature, often the average run length ARL is used in performance comparisons studies of Phase II methods.

Several authors have proposed Phase II control charting approaches for monitoring simple linear profiles with assumed known values for the intercept, slope and variance parameters. In the following sub-sections the simple linear profile Phase II approaches are presented.

2.B.1 Kang and Albin's (2000) Phase II Approaches

Kang and Albin (2000) proposed two control chart methods for Phase II monitoring of linear profiles. Their first approach is a bivariate T^2 chart based on

successive vectors of the least squares estimators of the Y -intercept and slope, assuming known parameter values. Here, the T^2 statistics are

$$T_j^2 = (\mathbf{z}_j - \boldsymbol{\mu})^T \boldsymbol{\Sigma}^{-1} (\mathbf{z}_j - \boldsymbol{\mu}), \quad j=1, 2, \dots, \quad (2.21)$$

where $\mathbf{z}_j = (a_{0j}, a_{1j})^T$ is the vector of sample estimators, and $\boldsymbol{\mu}$ and $\boldsymbol{\Sigma}$ are as defined in Equation (2.3). When the process is in-control, the T^2 statistic in Equation (2.21) follows a central chi-squared distribution with 2 degrees of freedom. The upper control limit of this chart used by Kang and Albin (2000) is

$$UCL = \chi_{2,\alpha}^2, \quad (2.22)$$

where $\chi_{2,\alpha}^2$ is the $100(1-\alpha)$ percentile of the chi-squared distribution with 2 degrees of freedom. Under out-of-control shifts in the process parameters (assuming that the X -values are the same for all samples), the T^2 statistic in Equation (2.21) follows a non-central chi-squared distribution with 2 degrees of freedom and non-centrality parameter

$$\tau = n(\lambda + \beta\bar{X})^2 + \beta^2 S_{XX},$$

where λ and β are the shifts in the intercept and slope, respectively. It can be shown that the exact ARL of this T^2 control chart is evaluated using the following formula:

$$ARL = \frac{1}{\Pr(T_j^2 > \chi_{2,\alpha}^2)}.$$

If the X -values are not the same for all samples, the ARL corresponding to a specified false alarm probability can be estimated using simulation.

The second Phase II method of Kang and Albin (2000) is an EWMA chart to monitor the average deviation from the in-control line. The deviations from the in-control regression line obtained at sample j are calculated using

$$e_{ij} = Y_{ij} - A_0 - A_1 X_{ij}, \quad i=1, 2, \dots, n_j,$$

and the average deviation for sample j is $\bar{e}_j = \sum_{i=1}^n e_{ij} / n_j$. The EWMA control chart statistics are given by

$$EWMA_j = \theta \bar{e}_j + (1 - \theta) EWMA_{j-1}, \quad (2.23)$$

where $0 < \theta \leq 1$ is usually called the smoothing parameter and $EWMA_0 = 0$. Assuming that $n_j = n, j = 1, 2, \dots$, the control limits for this EWMA chart used by Kang and Albin (2000) are

$$LCL = -L_1 \sigma \sqrt{\theta / n(2 - \theta)} \quad \text{and} \quad UCL = L_1 \sigma \sqrt{\theta / n(2 - \theta)}, \quad (2.24)$$

where $L_1 > 0$ is a constant chosen to give a specified in-control ARL .

Kang and Albin (2000) also suggested an R -chart to be used in conjunction with this EWMA chart to monitor the variation about the regression line. For the R -chart, they plotted the sample ranges $R_j = \max_i(e_{ij}) - \min_i(e_{ij}), j = 1, 2, \dots$, on a chart with the following control limits:

$$LCL = \sigma(d_2 - L_2 d_3) \quad \text{and} \quad UCL = \sigma(d_2 + L_2 d_3), \quad (2.25)$$

where $L_2 > 0$ is a constant selected to produce a specified in-control ARL , and d_2 and d_3 are constants depending on the sample size n . Ryan (2000) and Montgomery(2001), for example, provide tables for the values of d_2 and d_3 corresponding to different values of the sample size n . A signal is given whenever one of the two charts produces an out-of-control signal. A disadvantage of the R -chart approach, however, is that if $n < 7$ there is no lower control limit for the R -chart, and consequently one cannot detect decreases in the process variance without using a runs rule.

If the sample sizes are not the same for all samples, one can determine the control limits of the EWMA chart and R -chart corresponding to a specified overall in-control ARL using simulation.

Kang and Albin (2000) recommended using this EWMA approach in Phase I, substituting the values of the unknown parameters by their estimates. However, it is not recommended using this method in Phase I for two reasons. First, EWMA charts are recommended in Phase II because of their power in detecting sustained shifts in parameters and their quick detection of small-to-moderate process shifts compared to Shewhart-type control charts. However, quick detection is not an issue in Phase I since we have access to a fixed set of historical data. Second, in applying an EWMA chart in Phase I, several samples could be contributing to any out-of-control signal. Therefore, it is not clearly defined how to identify and delete the out-of-control regression lines to achieve stability in the process before estimating the in-control regression parameters.

2.B.2 Kim et al.'s (2003) Phase II Approach

Kim et al. (2003) proposed another method for monitoring a Phase II linear profile process assuming known parameter values. Their idea was to code the X -values within each sample as described in Section 2.A.2. Since coding the X -values this way leads to independent regression estimators, Kim et al. (2003) recommended monitoring the two regression coefficients using separate EWMA charts. They also recommended replacing the R -chart of Kang and Albin (2000) by EWMA charts for monitoring the process standard deviation, including one proposed by Crowder and Hamilton (1992). A signal is produced as soon as any one of the three EWMA charts for the Y -intercept, the slope, and the variation about the regression line produces an out-of-control signal.

The EWMA chart statistics for monitoring the Y -intercept B_0 used by Kim et al. (2003) are

$$EWMA_{I(j)} = \theta b_{0j} + (1 - \theta)EWMA_{I(j-1)}, \quad (2.26)$$

where $0 < \theta \leq 1$ is a smoothing constant and $EWMA_{I(0)} = B_0$. An out-of-control signal is given by this chart as soon as the $EWMA_I$ statistic crosses the control limits

$$LCL = B_0 - L_I \sigma \sqrt{\theta / n(2 - \theta)} \quad \text{and} \quad UCL = B_0 + L_I \sigma \sqrt{\theta / n(2 - \theta)}, \quad (2.27)$$

where $L_I > 0$ is a constant selected to produce a specified in-control ARL . The EWMA statistics for monitoring the slope B_1 are given by

$$EWMA_{S(j)} = \theta b_{1j} + (1 - \theta)EWMA_{S(j-1)}, \quad (2.28)$$

where $0 < \theta \leq 1$ is again a smoothing constant and $EWMA_{S(0)} = B_1$. The control limits for the slope chart are given by

$$LCL = B_1 - L_S \sigma \sqrt{\theta/n(2-\theta)} \quad \text{and} \quad UCL = B_1 + L_S \sigma \sqrt{\theta/n(2-\theta)}, \quad (2.29)$$

where $L_S > 0$ is a constant chosen to produce a specified in-control ARL . Finally, to monitor the process variance, Kim et al. (2003) proposed an EWMA chart based on the approach of Crowder and Hamilton (1992). The EWMA statistics for monitoring σ^2 are

$$EWMA_{E(j)} = \max \{ \theta (\ln MSE_j) + (1 - \theta)EWMA_{E(j-1)}, \ln \sigma_0^2 \}, \quad (2.30)$$

where $0 < \theta \leq 1$ is again a smoothing constant and $EWMA_{E(0)} = \ln \sigma_0^2$. Here σ_0^2 is the in-control value of the process variance σ^2 . The control limit for detecting increases in the process variance used by Kim et al. (2003) is

$$UCL = \ln \sigma_0^2 + L_E [\theta \text{Var} (\ln MSE_j) / (2 - \theta)]^{1/2}, \quad (2.31)$$

where the multiplier $L_E > 0$ is chosen to produce a specified in-control ARL and

$$\text{Var} (\ln MSE_j) \approx \frac{2}{n-2} + \frac{2}{(n-2)^2} + \frac{4}{3(n-2)^3} - \frac{16}{15(n-2)^5}. \quad (2.32)$$

Kim et al. (2003) compared their proposed EWMA charts method to the methods of Kang and Albin (2000) through simulation. They found that their proposed method is more effective than the competing methods in detecting sustained shifts in a process parameter. It is clear that their method also provides easier interpretation of an out-of-control signal than the Kang and Albin's (2000) methods, since each parameter in the model is monitored using a separate chart using their proposed approach.

2.C Model Assumptions

The normality assumption for the models in Equations (2.1) and (2.20) is required for determining the statistical performance of any of the Phase I and Phase II proposed methods. For example, the simulation study reported in Chapter 3 shows that departures from this assumption can affect the statistical performance of all of the Phase I methods. In particular, the false alarm rate can increase dramatically. Thus, it is necessary to test for the appropriateness of the normality assumption before applying a Phase I or Phase II method. There are many statistical methods for checking the normality of the error terms, as described in Neter et al. (1990, chap. 4) and Ryan (1997, pp. 52-53).

Also, departures from linearity affect the performance of the proposed methods. In particular, the control chart for the variance may signal instability in the process variance due to a lack-of-fit affecting the regression model. Therefore, it is imperative to check for the linearity of the m regression lines before applying a Phase I or Phase II method. Neter et al. (1990, p. 131), for example, described a lack-of-fit test appropriate for the case when there are replications at one or more X -levels. Also, see Burn and Ryan (1983) for a lack-of-fit test suitable for the case when no replications are available.

Chapter 3: Performance Comparisons for Some Phase I Approaches

This chapter presents simulation results that compare the performance of some of the recommended Phase I approaches in terms of the overall probabilities of a signal. Also this chapter illustrates the use of these methods using a real data set from a calibration application presented in Mestek et al. (1994).

3.A Performance Comparisons

As mentioned in Chapter 1, there have been several sets of recommendations for the Phase I analysis of linear profile data sets. However, no performance comparisons study has been conducted to determine the most appropriate and effective approaches. In this chapter I use simulation to investigate the performance of four control chart methods for monitoring linear profile processes in Phase I in terms of the overall probability of a signal. These methods are Method A: the T^2 control chart proposed by Stover and Brill (1998), Method B: the T^2 control chart proposed by Kang and Albin (2000), Method C: the three Shewhart-type control charts proposed by Kim et al. (2003), and Method D: the proposed method of using the global F -test based on the statistic in Equation (2.19) in conjunction with the control chart with control limits in Equation (2.15) for monitoring the error term variance.

In this simulation the underlying in-control model with $A_0=0$ and $A_1=1$ was considered, i.e., $Y_{ij} = X_i + \varepsilon_{ij}$, $i = 1, 2, \dots, n$, where the ε_{ij} 's are i.i.d. $N(0, 1)$ random variables. The fixed X -values of 0(0.2)1.8 were used in this simulation ($n=10$, $\bar{X}=0.9$, and $S_{XX} = 3.3$). Also, the numbers of samples $m=5, 20, 40$, and 60 were used in this simulation. For one case considered in these simulations the fixed X -values were used twice to give a linear profile model with $n=20$, and in another case they were used three times to give a linear profile model with $n=30$. Also, in some cases considered in these simulations different sets of the fixed X -values were used.

3.A.1 Estimation of False Alarm Probabilities

First, the control limit (limits) for each method was (were) set based on a nominal false alarm probability of $\alpha_1 = 1 - \sqrt[m]{1 - \alpha}$ to give a nominal overall false alarm probability of $\alpha = 0.01, 0.015, 0.02, 0.025, 0.03, 0.035, 0.04, 0.045, 0.05, \text{ or } 0.1$. Equations (2.8) and (2.10) were used to determine the *UCL* based on a nominal false alarm probability of α_1 for Method A and Method B, respectively. For Method C, Equations (2.12), (2.13), and (2.15) were used to determine the control limits of the three Shewhart control charts for the *Y*-intercept, slope, and error term variance, respectively. The control limits for each chart were set based on a false alarm probability of $\alpha_2 = 1 - \sqrt[3]{1 - \alpha_1}$. For Method D, the global *F*-test was performed at a significance level of $\alpha_3 = 1 - \sqrt{1 - \alpha}$ and the control limits for the chart for monitoring the error term variance were set based on a false alarm probability of $\alpha_4 = 1 - \sqrt[m]{1 - \alpha_3}$.

Tables 3.1-3.4 give the overall false alarm probabilities when $m=5, 20, 40,$ and $60,$ respectively. For these tables, the sample size $n=10$ was used. The first columns of these tables give the desired nominal overall false alarm probabilities. The following four columns in each table give the simulated overall false alarm probabilities when applying Methods A, B, C, and D, respectively. Each of these estimates was obtained independently from 1,000,000 Phase I simulations. As shown in Tables 3.1-3.4, there is no practical difference between the simulated and nominal overall false alarm probabilities for all values of m considered in these simulations.

Tables 3.5-3.6 give the overall false alarm probabilities when $n=20$ and $30,$ respectively. The number of samples $m=20$ was used to obtain these tables. Again, as shown in both tables, there is no practical difference between the simulated and nominal overall false alarm probabilities.

For Tables 3.7-3.8, different sets of the fixed X -values from that considered for Tables 3.1-3.6 were used to simulate the overall false alarm probabilities. The fixed X -values of $-30, -23, -12, -4, 0, 3, 10, 20, 25,$ and 35 were used to estimate the overall false alarm probabilities in Table 3.7, while the fixed X -values of $-600, -450, -380, -260, -100, 0, 90, 210, 400,$ and 500 were used to estimate those in Table 3.8. Unlike the X -values used to estimate the overall false alarm probabilities in Tables 3.1-3.6, the X -values used in these two sets are unequally spaced. Again, there is no practical difference between the simulated and nominal overall false alarm probabilities when both sets were used as shown in Tables 3.7-3.8.

Table 3.1: Overall false alarm probabilities: Nominal vs. Simulated ($m=5, n=10$).

Nominal	Simulated			
	Method A	Method B	Method C	Method D
0.010	0.0098	0.0096	0.0097	0.0097
0.015	0.0150	0.0144	0.0146	0.0148
0.020	0.0200	0.0192	0.0195	0.0197
0.025	0.0252	0.0241	0.0244	0.0251
0.030	0.0300	0.0286	0.0295	0.0299
0.035	0.0350	0.0332	0.0341	0.0351
0.040	0.0406	0.0372	0.0383	0.0398
0.045	0.0453	0.0424	0.0434	0.0443
0.050	0.0502	0.0466	0.0477	0.0493
0.100	0.1013	0.0920	0.0951	0.0992

Table 3.2: Overall false alarm probabilities: Nominal vs. Simulated ($m=20, n=10$).

Nominal	Simulated			
	Method A	Method B	Method C	Method D
0.010	0.0099	0.0098	0.0099	0.0100
0.015	0.0150	0.0149	0.0150	0.0151
0.020	0.0201	0.0200	0.0200	0.0201
0.025	0.0251	0.0244	0.0248	0.0249
0.030	0.0304	0.0297	0.0299	0.0299
0.035	0.0353	0.0347	0.0348	0.0349
0.040	0.0402	0.0395	0.0401	0.0400
0.045	0.0457	0.0447	0.0451	0.0451
0.050	0.0507	0.0496	0.0500	0.0500
0.100	0.1030	0.0975	0.0986	0.0989

Table 3.3: Overall false alarm probabilities: Nominal vs. Simulated ($m=40, n=10$).

Nominal	Simulated			
	Method A	Method B	Method C	Method D
0.010	0.0097	0.0101	0.0099	0.0099
0.015	0.0144	0.0147	0.0143	0.0144
0.020	0.0210	0.0199	0.0203	0.0202
0.025	0.0248	0.0257	0.0261	0.0253
0.030	0.0300	0.0298	0.0299	0.0299
0.035	0.0342	0.0350	0.0343	0.0348
0.040	0.0407	0.0396	0.0404	0.0401
0.045	0.0458	0.0461	0.0460	0.0457
0.050	0.0521	0.0498	0.0503	0.0501
0.100	0.1024	0.0986	0.0992	0.0998

Table 3.4: Overall false alarm probabilities: Nominal vs. Simulated ($m=60, n=10$).

Nominal	Simulated			
	Method A	Method B	Method C	Method D
0.010	0.0100	0.0097	0.0099	0.0100
0.015	0.0145	0.0150	0.0149	0.0150
0.020	0.0197	0.0192	0.0192	0.0195
0.025	0.0257	0.0254	0.0252	0.0251
0.030	0.0305	0.0301	0.0301	0.0300
0.035	0.0352	0.0344	0.0349	0.0349
0.040	0.0401	0.0398	0.0399	0.0399
0.045	0.0450	0.0447	0.0455	0.0452
0.050	0.0512	0.0507	0.0504	0.0502
0.100	0.1040	0.0984	0.0983	0.0992

Table 3.5: Overall false alarm probabilities: Nominal vs. Simulated ($m=20, n=20$).

Nominal	Simulated			
	Method A	Method B	Method C	Method D
0.010	0.0101	0.0103	0.0106	0.0101
0.015	0.0149	0.0141	0.0149	0.0149
0.020	0.0196	0.0189	0.0195	0.0197
0.025	0.0258	0.0250	0.0250	0.0250
0.030	0.0304	0.0288	0.0301	0.0300
0.035	0.0347	0.0341	0.0342	0.0346
0.040	0.0410	0.0395	0.0399	0.0398
0.045	0.0468	0.0453	0.0458	0.0452
0.050	0.0517	0.0497	0.0497	0.0498
0.100	0.1016	0.0993	0.0990	0.0997

Table 3.6: Overall false alarm probabilities: Nominal vs. Simulated ($m=20, n=30$).

Nominal	Simulated			
	Method A	Method B	Method C	Method D
0.010	0.0101	0.0093	0.0101	0.0100
0.015	0.0154	0.0152	0.0152	0.0151
0.020	0.0201	0.0199	0.0196	0.0198
0.025	0.0258	0.0254	0.0246	0.0248
0.030	0.0295	0.0287	0.0297	0.0299
0.035	0.0357	0.0342	0.0343	0.0344
0.040	0.0401	0.0389	0.0395	0.0397
0.045	0.0460	0.0453	0.0456	0.0455
0.050	0.0504	0.0491	0.0491	0.0496
0.100	0.1050	0.1000	0.0997	0.0998

Table 3.7: Overall false alarm probabilities: Nominal vs. Simulated ($m=20$ and $X= -30, -23, -12, -4, 0, 3, 10, 20, 25,$ and 35).

Nominal	Simulated			
	Method A	Method B	Method C	Method D
0.010	0.0100	0.0095	0.0098	0.0100
0.015	0.0154	0.0149	0.0146	0.0149
0.020	0.0209	0.0204	0.0194	0.0197
0.025	0.0249	0.0250	0.0254	0.0248
0.030	0.0302	0.0304	0.0308	0.0301
0.035	0.0356	0.0349	0.0341	0.0348
0.040	0.0394	0.0399	0.0403	0.0401
0.045	0.0455	0.0447	0.0452	0.0452
0.050	0.0514	0.0495	0.0492	0.0496
0.100	0.1062	0.0989	0.0998	0.0999

Table 3.8: Overall false alarm probabilities: Nominal vs. Simulated ($m=20$ and $X=-600, -450, -380, -260, -100, 0, 90, 210, 400,$ and 500).

Nominal	Simulated			
	Method A	Method B	Method C	Method D
0.010	0.0103	0.0100	0.0102	0.0101
0.015	0.0150	0.0150	0.0143	0.0149
0.020	0.0197	0.0191	0.0200	0.0201
0.025	0.0252	0.0250	0.0250	0.0251
0.030	0.0316	0.0304	0.0303	0.0301
0.035	0.0343	0.0345	0.0354	0.0352
0.040	0.0427	0.0390	0.0406	0.0407
0.045	0.0456	0.0438	0.0443	0.0445
0.050	0.0511	0.0498	0.0510	0.0502
0.100	0.1037	0.0983	0.1005	0.1001

In general, for all the cases considered in these simulations there was no practical difference between the simulated and nominal overall false alarm probabilities. Therefore, the dependencies of the control chart statistics for the methods have no practical effect on one's use of the marginal distribution (distributions) to approximate closely the overall false alarm probabilities.

3.A.2 Estimation of Out-of-Control Probabilities of Signal

This section compares the performance of the competing methods in terms of the overall probabilities of an out-of-control signal indicating instability when there were shifts in model parameters. The fixed X -values of $0(0.2)1.8$ were first considered in linear profile data sets with number of samples $m=20$ or 60 . The types of shifts considered in this simulation are fixed shifts in k out of the m individual model parameters, where $k=1,$

2, 5, or 10 if $m=20$ and $k=1, 3, 15,$ or 20 if $m=60$. The locations of the shifts do not affect the performance of the methods.

Four different types of shifts were considered in the model parameters. These corresponded to shifts in the Y -intercept, in the slope under the model in Equation (2.1), in the slope under the model in Equation (2.11), and in the process standard deviation. Shifts in the intercept are measured in units of σ/\sqrt{n} , shifts in the slopes are measured in units of $\sigma/\sqrt{S_{XX}}$, and shifts in the process standard deviation are measured as multiples of σ .

In some performance comparisons considered in these simulations with $m=20$, the fixed X -values were used twice to give a linear profile model with $n=20$. Also, in some performance comparisons considered in these simulations with $m=20$, the fixed X -values of $-30, -23, -12, -4, 0, 3, 10, 20, 25,$ and 35 were used.

For Methods A and B, if $m=20$ and $n=10$, the upper control limits were set based on a false alarm probability of $\alpha_1=0.002039$ to produce a nominal overall false alarm probability of $\alpha=0.04$. Thus, in this case, for Method A we have $UCL=9.34182$ and for Method B we have $UCL=12.8830$. For Method C, the control limits of each control chart were set based on a false alarm probability of $\alpha_2=0.00068$, so that the overall false alarm probability produced by this method was $\alpha=0.04$. The critical value corresponding to the 99.966th percentile of the t -distribution required to compute the control limits in Equations (2.12) and (2.13) is 3.465. Also, the control limits in Equation (2.15) for monitoring the error term variance were $LCL=0.07871$ and $UCL=3.8853$. For Method D, the control limits for the chart for monitoring the error term variance were $LCL=0.08776$ and $UCL=3.73678$. These limits were determined based on a false alarm probability of $\alpha_4=0.00102$. The global F -test was performed at a significance level of $\alpha_3=0.0202041$. The 99.898th percentile of the F -distribution used to test the equality of all the regression lines is 1.6281492. Thus, the overall false alarm probability corresponding to Method D was also $\alpha=0.04$. Table 3.9 shows the different false alarm probabilities, percentiles,

and control limits used for each Phase I method for the different cases considered in the performance comparisons.

Table 3.9: False alarm probabilities, percentiles, and control limits used for the different cases considered in the performance comparisons.

	$(m=20, n=10)$	$(m=20, n=20)$	$(m=60, n=10)$
False alarm probabilities	$\alpha = 0.04$ $\alpha_1 = 0.002039$ $\alpha_2 = 0.00068$ $\alpha_3 = 0.0202041$ $\alpha_4 = 0.00102$	$\alpha = 0.04$ $\alpha_1 = 0.002039$ $\alpha_2 = 0.00068$ $\alpha_3 = 0.0202041$ $\alpha_4 = 0.00102$	$\alpha = 0.04$ $\alpha_1 = 0.00068$ $\alpha_2 = 0.000227$ $\alpha_3 = 0.0202041$ $\alpha_4 = 0.0003401$
<i>UCL</i> for Method A	9.341597	9.341597	13.099147
<i>UCL</i> for Method B	12.88297	12.606272	14.810329
Percentile of the <i>t</i> -distribution required for Method C	3.4652442	3.4272914	3.715389
Control limits for the variance using Method C	<i>LCL</i> =0.0787074 <i>UCL</i> =3.885273	<i>LCL</i> =0.2296672 <i>UCL</i> =2.6444826	<i>LCL</i> =0.0595421 <i>UCL</i> =4.048459
Percentile of the <i>F</i> -distribution required for Method D	1.6281492	1.5705054	1.3307411
Control limits for the variance using Method D	<i>LCL</i> =0.0877562 <i>UCL</i> =3.736782	<i>LCL</i> =0.2432506 <i>UCL</i> =2.5691832	<i>LCL</i> =0.0662504 <i>UCL</i> =3.9172931

Figure 3.1-3.4 show the simulated overall probabilities of an out-of-control signal for shifts in the regression parameters when $m=20$ and $X=0(0.2)1.8$. The overall probabilities of out-of-control signals for shifts in the Y -intercept from A_0 to $A_0 + \lambda \sigma / \sqrt{n}$ are shown in Figure 3.1. These estimates were obtained from 100,000 simulations for $\lambda = 0.5(0.5) 5$. As shown in Figure 3.1, the F -test method, Method D, is much better than the competing methods for detecting shifts in the Y -intercept when $k=5$ and $k=10$. However, both Methods B and C give better results for $k=1$ and $k=2$. Note that Method B performs uniformly slightly better than Method C over the entire range considered for Y -intercept shifts. For $k=1$, Method D has the worst performance.

Another important observation from Figure 3.1 is that Method A is insensitive to shifts in the Y -intercept. Except for $k=1$ and $k=2$, the probability of an out-of-control signal produced by this method slightly decreases with increases in λ . Overall, Method A performs very poorly. Similar results were obtained in other simulation studies conducted by Sullivan and Woodall (1996a) and Vargas (2003). They found that the T^2 control chart for individual multivariate observations when estimating the population covariance matrix with the usual pooled sample covariance matrix is not effective in detecting a sustained shift in the mean vector. They also mentioned that in some cases the probability of an out-of-control signal produced by this method decreases with increasingly severe shifts, as seen in the current simulation. They stated that the reason for these results is that the population covariance matrix is poorly estimated by the pooled sample covariance matrix when the mean vector is not stable.

Figure 3.2 shows the simulated overall probabilities of an out-of-control signal for different shifts in the slope under the model in Equation (2.1) from A_1 to $A_1 + \beta \sigma / \sqrt{S_{xx}}$. The same values for β as those considered for λ were used in this simulation. For this type of shift, Method D performs uniformly better than the competing methods for $k= 10$ and $k = 5$, while both Methods B and C give better results for $k = 2$ and $k = 1$. Also in this case Method B performs uniformly better than Method C over the entire range considered for slope shifts. Again, Method A has the worst

performance for all values of k considered except for $k = 1$. Method D has the worst performance when $k=1$.

Figure 3.3 shows the simulated overall probabilities of an out-of-control signal for shifts in the slope under the model in Equation (2.11) from B_1 to $B_1 + \delta \sigma / \sqrt{S_{XX}}$, for the same values for δ as those considered earlier for λ and β . This illustrates much better performance of Method D unless $k=1$ or 2. Also for this type of shift, Method B performs slightly better than Method C and Method A again has very poor performance.

Finally, Figure 3.4 presents the simulated overall probabilities of an out-of-control signal for different shifts in the process standard deviation from σ to $\gamma\sigma$, $\gamma = 1.2(0.2) 3$. As shown in Figure 3.4, Method D and Method C perform much better than Methods A and B. Method C and Method D have very similar performance for all values of k considered.

Contrary to its good performance under slope and Y -intercept shifts, Method B has the worst performance among the competing methods under process standard deviation shifts, especially for large shifts. One could modify Method B by adding a univariate control chart for monitoring the standard deviation in conjunction with the T^2 control chart based on statistics in Equation (2.9) in order to increase its sensitivity to standard deviation shifts. However, in this case its performance in detecting slope and Y -intercept shifts would diminish because of the increased control limit required to maintain the same overall probability of a false alarm. In fact, it is expected that in this case Method C might give uniformly better results. Method C has a strong advantage over Method B in terms of interpretability.

Figure 3.1: Probability of out-of-control signal under intercept shifts from A_0 to $A_0 + \lambda \sigma / \sqrt{n}$ ($m=20$ and $X=0(0.2)1.8$).

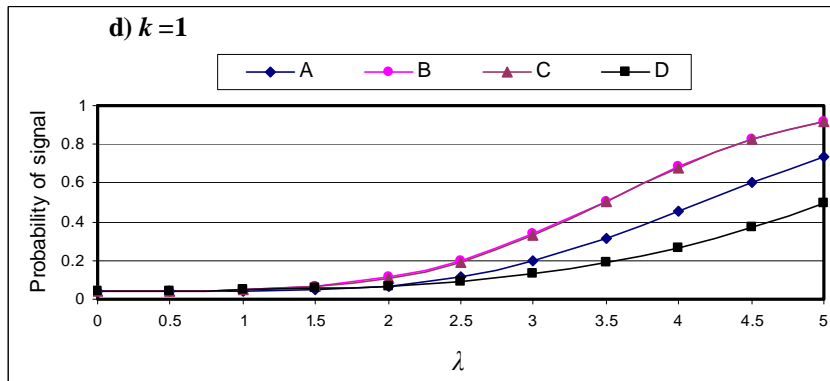
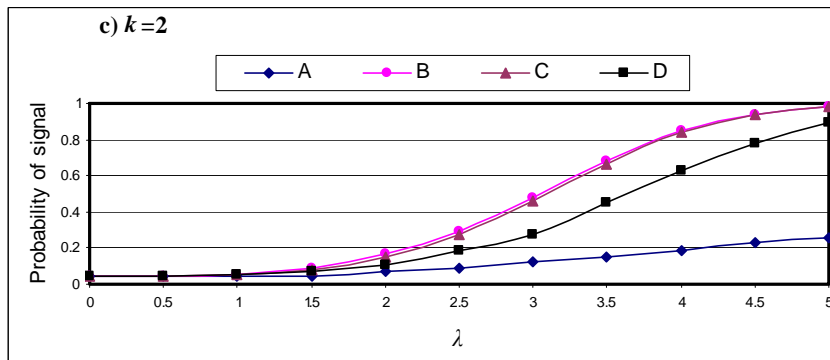
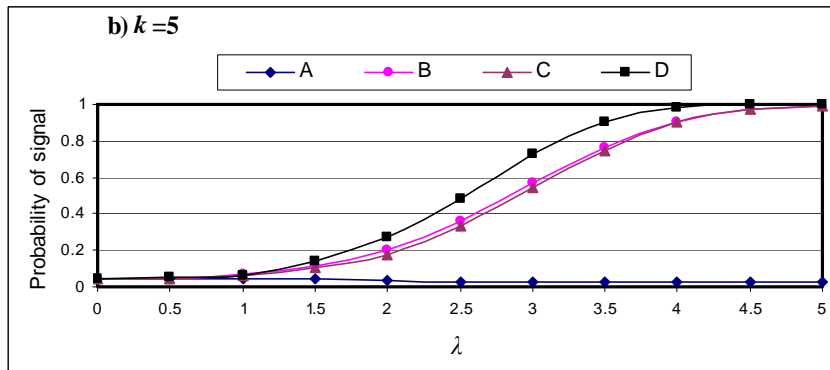
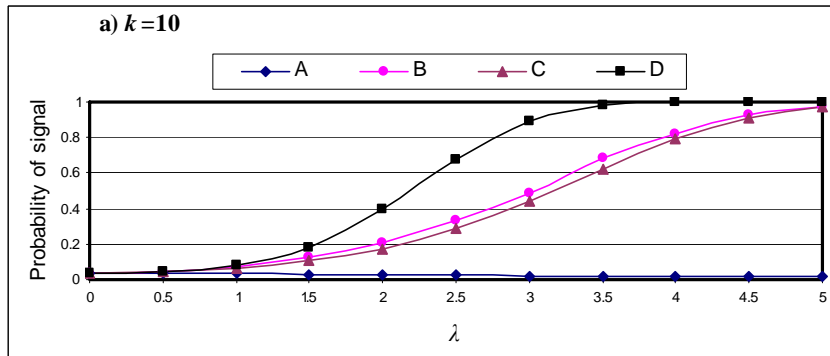


Figure 3.2: Probability of out-of-control signal under slope shifts from A_1 to $A_1 + \beta \sigma / \sqrt{S_{xx}}$ ($m=20$ and $X=0(0.2)1.8$).

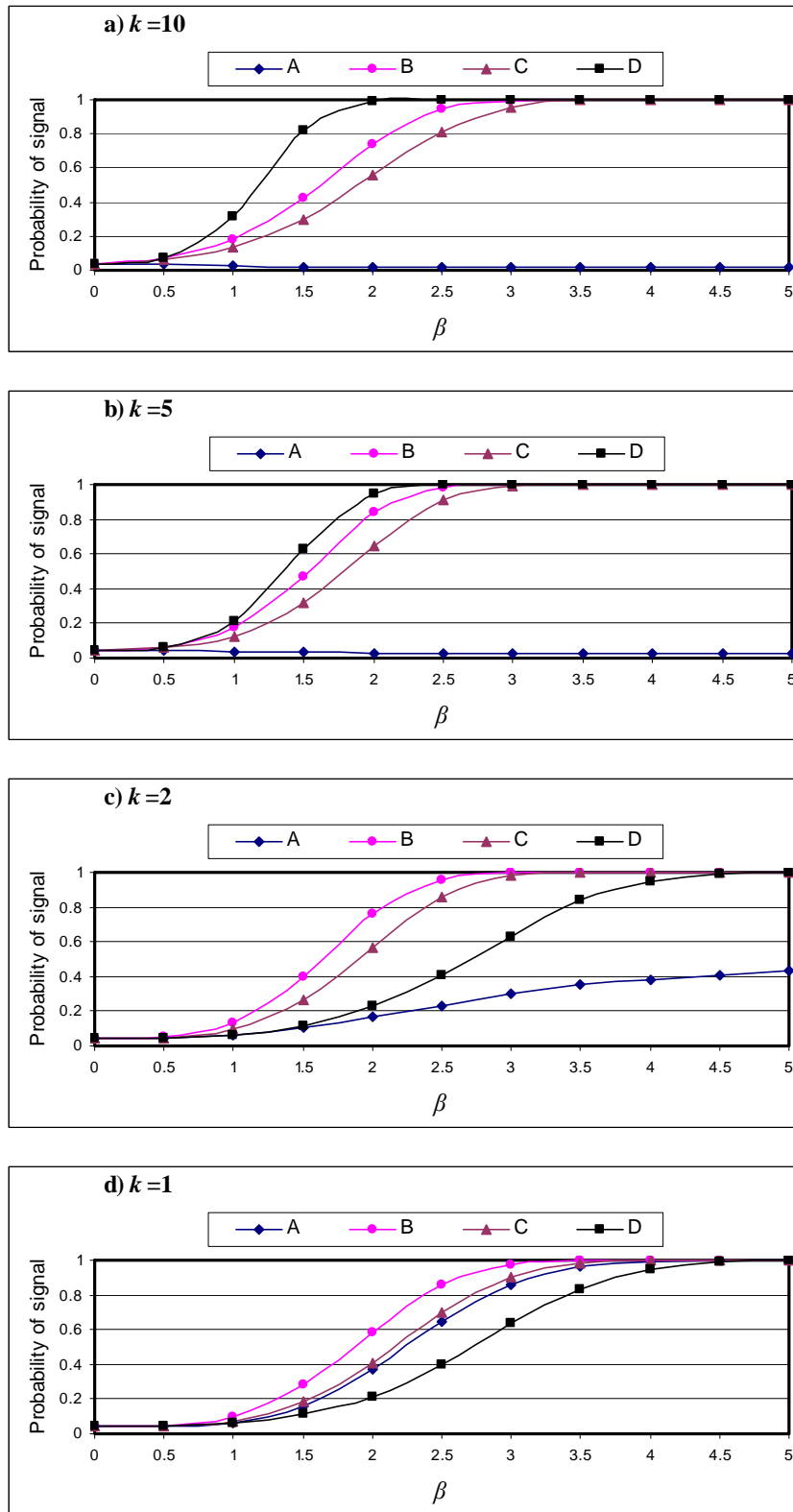


Figure 3.3: Probability of out-of-control signal under slope shifts from B_1 to $B_1 + \delta \sigma / \sqrt{S_{xx}}$ ($m=20$ and $X=0(0.2)1.8$).

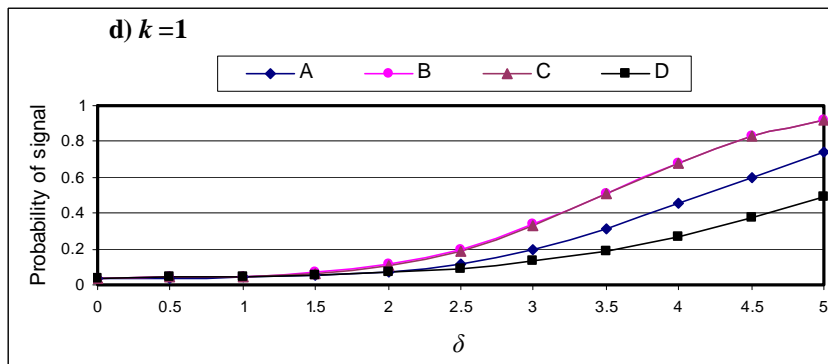
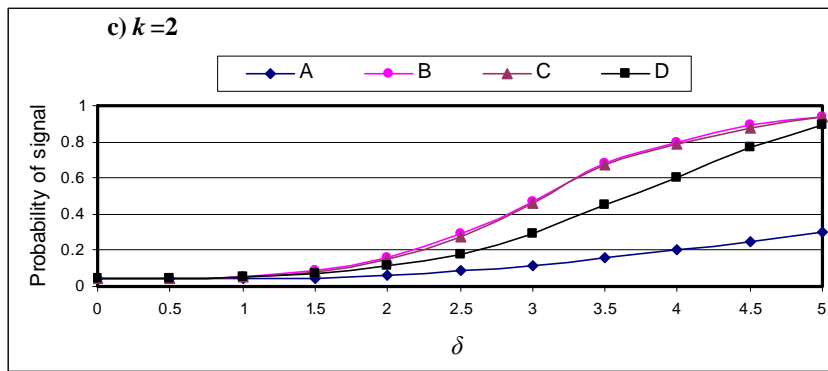
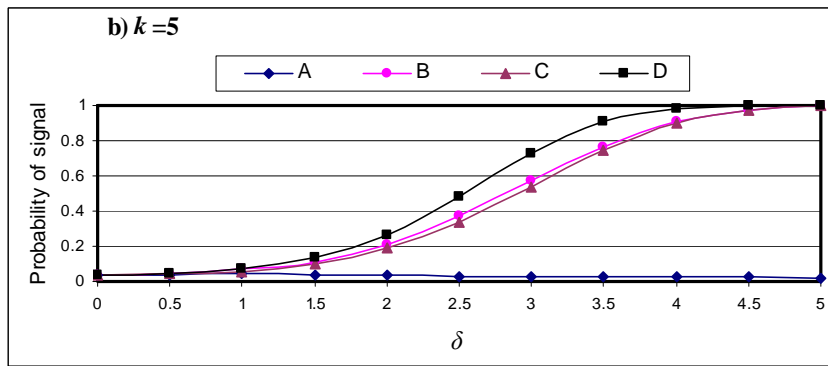
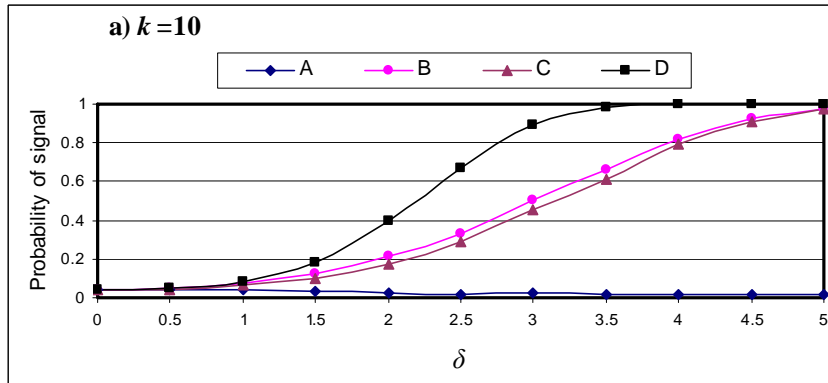
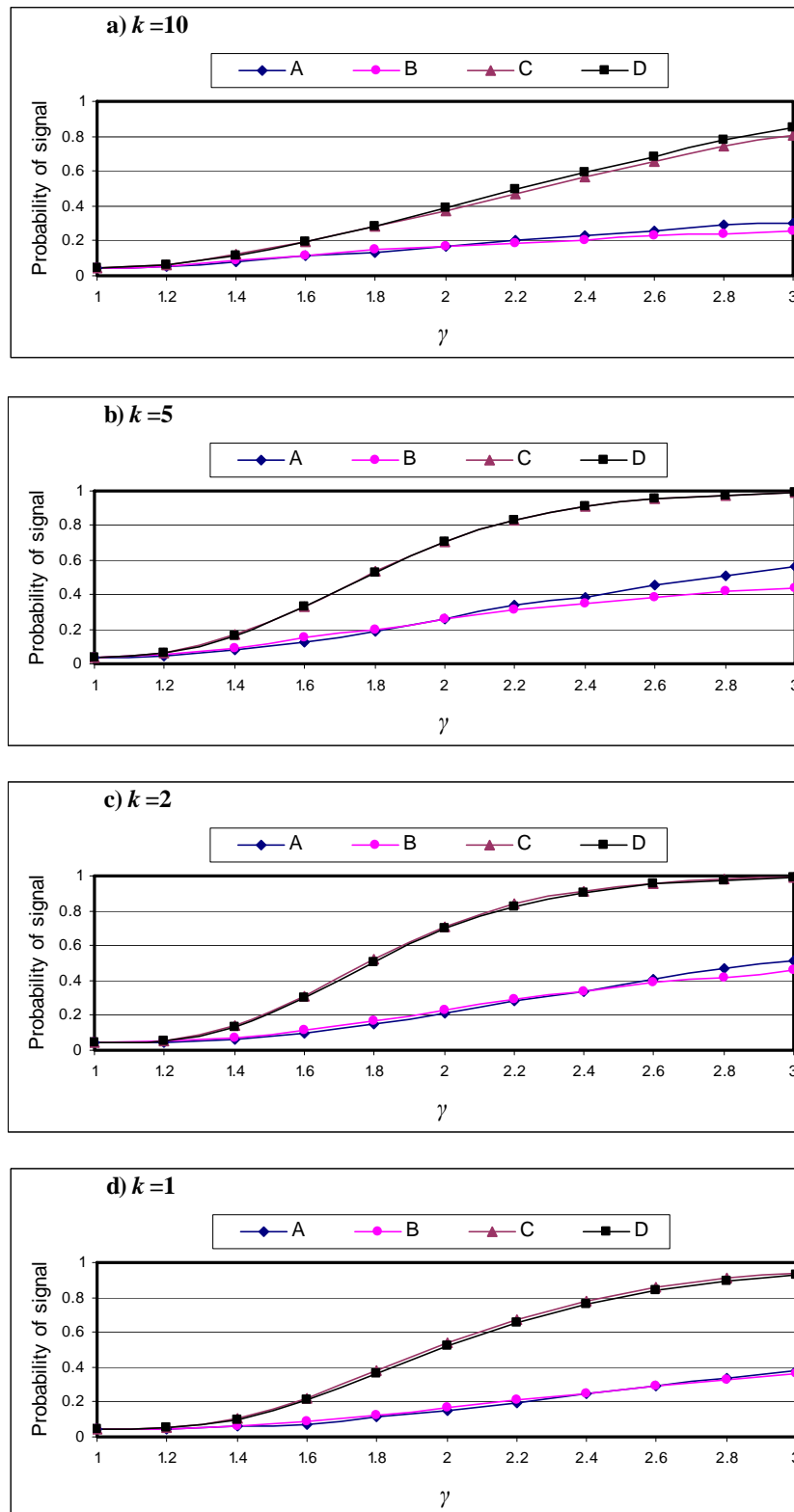


Figure 3.4: Probability of out-of-control signal under standard deviation shifts from σ to $\gamma\sigma$ ($m=20$ and $X=0(0.2)1.8$).



Figures 3.5-3.8 show the simulated overall probabilities of an out-of-control signal for shifts in the Y -intercept, slope under the model in Equation (2.1), slope under the model in Equation (2.11), and process standard deviation, respectively, when $m=60$ and $X=0(0.2)1.8$. Also, Figures 3.9-3.12 show these probabilities when $m=20$ and $X=0(0.2)1.8$ were used twice within each sample to give a linear profile model with $n=20$. Finally Figures 3.13-3.16 show these probabilities when $m=20$ and $X= -30, -23, -12, -4, 0, 3, 10, 20, 25,$ and 35 were used.

Inspection of Figures 3.5-3.16 show that the overall probability of an out-of-control signal corresponding to a specified shift in a process parameter increases as m or n increases. For all the cases considered in Figures 3.5-3.16, Method D is much better than the competing methods for detecting shifts in the Y -intercept and slope affecting much of the Phase I data. Both Methods B and C, however, give better results for shifts affecting only a few samples. For $k=1$ and $m=20$ or 60 , Method D has the worst performance. Method A has very poor performance except for $k=1$. Under process standard deviation shifts, Method B has the worst performance among the competing methods. Method C and D have the best performance in detecting standard deviation shifts.

In general, these simulation studies indicate that Method C and Method D have the best overall performance in detecting shifts in a process parameter. Under a parameter shift affecting much of the Phase I data, Method D performs uniformly better than the competing methods. Methods B and C have roughly similar performance in detecting shifts in the Y -intercept and in the slope under both models in Equations (2.1) and (2.11). However, Method C has greater statistical power in detecting shifts in the process standard deviation. Method A has very poor performance in detecting shifts in any process parameter.

Figure 3.5: Probability of out-of-control signal under intercept shifts from A_0 to $A_0 + \lambda \sigma / \sqrt{n}$ ($m=60$ and $X=0(0.2)1.8$).

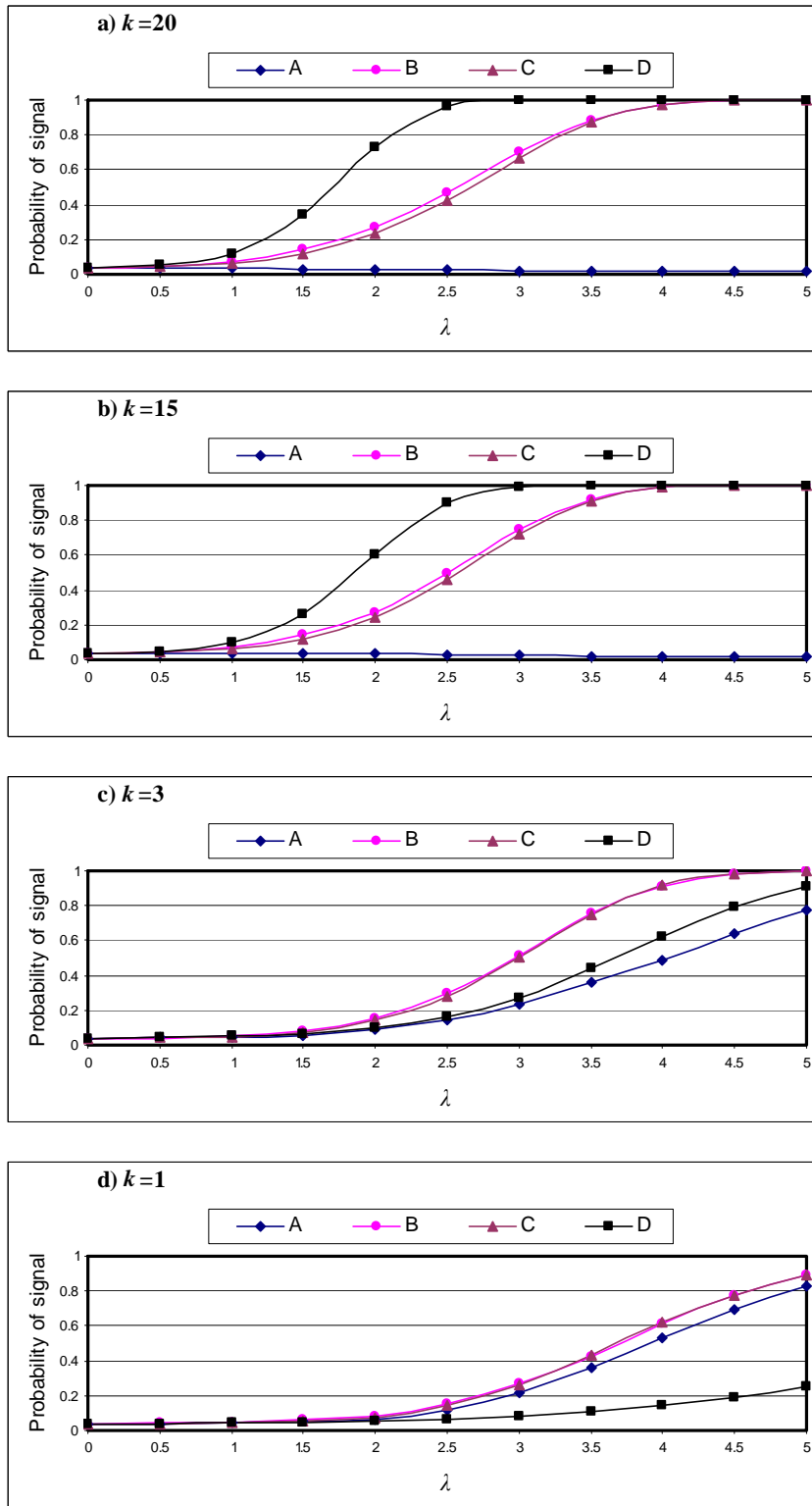


Figure 3.6: Probability of out-of-control signal under slope shifts from A_1 to $A_1 + \beta \sigma / \sqrt{S_{xx}}$ ($m=60$ and $X=0(0.2)1.8$).

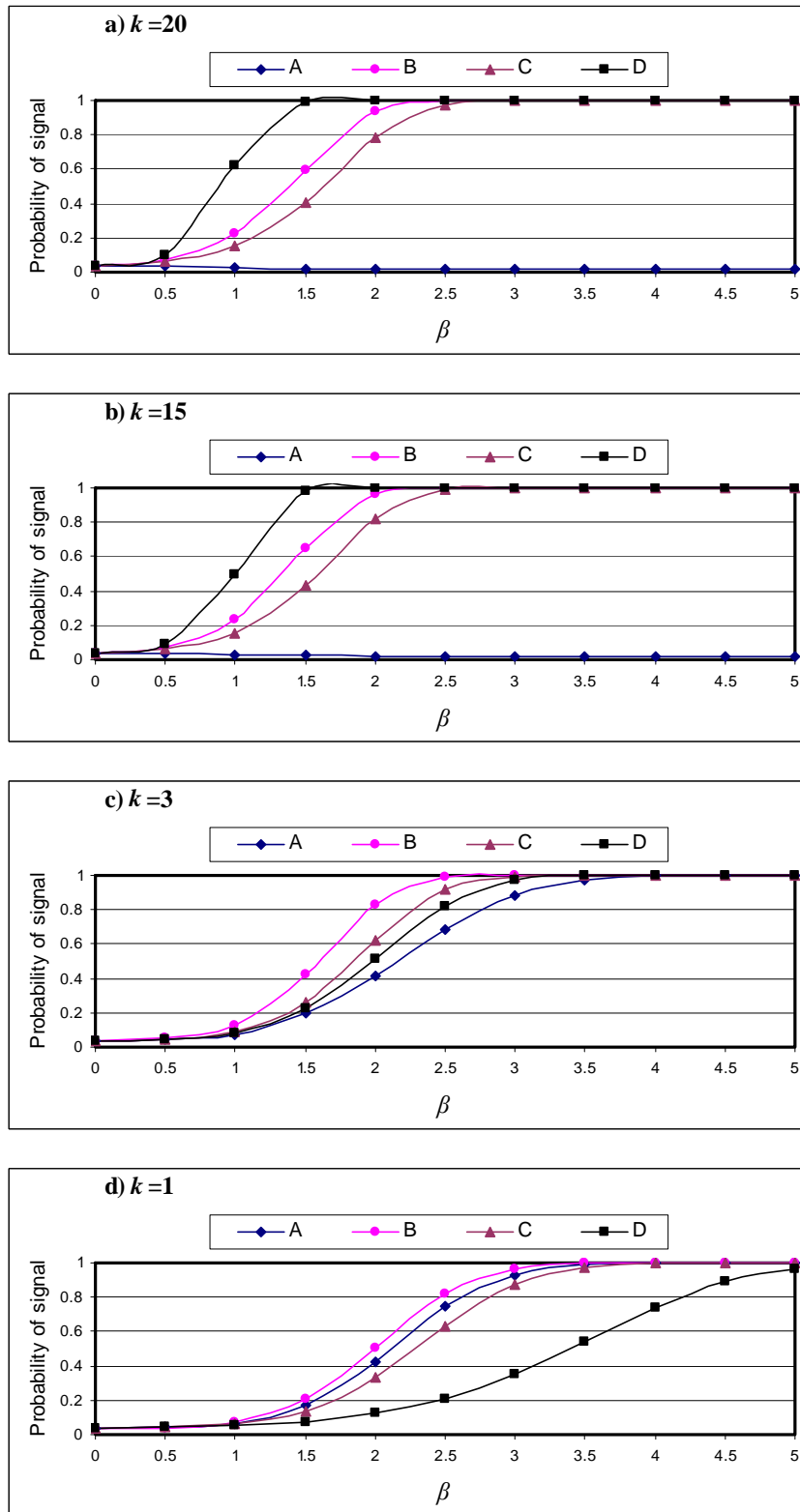


Figure 3.7: Probability of out-of-control signal under slope shifts from B_1 to $B_1 + \delta \sigma / \sqrt{S_{xx}}$ ($m=60$ and $X=0(0.2)1.8$).

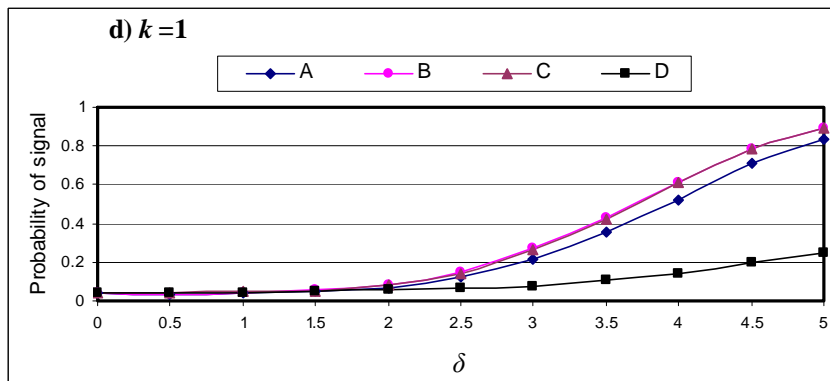
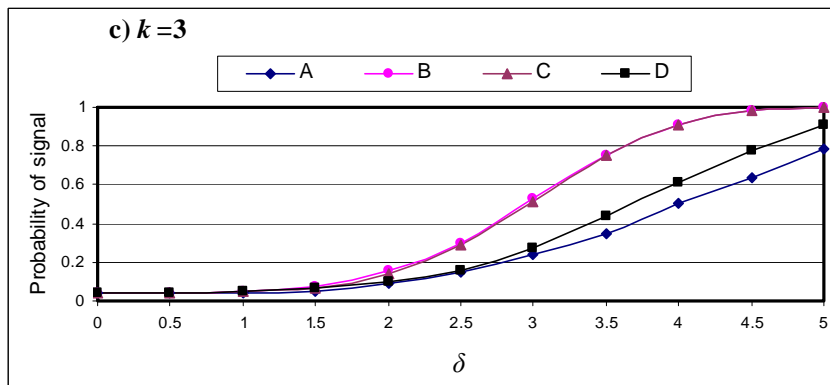
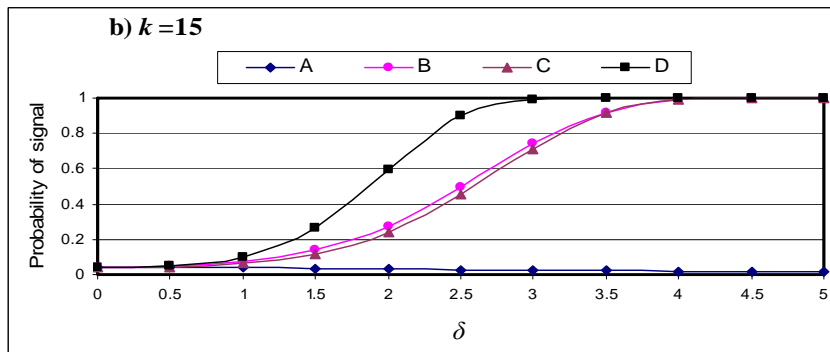
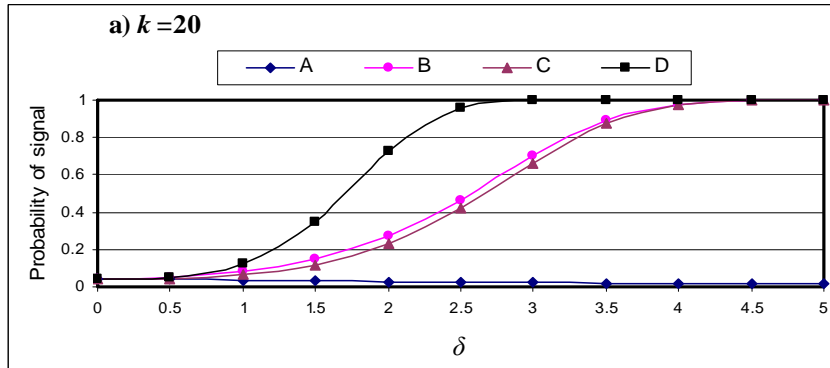


Figure 3.8: Probability of out-of-control signal under standard deviation shifts from σ to $\gamma\sigma$ ($m=60$ and $X=0(0.2)1.8$).

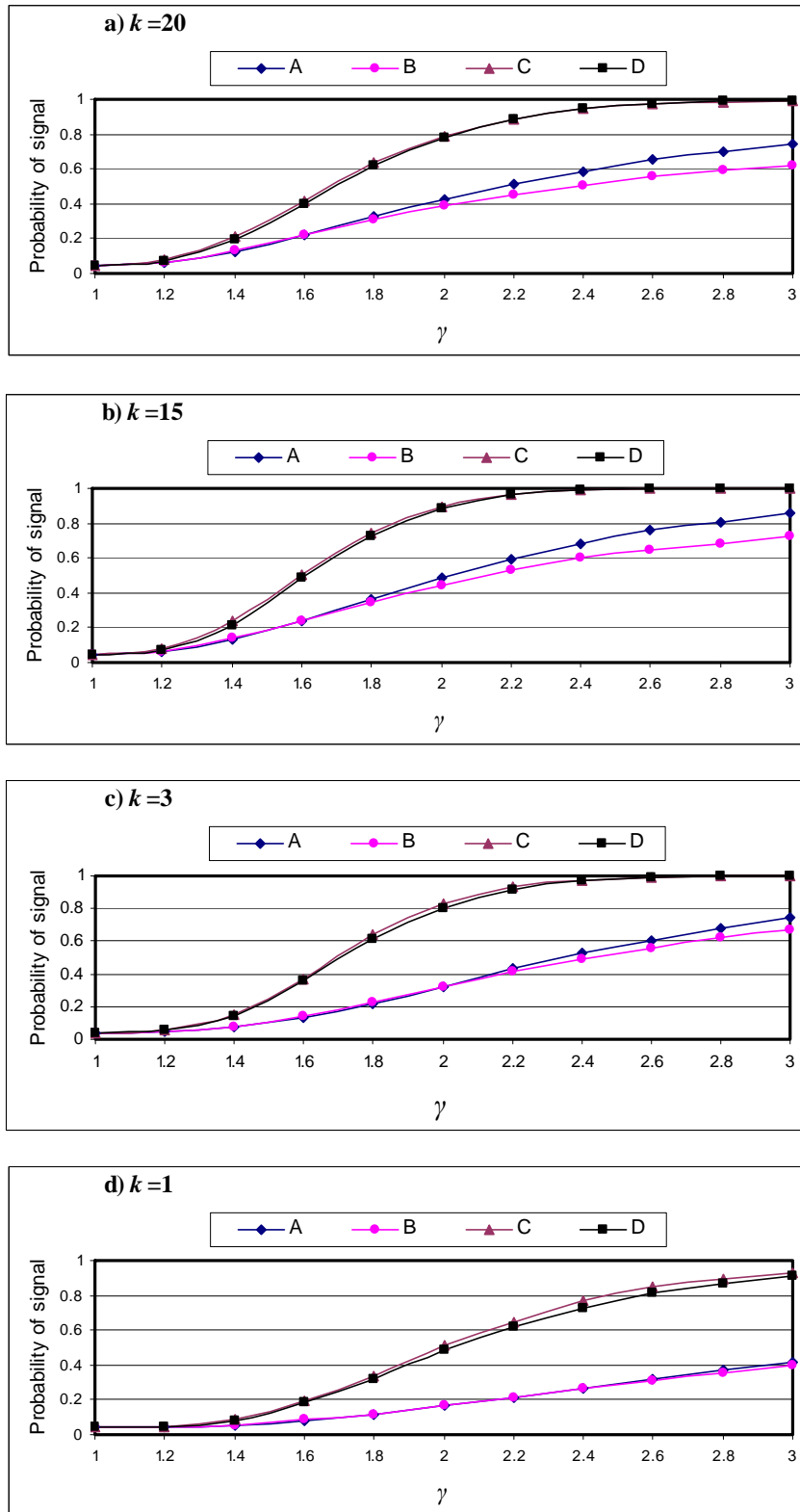


Figure 3.9: Probability of out-of-control signal under intercept shifts from A_0 to $A_0 + \lambda \sigma / \sqrt{n}$ ($m=20$ and the values of $X=0(0.2)1.8$ are used twice).

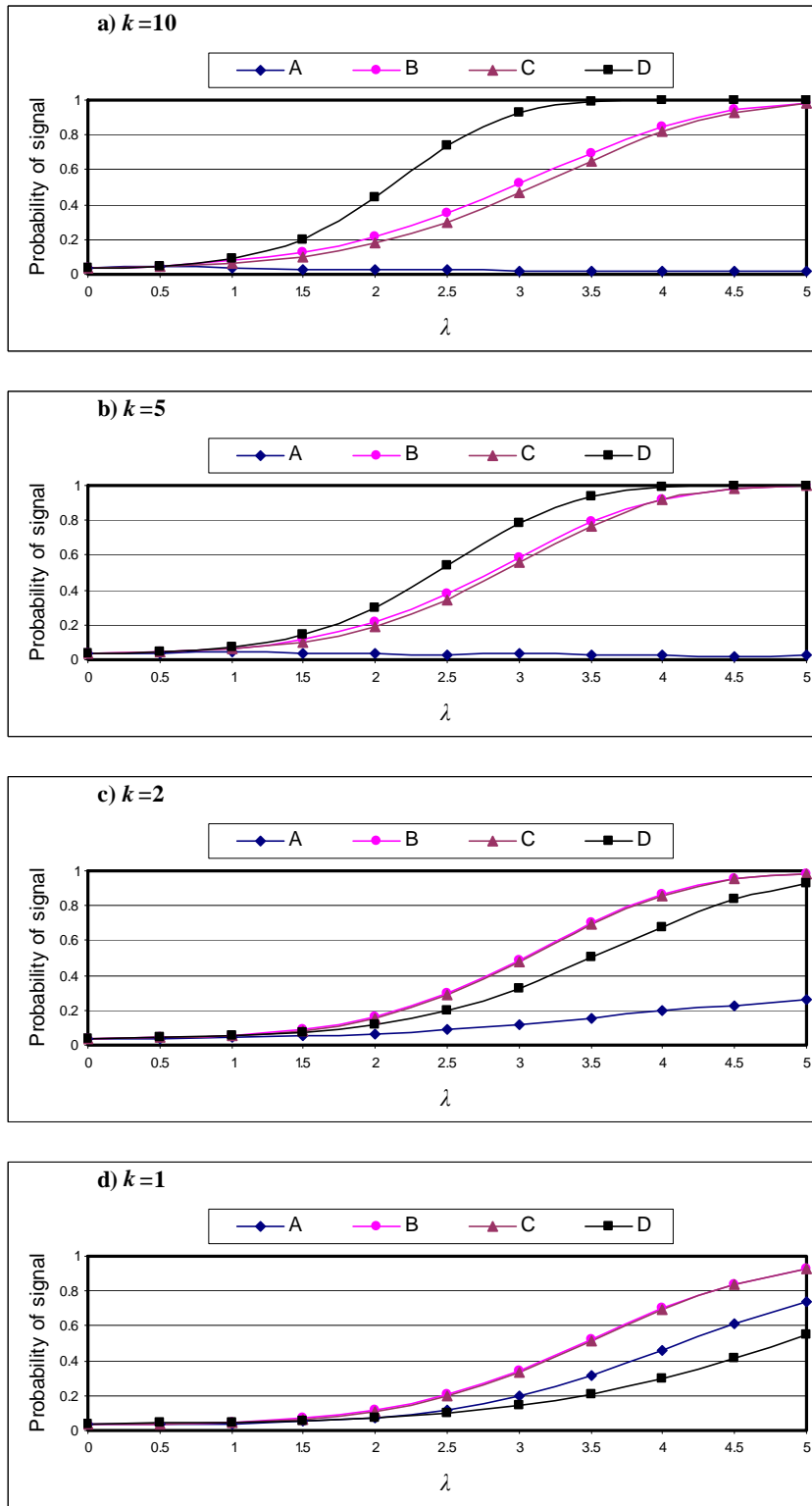


Figure 3.10: Probability of out-of-control signal under slope shifts from A_1 to $A_1 + \beta \sigma / \sqrt{S_{xx}}$ ($m=20$ and the values of $X=0(0.2)1.8$ are used twice).

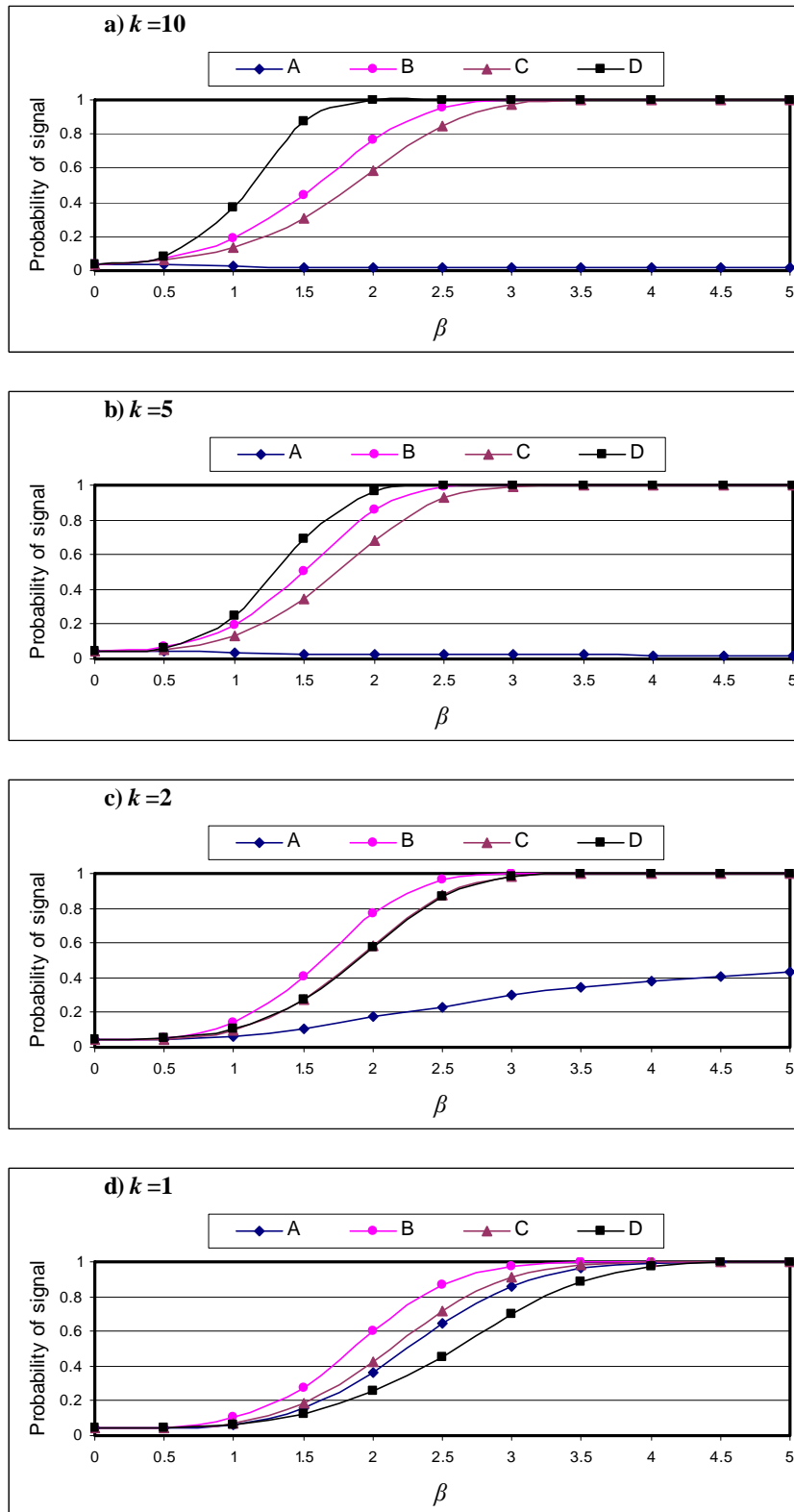


Figure 3.11: Probability of out-of-control signal under slope shifts from B_1 to $B_1 + \delta \sigma / \sqrt{S_{xx}}$ ($m=20$ and the values of $X=0(0.2)1.8$ are used twice).

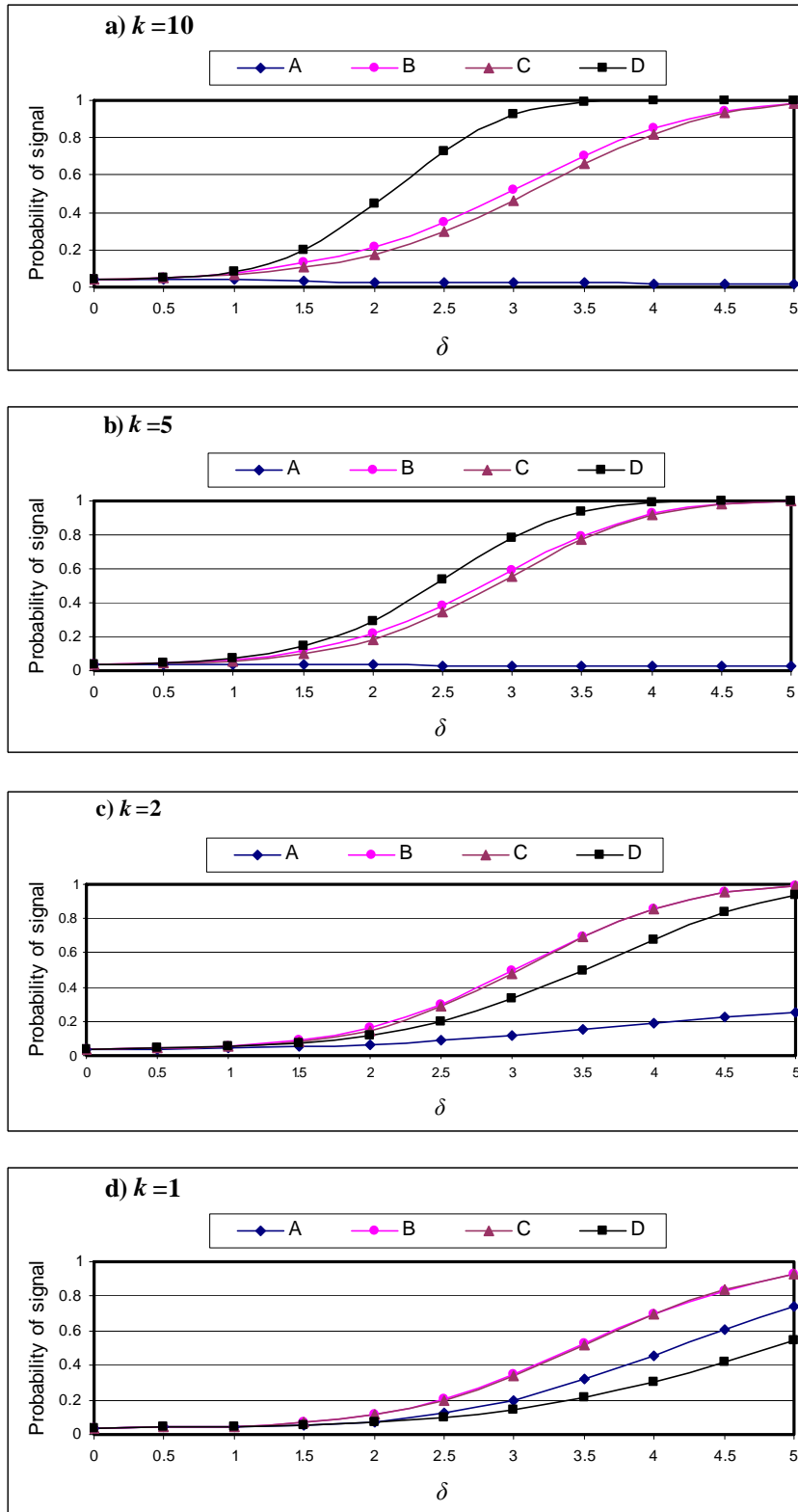


Figure 3.12: Probability of out-of-control signal under standard deviation shifts from σ to $\gamma\sigma$ ($m=20$ and the values of $X=0(0.2)1.8$ are used twice).

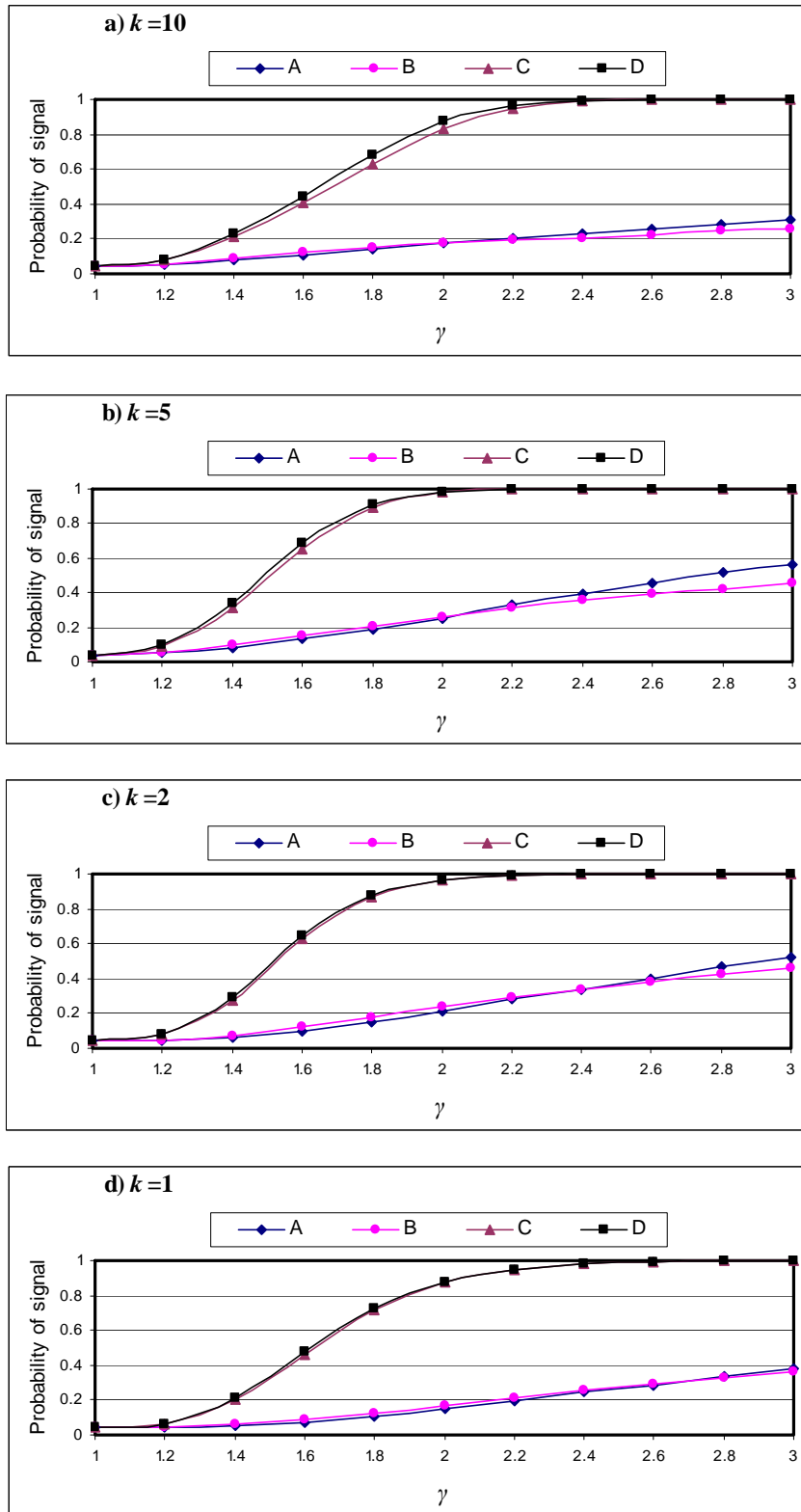


Figure 3.13: Probability of out-of-control signal under intercept shifts from A_0 to $A_0 + \lambda \sigma / \sqrt{n}$ ($m=20$ and $X = -30, -23, -12, -4, 0, 3, 10, 20, 25,$ and 35).

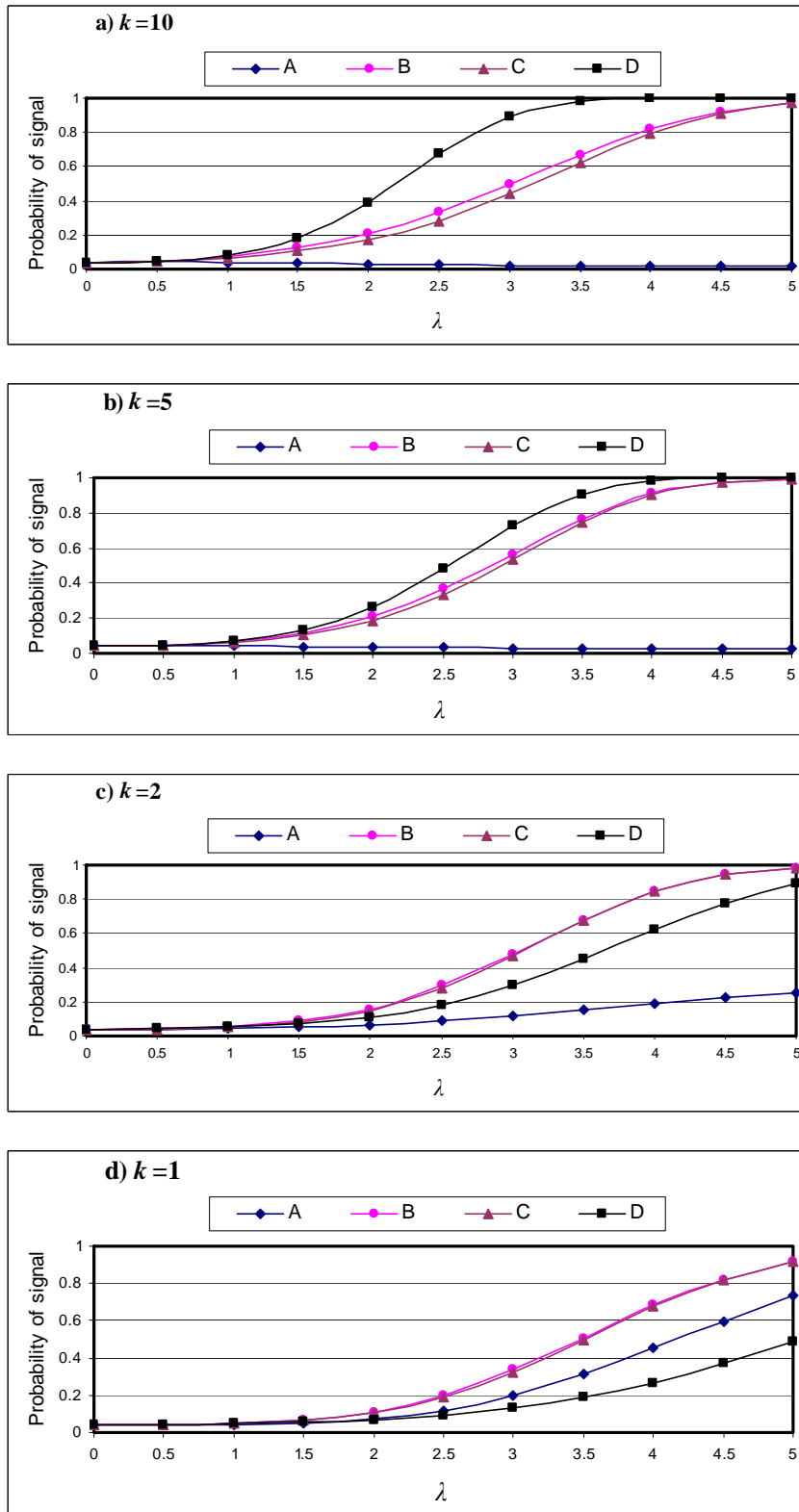


Figure 3.14: Probability of out-of-control signal under slope shifts from A_1 to $A_1 + \beta \sigma / \sqrt{S_{xx}}$ ($m=20$ and $X = -30, -23, -12, -4, 0, 3, 10, 20, 25,$ and 35).

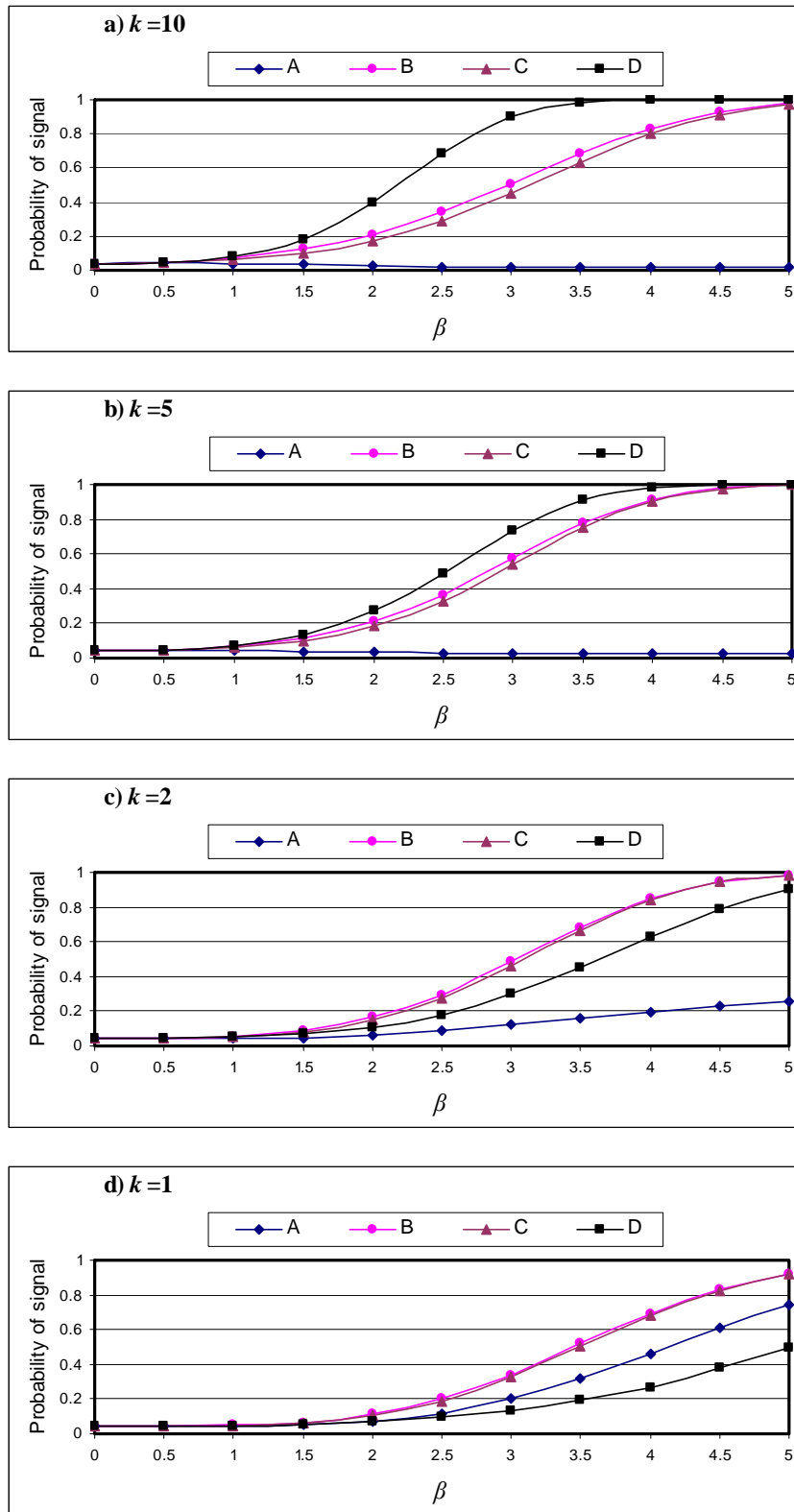


Figure 3.15: Probability of out-of-control signal under slope shifts from B_1 to $B_1 + \delta \sigma / \sqrt{S_{xx}}$ ($m=20$ and $X = -30, -23, -12, -4, 0, 3, 10, 20, 25,$ and 35).

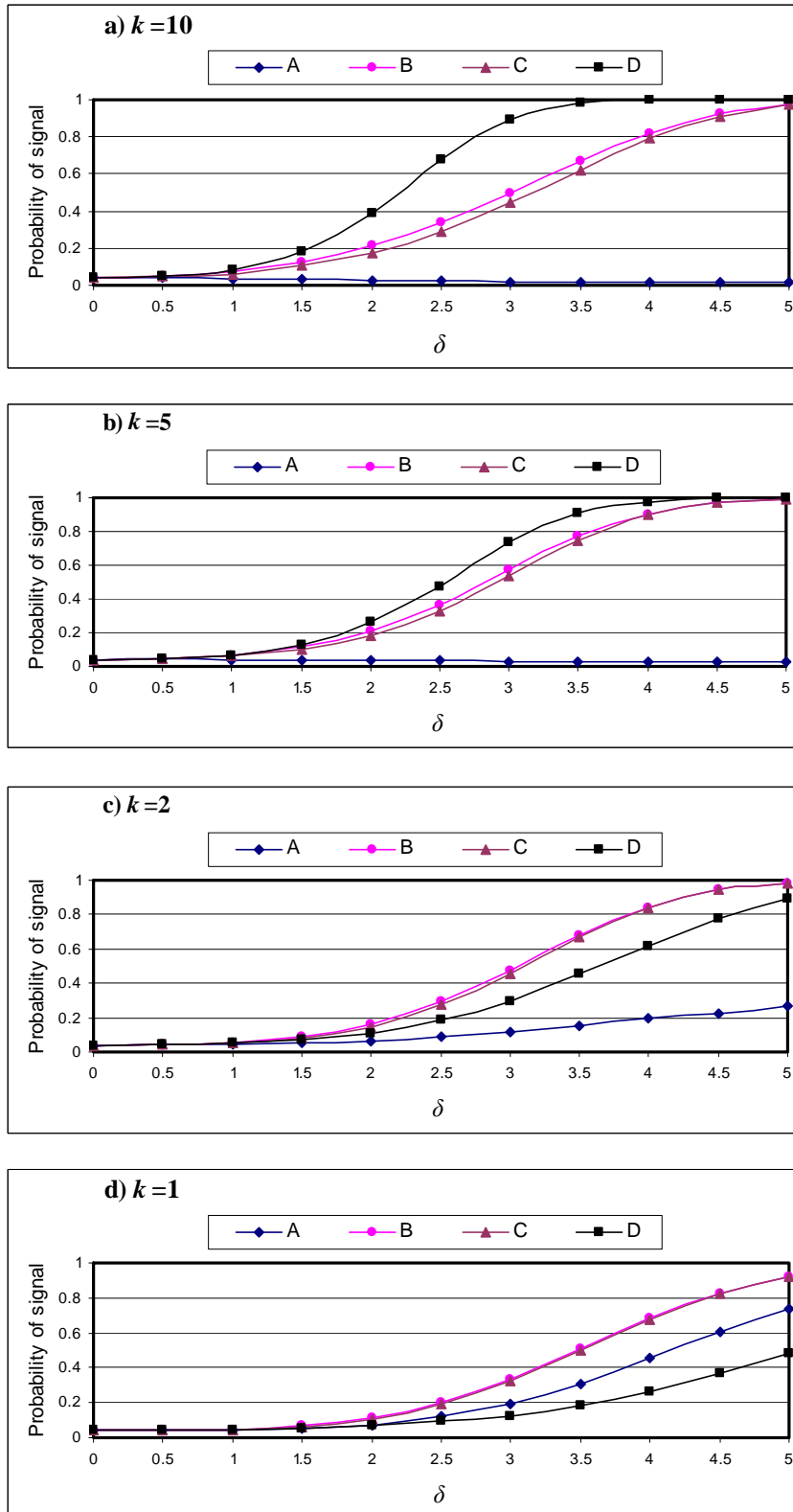
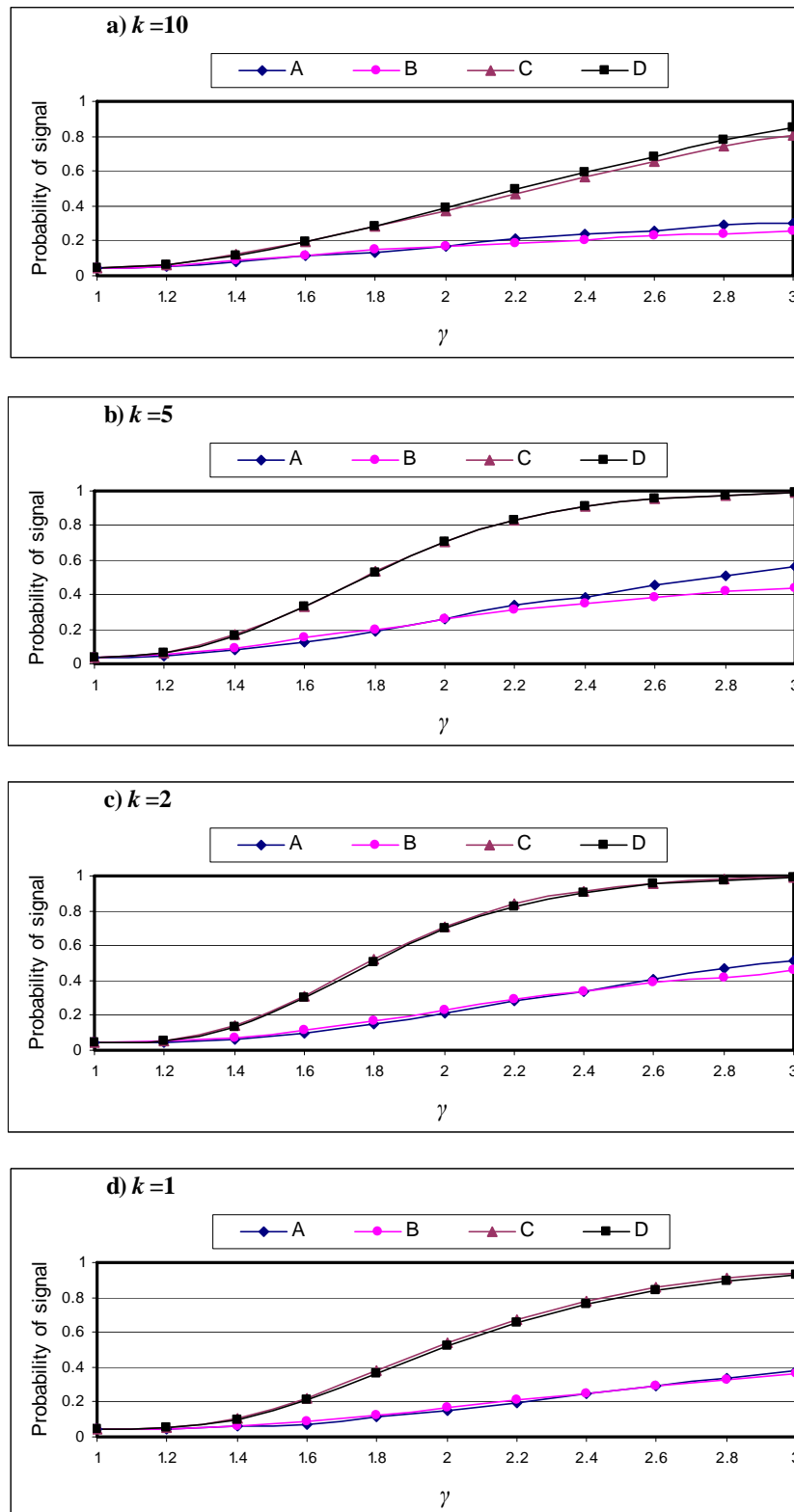


Figure 3.16: Probability of out-of-control signal under standard deviation shifts from σ to $\gamma\sigma$ ($m=20$ and $X= -30, -23, -12, -4, 0, 3, 10, 20, 25,$ and 35).



3.A.3 Violations of the Normality Assumption

The normality assumption for the linear profile model in Equation (2.1) is required for determining the statistical performance of any of the proposed Phase I methods. Tables 3.10-3.14 show the overall false alarm probabilities produced by the competing methods, assuming that the ε_{ij} 's are i.i.d. double exponential random variables with mean 0 and variance 1, double exponential random variables with mean 0 and variance 2, exponential random variables with mean 1, t -distributed random variables with 3 degrees of freedom, and t -distributed random variables with 5 degrees of freedom, respectively. For these tables, the number of samples $m=20$ and the fixed X -values= $0(0.2)1.8$ were used. As shown in these tables, departures from the normality assumption can greatly affect the statistical performance of all of the Phase I methods. The false alarm rate can increase dramatically if this assumption is violated. Thus, it is strongly recommended that a test be carried out for the appropriateness of the normality assumption before applying a Phase I method. As mentioned in Chapter 2, there are many statistical methods for checking the normality of the error terms; see, for example, Neter et al. (1990, chap. 4) and Ryan (1997, pp. 52-53).

Table 3.10: Overall false alarm probabilities when the ε_{ij} 's are i.i.d. double exponential random variables with mean 0 and variance 1.

Nominal	Simulated			
	A	B	C	D
0.01	0.3128	0.2835	0.5706	0.1695
0.02	0.5014	0.4329	0.7354	0.2231
0.03	0.645	0.5492	0.8207	0.2815
0.04	0.7571	0.64	0.8856	0.3165
0.05	0.8233	0.6946	0.9116	0.3522
0.10	0.9819	0.8821	0.9856	0.4732

Table 3.11: Overall false alarm probabilities when the ε_{ij} 's are i.i.d. double exponential random variables with mean 0 and variance 2.

Nominal	Simulated			
	A	B	C	D
0.01	0.3091	0.2891	0.5828	0.1653
0.015	0.4178	0.3655	0.6612	0.1852
0.03	0.6393	0.5475	0.8203	0.2831
0.04	0.7531	0.6312	0.8834	0.3102
0.05	0.8272	0.7004	0.9146	0.3451
0.10	0.9774	0.8857	0.9827	0.4731

Table 3.12: Overall false alarm probabilities when the ε_{ij} 's are i.i.d. exponential random variables with mean 1.

Nominal	Simulated			
	A	B	C	D
0.01	0.4128	0.3698	0.7801	0.3671
0.02	0.5794	0.499	0.8863	0.4482
0.03	0.7118	0.5918	0.9317	0.5065
0.04	0.7811	0.6642	0.9562	0.553
0.05	0.8562	0.7192	0.9675	0.5839
0.10	0.9797	0.8819	0.994	0.7012

Table 3.13: Overall false alarm probabilities when the ε_{ij} 's are i.i.d. t -distributed random variables with 3 degrees of freedom.

Nominal	Simulated			
	A	B	C	D
0.01	0.4962	0.442	0.8215	0.5354
0.02	0.6714	0.5753	0.9016	0.5928
0.03	0.7792	0.6662	0.9403	0.6348
0.04	0.8495	0.7307	0.9585	0.6651
0.05	0.8983	0.7792	0.9721	0.6941
0.10	0.9904	0.9151	0.9954	0.767

Table 3.14: Overall false alarm probabilities when the ε_{ij} 's are i.i.d. t -distributed random variables with 5 degrees of freedom.

Nominal	Simulated			
	A	B	C	D
0.01	0.3161	0.288	0.547	0.2055
0.02	0.5051	0.4408	0.6908	0.2604
0.03	0.6318	0.5392	0.7711	0.2881
0.04	0.741	0.6239	0.8416	0.3249
0.05	0.8163	0.6908	0.8865	0.3469
0.10	0.9801	0.8865	0.9715	0.4537

3.B Calibration Example

This section presents a Phase I analysis of the calibration data set presented by Mestek et al. (1994). Their purpose was to study the stability of the calibration curve in the photometric determination of Fe^{3+} with sulfosalicylic acid. The data set for this example is in Table 3.15. The example includes twenty-two calibration curves. Each calibration curve was set up by the following procedure. Five volumes of 0, 1, 2, 3 and 4 mL of 50 $\mu\text{g}/\text{mL}$ Fe^{3+} solution were diluted with water to 25 mL. Then, for each volume, 2.5 mL of a 20% solution of sulfosalicylic acid and 1.5 mL of a concentrated solution of ammonia were added to the diluted solution. Each volume was replicated twice, so that each calibration curve consists of 10 points. For each volume, the absorbance of the solution at 420 nm was measured on a Spekol 11 using 1 cm cells.

The first three columns of Table 3.16 contain the least squares estimates for the intercept, slope, and sample error variance for each calibration curve. The intercept and slope averages are $\bar{a}_0 = -0.456$ and $\bar{a}_1 = 2.047$, respectively, while the estimate of the error variance is $MSE = 1.6114$.

Before applying the proposed Phase I methods, some diagnostics to check for the appropriateness of the normality assumption and the linearity of the relationship between

the response and the independent variable for each of the samples were obtained. These suggested the reasonableness of the normality assumption of the error terms. The last two columns of Table 3.16 contain the F -values and the p -values, respectively, of the lack-of-fit tests. The p -values suggest that there is no significant evidence of departures from linearity.

Table 3.15: Example Data with the response measured according to each Fe^{3+} level (from Mestek et al. (1994)).

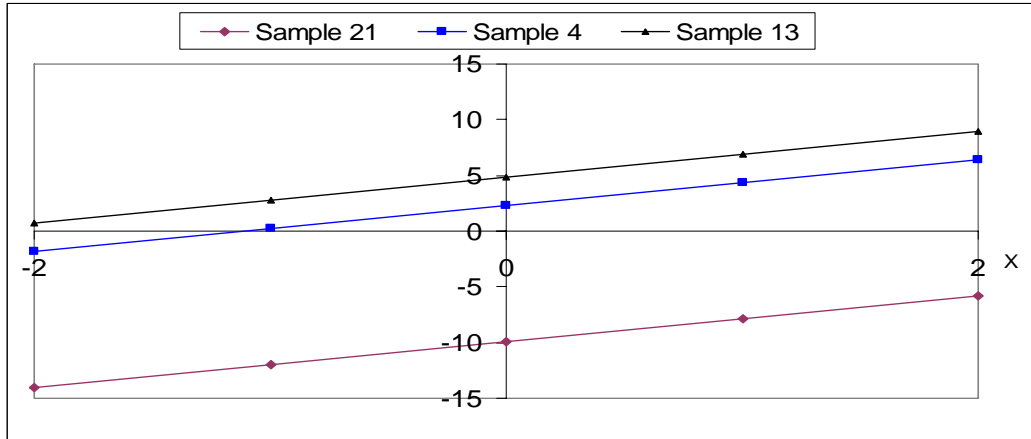
Sample No.	0 $\mu\text{g Fe}^{3+}$	50 $\mu\text{g Fe}^{3+}$	100 $\mu\text{g Fe}^{3+}$	150 $\mu\text{g Fe}^{3+}$	200 $\mu\text{g Fe}^{3+}$
1	1, 3	104, 104	206, 206	307, 308	409, 412
2	4, 2	104, 103	206, 204	308, 307	412, 413
3	3, 2	105, 104	207, 207	311, 309	414, 411
4	4, 2	104, 104	206, 207	308, 312	411, 413
5	-9, -8	92, 95	195, 197	296, 299	397, 400
6	3, 3	107, 105	209, 207	311, 308	412, 410
7	3, 2	104, 105	207, 208	311, 308	414, 410
8	2, 2	105, 104	208, 208	310, 309	412, 412
9	-6, -7	95, 94	196, 197	297, 300	401, 401
10	2, 4	104, 105	206, 207	311, 310	413, 412
11	1, 2	103, 104	205, 206	309, 307	412, 411
12	-7, -7	94, 96	198, 199	298, 301	404, 402
13	5, 7	105, 107	210, 208	313, 315	415, 415
14	3, 2	106, 104	208, 207	311, 308	411, 414
15	-8, -6	94, 95	196, 199	299, 302	400, 404
16	4, 6	104, 106	207, 210	311, 310	415, 413
17	2, 4	105, 106	206, 208	308, 310	410, 413
18	2, 0	104, 103	206, 206	309, 308	414, 409
19	0, 1	101, 102	203, 206	305, 307	409, 411
20	1, 4	104, 106	206, 208	311, 309	410, 414
21	-9, -10	92, 92	194, 194	298, 297	400, 398
22	-8, -8	95, 95	195, 199	298, 301	401, 403

Table 3.16: The linear regression results for the 22 samples.

Sample	Intercept	Slope	MSE_j	F-value	p-value
1	1.900	2.041	1.000	0.230	0.875
2	1.700	2.046	2.528	4.480	0.070
3	2.200	2.051	1.000	0.120	0.943
4	2.300	2.048	1.960	0.430	0.743
5	-8.200	2.036	2.190	0.170	0.914
6	3.600	2.039	1.563	0.310	0.818
7	2.400	2.048	1.796	0.050	0.985
8	2.200	2.050	0.325	2.670	0.159
9	-7.00	2.038	0.922	0.390	0.767
10	2.400	2.050	0.922	1.420	0.341
11	1.100	2.049	0.740	0.810	0.539
12	-7.100	2.049	1.440	0.470	0.715
13	4.800	2.052	2.592	2.670	0.159
14	2.500	2.049	1.538	0.050	0.984
15	-7.300	2.048	2.657	0.150	0.923
16	3.900	2.047	2.250	1.050	0.446
17	3.100	2.041	1.440	0.080	0.966
18	0.900	2.052	1.960	0.020	0.995
19	-0.200	2.047	1.769	0.800	0.546
20	2.500	2.048	2.372	0.040	0.990
21	-9.900	2.045	0.640	1.190	0.401
22	-7.800	2.049	1.850	0.040	0.988

Having checked the model assumptions, the researcher applied the method of Jones and Rice (1992) using a principal component analysis to identify the primary patterns of variation among the 22 calibration curves. The first principal component accounts for approximately 95% of the total original variation. Figure 3.17 shows the three fitted calibration curves corresponding to the minimum, median, and maximum first principal component scores. These correspond to Samples 21, 4, and 13, respectively. It is clear from Figure 3.17 that these curves differ primarily in the Y -intercept. Therefore, one concludes that 95% of the overall variability is due to the variability in the Y -intercept.

Figure 3.17: Calibration curves corresponding to the minimum, median, and maximum first principal component scores.



The control chart for Method A, as recommended by Stover and Brill (1998), is given in Figure 3.18. The *UCL* of this chart was determined based on a false alarm probability of $\alpha_1 = 0.00233$ to produce an overall false alarm probability of $\alpha = 0.05$. Using Equation (2.8), the *UCL* of this chart is 9.456. Examination of Figure 3.18 suggests that all the calibration curves are in control.

Figure 3.18: Control chart for Method A.

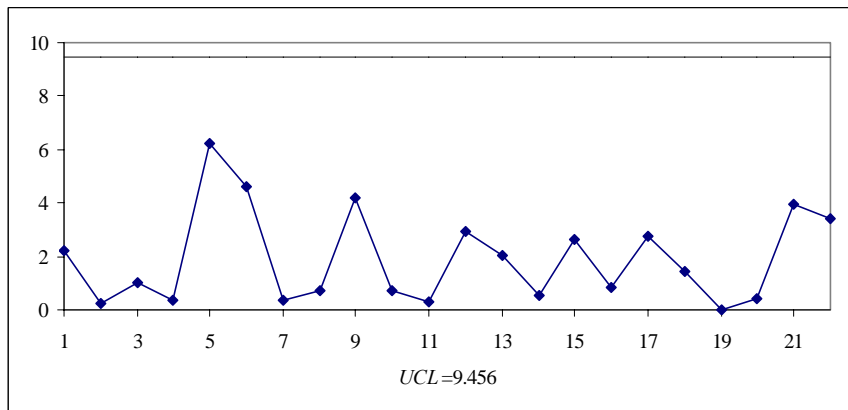
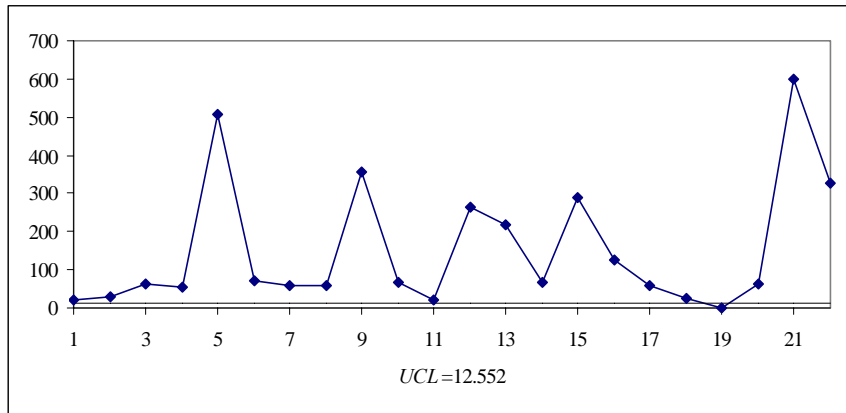


Figure 3.19 gives a control chart for Method B with $UCL=12.552$. This UCL was calculated using Equation (2.10) based on $\alpha_1 = 0.00233$ to produce an overall false alarm probability of $\alpha = 0.05$. The results obtained by using this method were quite contrary to the results obtained from Method A. Figure 3.19 indicates that the calibration curves are very unstable.

Figure 3.19: Control chart for Method B.



Figures 3.20, 3.21, and 3.22 give control charts for the process variance, Y -intercept, and slope, respectively, using Method C. The control limits for the three control charts are calculated using Equations (2.16), (2.12), and (2.13), respectively. Each set of chart limits was determined based on $\alpha_2 = 0.00078$ to produce an overall false alarm probability of $\alpha = 0.05$. According to the chart in Figure 3.20, the error term variance appears stable. Figure 3.21, however, shows that the intercept is out-of-control. On the other hand, the slope, as shown in Figure 3.22, is stable. This result agrees with the result obtained from Method B. However, using Method C one can more easily explain out-of-control signals. The calibration curves are out of control because their intercepts are unstable. The importance of this instability would have to be evaluated based on practical considerations. If this variation were considered to be common cause variation, then this would affect the determination of appropriate control limits for Phase II. In particular, it would be more appropriate to base the control limits on the average moving range as done with the conventional univariate X -chart for individuals data.

Figure 3.20: Method C control chart for the error term variance.

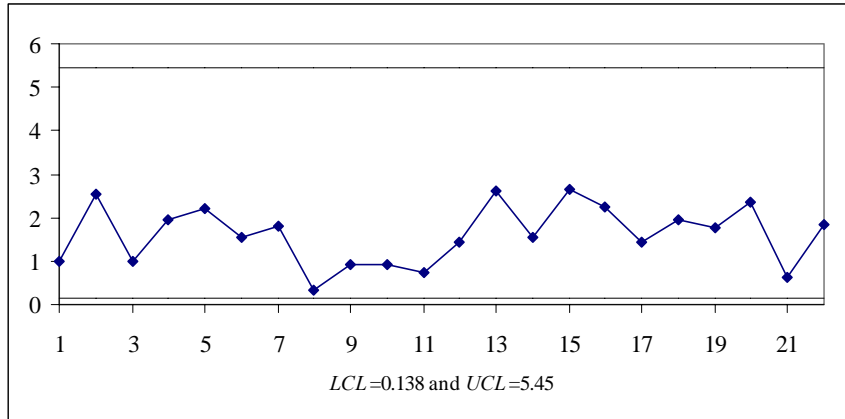


Figure 3.21: Method C control chart for the intercept.

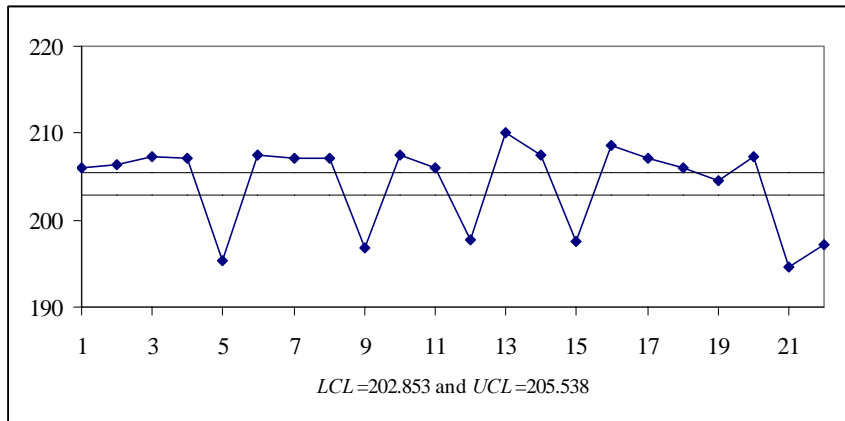
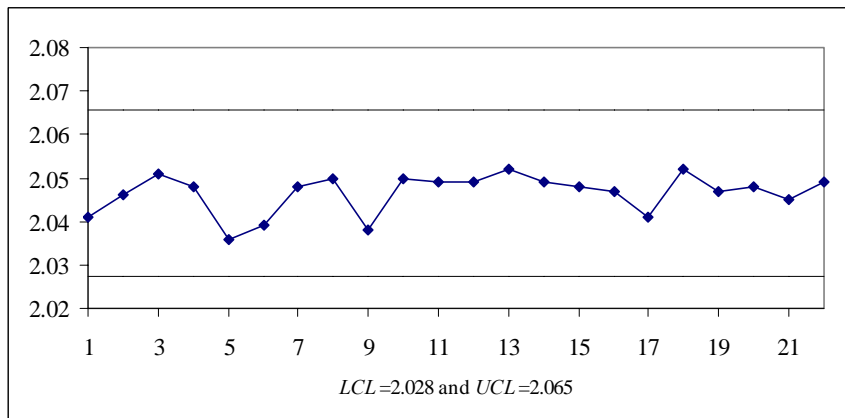


Figure 3.22: Method C control chart for the slope.



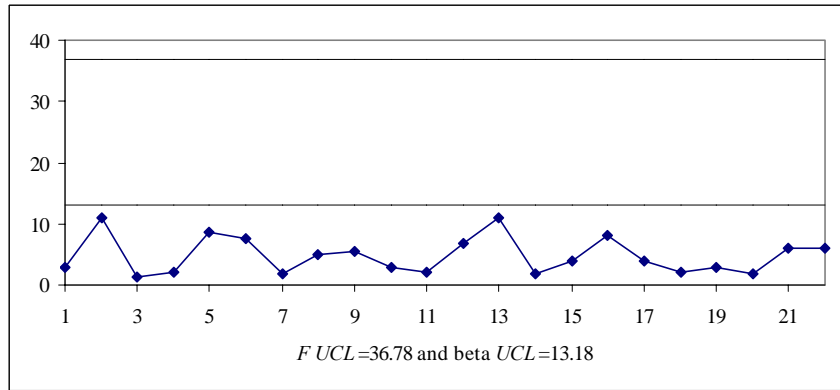
For Method D, the global F -test was performed based on the statistic in Equation (2.19) in conjunction with the third control chart of Method C for monitoring the process variance with limits calculated using Equation (2.16). The control limits for this chart were set using $\alpha_4 = 0.001165$ and the global F -test was performed at the significance level $\alpha_3 = 0.0253$. Therefore, the nominal overall false alarm probability produced by Method D is also $\alpha = 0.05$. In this case the control chart for monitoring the process variance is exactly the same as that of Figure 3.20, but with different control limits because of the use of different false alarm probabilities. The new control limits are $LCL=0.1532$ and $UCL=5.2718$. However, it can be seen that all the sample variance values are also within these new control limits. Therefore, one concludes that the error term variance is stable.

The F -value for testing the equality of all the regression lines is $F = 75.8019$ with a p -value of 0.00. Therefore, one rejects the null hypothesis that all of the regression lines are identical, i.e., the process is out-of-control. For diagnostic purposes, the X -values were coded and then separate 3-sigma control charts for the Y -intercept and for the slope were applied. The 3-sigma control limits for the Y -intercept are 202.99 and 205.4 while the 3-sigma control limits for the slope are 2.03 and 2.064. All of the slope estimates are within these control limits while all of the Y -intercept estimates are outside the control limits, except the intercept estimate for sample 19. Hence, one also concludes that the process is out-of-control because the intercept is not stable.

In their analysis of this example, Mestek et al. (1994) considered monitoring vectors containing the absorbance averages corresponding to the Fe^{3+} volumes. Using a pooled sample covariance matrix of vectors containing the absorbance averages, they calculated the T^2 statistics in Equation (2.5). They used a T^2 -distribution with 5 and 22 degrees of freedom to determine the UCL of this control chart and found that all the calibration curves are in-control. However, as mentioned previously, the T^2 -distribution is not the correct marginal distribution for their T^2 statistics. The correct marginal distribution is the beta distribution with parameters 2.5 and 8. Figure 3.23 shows a control chart for their T^2 statistics with upper control limits calculated using both the beta

and T^2 -distributions based on a nominal overall false alarm probability of $\alpha = 0.05$. As shown in Figure 3.23, all the calibration curves appear in-control, regardless of the UCL used.

Figure 3.23: Control chart using Mestek et al.'s (1994) T^2 approach. The lower UCL is obtained using the beta distribution and the higher UCL is obtained using the T^2 distribution.



Mestek et al. (1994) treated each sample as a group of two sub-samples, each with five observations. In this case, the sample covariance matrix of vectors containing the group averages would not be the best estimator of the population covariance matrix. Supposing that each sample consists of q sub-samples (each with n observations), a better estimator for the population covariance matrix then could be obtained by the pooled covariance matrix $\mathbf{S}_p = \sum_{j=1}^m \mathbf{S}_j / m$, where \mathbf{S}_j is the usual sample covariance matrix for group j (usually \mathbf{S}_j is called the within-group covariance matrix and \mathbf{S}_p is called the between groups covariance matrix). It can be shown, see Mason et al. (2001), that

$$T_j^2 = mq(\bar{\mathbf{y}}_j - \bar{\bar{\mathbf{y}}})^T \mathbf{S}_p^{-1} (\bar{\mathbf{y}}_j - \bar{\bar{\mathbf{y}}}) / (m-1) \quad j=1, 2, \dots, m, \quad (3.1)$$

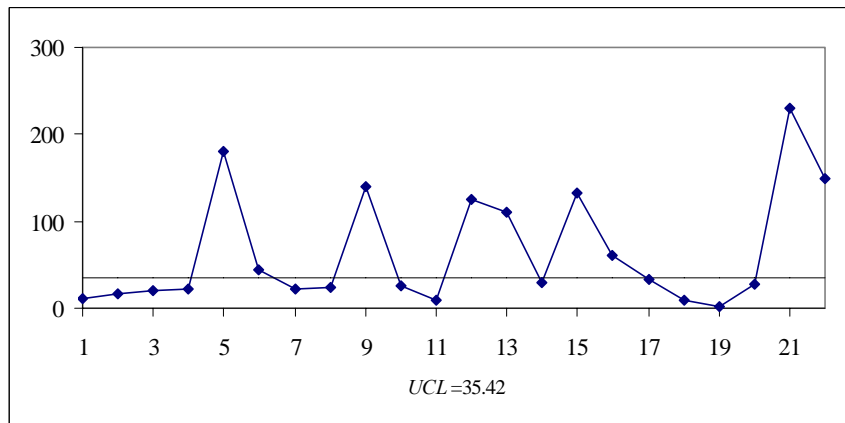
each have a T^2 -distribution with n and $m(q-1)-n+1$ degrees of freedom where $\bar{\mathbf{y}}_j = (\bar{y}_{1j}, \bar{y}_{2j}, \dots, \bar{y}_{nj})$ is a vector containing the response average values of the j^{th} group, $\bar{y}_{ij} = \sum_{l=1}^q y_{ijl} / q$, ($i=1, 2, \dots, n$), and y_{ijl} is the i^{th} response value in the sub-sample l ($l=1, 2, \dots, q$) and group j ($j=1, 2, \dots, m$). Also, $\bar{\bar{\mathbf{y}}} = (\bar{y}_1, \bar{y}_2, \dots, \bar{y}_n)$ is a vector of the overall

response averages, where $\bar{y}_i = \sum_{j=1}^m \bar{y}_{ij} / m$, ($i=1, 2, \dots, n$). Using the relationship between the T^2 - and F -distributions, an appropriate UCL for the T^2 values in Equation (3.1) is

$$UCL = mn(q-1)F_{n,m(q-1)-n+1,\alpha} / [m(q-1) - n + 1]. \quad (3.2)$$

Figure 3.24 shows a control chart for the T^2 statistics in Equation (3.1). Again, the UCL was set based on a nominal overall false alarm probability of $\alpha = 0.05$. As shown in Figure 3.24, the process is not in control. This result shows how the T^2 control chart approach proposed by Mestek et al. (1994) is sensitive to the method used for estimating the population covariance matrix. Mestek et al.'s (1994) T^2 control chart is an ineffective approach, in general, because of its use of a poor estimator for the population covariance matrix.

Figure 3.24: Control chart for the T^2 statistics in Equation (3.1).



3.C Summary

Through a simulation study the researcher compared the performance of four methods of monitoring linear profiles in Phase I. These are the T^2 control chart proposed by Stover and Brill (1998) (Method A), the T^2 control chart proposed by Kang and Albin (2000) (Method B), and the three Shewhart-type control charts proposed by Kim et al. (2003) (Method C) and the F -test method (Method D). Method D is much more effective

than the other methods in detecting shifts affecting much of the Phase I data. On the other hand, for shifts for the slope and Y -intercept affecting only a few samples of the Phase I data, both the Kang and Albin (2000) method and the Kim et al. (2003) method gave better results. However, the Kang and Albin (2000) method was shown to be ineffective in detecting shifts in the process standard deviation. The Kim et al. (2003) method is much more interpretable than the Kang and Albin (2000) method. Departure from normality, however, affects the statistical performance of all the Phase I methods as shown in the simulation study presented in Section 3.A.3.

Both the simulation study and the calibration example show that the T^2 control chart proposed by Stover and Brill (1998) is ineffective in detecting shifts in the process parameters. As mentioned in Sullivan and Woodall (1996a), the reason is that the population covariance matrix can be poorly estimated by the pooled sample covariance matrix when applying a T^2 control chart with individual vector observations. The same conclusion applies to the overparameterized T^2 control chart proposed by Mestek et al. (1994).

Chapter 4: A Change Point Method Based on Linear Profile Data

As mentioned in Chapter 1, many authors have studied the change point problem in different regression models, but under a different sampling framework than that of the linear profile data. These authors assumed that either there is a single data set or data are obtained sequentially one observation at a time. In the literature, the change point problem in a regression model is usually referred to as segmented regression.

A s -segment piecewise simple linear regression model is one given by

$$\begin{aligned}
 Y_i &= A_{01} + A_{11}X_i + \varepsilon_i, & \theta_0 < i \leq \theta_1 \\
 Y_i &= A_{02} + A_{12}X_i + \varepsilon_i, & \theta_1 < i \leq \theta_2 \\
 &\vdots \\
 &\vdots \\
 Y_i &= A_{0s} + A_{1s}X_i + \varepsilon_i, & \theta_{s-1} < i \leq \theta_s,
 \end{aligned} \tag{4.1}$$

where $i=1, 2, \dots, N$ and the θ_j 's are the change points between segments (usually $\theta_0 = 0$ and $\theta_s = N$) and the ε_i 's are the error terms. The ε_i 's are assumed to be i.i.d $N(0, \sigma_j^2)$, where σ_j^2 is the segment error term variance, where $j=1, 2, \dots, s$. The segmented regression technique is used to estimate the number of segments s and the locations of the change points θ_j 's.

In the linear profile applications, multiple data sets are collected over time in more of a functional data sampling framework. Generally speaking, the sampling framework of a linear profile data set is identical to that of a panel data set in the econometrics studies. This study proposes a change point method based on the segmented regression technique to test the constancy of the profile parameters over time. This method can be used to assess the stability of and to detect change points in a Phase I simple linear regression profile data set.

4.A A Change Point Approach

In this section the proposed change point method for testing the constancy of the regression parameters in a linear profile data set is presented. The observed data are m random samples, with each sample consisting of a sequence of n_j pairs of observations (X_{ij}, Y_{ij}) , $i=1, 2, \dots, n_j$, $n_j > 2$, $j=1, 2, \dots, m$. The linear profile model relating the explanatory variable X to the response Y is in Equation (2.1) in Chapter 2. It is assumed that the ε_{ij} 's are i.i.d. $N(0, \sigma_j^2)$ random variables and that the X -values in each sample are known constants.

The first step of the proposed change point approach is to combine the m samples of profiles into one sample of size N . Then, one applies the segmented simple linear regression model in Equation (4.1) to the combined sample. Since in the linear profile model we assume that no parameter changes take place within each sample, then the change points θ_j 's are restricted to the indices i corresponding to the ends of the profile samples, i.e., $\theta_0 = 0$, $\theta_1 = n_1$, $\theta_2 = n_1 + n_2, \dots$, $\theta_m = N$. Hawkins (1976) gave formulas for the maximum likelihood estimator (MLE) of the change points of the segmented multiple regression model, for both the heteroscedastic and homoscedastic models. In this study, only the heteroscedastic model is considered. Hawkins (2001) noted the form of the LRT statistic for testing the null hypothesis of a single segment versus the alternative of s segments. It can be shown that the LRT statistic used to test the null hypothesis of a single segment against the alternative of $s=2$ segments is lrt_{m_1} , where

$$lrt_{m_1} = N \log \hat{\sigma}^2 - N_1 \log \hat{\sigma}_1^2 - N_2 \log \hat{\sigma}_2^2, \quad m_1=1, 2, \dots, m-1, \quad (4.2)$$

and $\hat{\sigma}^2$ is the MLE of the error term variance for the regression model fitted for all the m samples pooled into one sample of size N , $\hat{\sigma}_1^2$ is the MLE of the error term variance for the regression model fitted for all the samples prior to m_1 pooled into one sample of size $N_1 = \sum_{j=1}^{m_1} n_j$, and $\hat{\sigma}_2^2$ is the MLE of the error term variance for the regression model fitted for all the samples following m_1 pooled into one sample of size $N_2 = N - N_1$. The LRT

statistic in Equation (4.2) is identical to that of Quandt (1958).

The literature of segmented regression includes two important approaches for the determination of the appropriate number of change points and the choice of segment boundaries. These are the DP algorithm of Hawkins (1976) and the binary segmentation approach originating with the work of Vostrikova (1981). Hawkins (2001) stated that the binary segmentation approach does not give the optimum splits if there are two or more of them. The DP algorithm is arguably much more accurate than the binary segmentation algorithm in fitting three or more segments to the data. If all the segment boundaries are known a priori, then the LRT statistic used in the binary segmentation procedure and that used for fitting $s > 2$ segments in the DP algorithm asymptotically follow a chi-squared distributions with 3 and $3s$ degrees of freedom, respectively. The distribution of the test statistic in each approach, however, no longer has a chi-squared distribution if we specify the split points by maximizing the LRT statistics. The reason for this, as stated by Hawkins (2001), is the failure of the Cramér regularity conditions. Several studies, however, showed that accurate bounds for the probability distribution of the test statistic used in the binary segmentation procedure can be obtained using the Bonferroni's inequality; see Worsley (1983). Csörgő and Horvath (1997) derived an asymptotic distribution for the square root of this test statistic. On the other hand, no approximations or asymptotic distributions are known for the test statistic used in the DP algorithm.

In the proposed change point approach for the analysis of linear profiles one applies the binary segmentation procedure to estimate the change points locations and to determine the appropriate number of change points. Using this procedure, one obtains the lrt_{m_1} statistics in Equation (4.2) for all possible values of m_1 , $m_1=1, 2, \dots, m-1$ and divides each by its expected value under the null hypothesis. The approach signals the presence of a change point if the maximum of these statistics exceeds a threshold. The value of m_1 that maximizes the lrt_{m_1} statistic in Equation (4.2) is the MLE of the change point location. Then, one splits the data set into two subsets at m_1 and applies the same binary splitting procedure described above to each subset. This procedure is repeated until no evidence of additional change points is given. This proposed change point approach for

linear profile data is similar to the proposed change point method of Sullivan and Woodall (1996b) to detect sustained step shifts in the process mean and/or variance in a Phase I individual univariate observations. This alternative approach not only provides a signal that the process is out-of-control in the SPC context, but also provides an estimate of when it went out-of-control. This gives it an advantage over competing control chart methods.

4.A.1 Factoring the lrt_{m_1} Statistic into Different Sources of Variability

The lrt_{m_1} statistic in Equation (4.2) can be written as

$$lrt_{m_1} = VAR_{\sigma^2} + VAR_{B_1} + VAR_{B_0}, \quad (4.3)$$

where

$$VAR_{\sigma^2} = N \log\{(N_1 r^{2N_2/N} + N_2 r^{-2N_1/N}) / N\}, \quad VAR_{B_1} = N \log\{1 + (c_2 d_{B_1}^2 / c_1)\},$$

$$VAR_{B_0} = N \log\{1 + [(c_4 + c_3 d_{B_0}^2) / (c_1 + c_2 d_{B_1}^2)]\}, \quad r = \hat{\sigma}_1 / \hat{\sigma}_2, \quad d_{B_0} = \bar{y}_2 - \bar{y}_1,$$

$$d_{B_1} = (S_{xy2} / S_{xx2}) - (S_{xy1} / S_{xx1}), \quad c_1 = N_1 \hat{\sigma}_1^2 + N_2 \hat{\sigma}_2^2, \quad c_2 = S_{xx1} S_{xx2} / S_{xx}, \quad c_3 = N_1 N_2 / N,$$

$$\text{and } c_4 = \{[N_1 N_2 (\bar{x}_2 - \bar{x}_1)^2 (S_{xx2} S_{xy1}^2 + S_{xx1} S_{xy2}^2) / N S_{xx} S_{xx1} S_{xx2}]$$

$$- [2N_1 N_2 (\bar{x}_2 - \bar{x}_1) (S_{xy1} + S_{xy2}) d_{B_0} / N S_{xx}] - [N_1^2 N_2^2 (\bar{x}_2 - \bar{x}_1)^2 d_{B_0}^2 / N^2 S_{xx}]\}.$$

$$\text{Here, } \bar{x} = \sum_{i=1}^N x_i / N, \quad \bar{x}_1 = \sum_{i=1}^{N_1} x_i / N_1, \quad \bar{x}_2 = \sum_{i=N_1+1}^N x_i / N_2, \quad \bar{y}_1 = \sum_{i=1}^{N_1} y_i / N_1, \quad \bar{y}_2 = \sum_{i=N_1+1}^N y_i / N_2,$$

$$S_{xx} = \sum_{i=1}^N (x_i - \bar{x})^2, \quad S_{xx1} = \sum_{i=1}^{N_1} (x_i - \bar{x}_1)^2, \quad S_{xx2} = \sum_{i=N_1+1}^N (x_i - \bar{x}_2)^2, \quad S_{xy1} = \sum_{i=1}^{N_1} (x_i - \bar{x}_1) y_i,$$

$$\text{and } S_{xy2} = \sum_{i=N_1+1}^N (x_i - \bar{x}_2) y_i, \text{ where } (x_i, y_i), i=1, 2, \dots, N, \text{ are } N \text{ bivariate observations}$$

resulting from pooling the m samples into one sample. The proof is in Appendix 4.A.

The expression simplifies considerably if the X -values are the same within each sample since $c_4 = 0$. Using the three factors VAR_{B_0} , VAR_{B_1} and VAR_{σ^2} one can determine to a

large extent the relative contributions of the Y -intercept, slope, and variance shifts to the statistic used to indicate the presence of a change point.

In the proposed approach, if the value of VAR_{σ^2} is large we consider this as

evidence that the variance is not stable. Since the accuracy of the estimators of the in-control regression coefficients relies heavily on the stability of the process variance, we do not test whether the regression coefficients are constant if the variance is shown to be unstable. Furthermore, a large value of VAR_{β_1} indicates that the regression lines are not parallel. In practice, if the regression lines are not parallel, we may not care whether their intercepts are equal. The idea of decomposing the LRT statistic into three components corresponding to the variance, slope, and intercept changes has been considered by several authors; see Gulliksen and Wilks (1950) and Fatti and Hawkins (1986), for example. The decomposition in Equation (4.3) is similar in several aspects to that of Gulliksen and Wilks (1950).

4.A.2 Expectation of the lrt_{m_1} Statistic

The in-control expected value for the lrt_{m_1} statistic in Equation (4.2) is not the same for all values of m_1 . For instance, the columns labeled as $E(lrt_{m_1})$ in Tables 4.1-4.5 give the simulated expected in-control values for the lrt_{m_1} statistics for all possible values of m_1 , using 100,000 Phase I data sets generated using the underlying assumed in-control model with $A_0=0$ and $A_1=1$, i.e.,

$$y_{ij} = x_i + \varepsilon_{ij}, i = 1, 2, \dots, n, j=1, 2, \dots, m.$$

The ε_{ij} 's were assumed to be i.i.d. $N(0, 1)$ random variables. In Tables 4.1-4.3 the fixed X -values of 0(0.2)1.8 were used. The number of samples $m=5, 20,$ and 60 were used for Tables 4.1, 4.2, and 4.3, respectively. For Table 4.4, the number of samples $m=20$ was used and the fixed X values 0(0.2)1.8 were used twice within each sample to give a linear profile model with $n=20$. For Table 4.5, the fixed X -values of $-30, -23, -12, -4, 0, 3, 10, 20, 25,$ and 35 and the number of samples $m=20$ were used. As shown in these tables, $E(lrt_{m_1})$ takes its largest values for large or small values of m_1 . Thus the Bartlett correction is used; that is dividing the lrt_{m_1} statistics by a normalizing factor C_{m_1} that makes the expected values the same for all values of m_1 . See Kendall and Stuart (1977, p.

250), for example. If we let $C_{m_1} = E(lrt_{m_1})$, then the statistics

$$lrtc_{m_1} = lrt_{m_1} / C_{m_1}, \quad m_1=1, 2, \dots, m-1,$$

all have an expected value of unity. The values of C_{m_1} , $m_1=1, 2, \dots, m-1$ can be approximated accurately as described in Section 4.5. Then the threshold for the largest adjusted LRT statistic corresponding to a given probability of a Type I error can be determined by simulation or approximated as described in Section 4.5.

Table 4.1: The simulated and approximate in-control expected values for the $lrtc_{m_1}$ statistic for $m=5$ and $X=0(0.2)1.8$.

m_1	$E(lrt_{m_1})$	e_{m_1}
1	3.560415	3.525048
2	3.293678	3.293637
3	3.301961	3.293637
4	3.55466	3.525048
5	<i>na</i>	<i>na</i>

Table 4.2: The simulated and approximate in-control expected values for the $lrtc_{m_1}$ statistic for $m=20$ and $X=0(0.2)1.8$.

m_1	$E(lrt_{m_1})$	e_{m_1}	m_1	$E(lrt_{m_1})$	e_{m_1}
1	3.542432	3.503238	11	3.069123	3.066866
2	3.239516	3.234127	12	3.084365	3.069711
3	3.163807	3.154726	13	3.083078	3.074882
4	3.126386	3.117358	14	3.094238	3.083189
5	3.097932	3.096229	15	3.101099	3.096229
6	3.08461	3.083189	16	3.126618	3.117358
7	3.084656	3.074882	17	3.159407	3.154726
8	3.075021	3.069711	18	3.247355	3.234127
9	3.070753	3.066866	19	3.556583	3.503238
10	3.070931	3.065956	20	<i>na</i>	<i>na</i>

Table 4.3: The simulated and approximate in-control expected values for the lrt_{m_1} statistic for $m=60$ and $X=0(0.2)1.8$.

m_1	$E(lrt_{m_1})$	e_{m_1}	m_1	$E(lrt_{m_1})$	e_{m_1}	m_1	$E(lrt_{m_1})$	e_{m_1}
1	3.539928	3.502206	21	3.038497	3.024667	41	3.018862	3.02632
2	3.233082	3.231937	22	3.042797	3.024012	42	3.020689	3.027352
3	3.145725	3.151232	23	3.03957	3.023456	43	3.018556	3.028547
4	3.105426	3.112383	24	3.039444	3.02299	44	3.018076	3.029934
5	3.088983	3.08956	25	3.033736	3.022607	45	3.022204	3.031549
6	3.06567	3.074567	26	3.035382	3.022301	46	3.023881	3.033438
7	3.056832	3.063987	27	3.031145	3.022067	47	3.023671	3.035662
8	3.042621	3.05614	28	3.028733	3.021902	48	3.024442	3.038303
9	3.037415	3.050104	29	3.030147	3.021804	49	3.030313	3.041473
10	3.037544	3.04533	30	3.028767	3.021771	50	3.031396	3.04533
11	3.03548	3.041473	31	3.024313	3.021804	51	3.037693	3.050104
12	3.035913	3.038303	32	3.02682	3.021902	52	3.044078	3.05614
13	3.030463	3.035662	33	3.024366	3.022067	53	3.055019	3.063987
14	3.032788	3.033438	34	3.021772	3.022301	54	3.068618	3.074567
15	3.034651	3.031549	35	3.021042	3.022607	55	3.095403	3.08956
16	3.034299	3.029934	36	3.023053	3.02299	56	3.120024	3.112383
17	3.028698	3.028547	37	3.026976	3.023456	57	3.152899	3.151232
18	3.029623	3.027352	38	3.023276	3.024012	58	3.246948	3.231937
19	3.031837	3.02632	39	3.019105	3.024667	59	3.532738	3.502206
20	3.03066	3.025431	40	3.022798	3.025431	60	na	na

Table 4.4: The simulated and approximate in-control expected values for the lrt_{m_1} statistic for $m=20$ and $X=0(0.2)1.8$ are used twice.

m_1	$E(lrt_{m_1})$	e_{m_1}	m_1	$E(lrt_{m_1})$	e_{m_1}
1	3.241877	3.232261	11	3.04568	3.033182
2	3.117655	3.113077	12	3.043869	3.034577
3	3.085592	3.075686	13	3.048764	3.037108
4	3.075676	3.057751	14	3.062193	3.041167
5	3.067265	3.047516	15	3.076805	3.047516
6	3.061247	3.041167	16	3.082913	3.057751
7	3.052074	3.037108	17	3.095536	3.075686
8	3.054829	3.034577	18	3.134699	3.113077
9	3.058104	3.033182	19	3.249598	3.232261
10	3.051691	3.032736	20	na	na

Table 4.5: The simulated and approximate in-control expected values for the lrt_{m_1} statistic for $m=20$ and $X=-30, -23, -12, -4, 0, 3, 10, 20, 25,$ and 35 .

m_1	$E(lrt_{m_1})$	e_{m_1}	m_1	$E(lrt_{m_1})$	e_{m_1}
1	3.519122	3.503238	11	3.078854	3.066866
2	3.224922	3.234127	12	3.075374	3.069711
3	3.145615	3.154726	13	3.079258	3.074882
4	3.110742	3.117358	14	3.089396	3.083189
5	3.084703	3.096229	15	3.10254	3.096229
6	3.077279	3.083189	16	3.119654	3.117358
7	3.072096	3.074882	17	3.158683	3.154726
8	3.071678	3.069711	18	3.235525	3.234127
9	3.072649	3.066866	19	3.540367	3.503238
10	3.076785	3.065956	20	<i>na</i>	<i>na</i>

4.B Performance Comparisons

This section presents simulation results, obtained using Proc IML in SAS software, that compare the performance of the proposed change point method (Method LRT) to that of the most effective Phase I linear profile control chart approaches. As shown in Chapter 3, the most effective Phase I methods are Method C: the Shewhart-type control charts proposed by Kim et al. (2003), Method D: The F -test based on the statistic in Equation (2.19) in conjunction with the control chart for monitoring the process variance using the control limits in Equation (2.15). Each signal probability was estimated using 100,000 simulated sets of profile data. The underlying in-control linear profile model considered in this study is the same as that considered in Section 4.A.3, i.e., $Y_{ij} = X_i + \varepsilon_{ij}$, $i = 1, 2, \dots, n_j$, $j=1, 2, \dots, m$, and the ε_{ij} 's are assumed to be i.i.d. $N(0, 1)$ random variables.

The cases considered in the performance comparisons are as follows. The fixed X -values of 0(0.2)1.8 were first considered in linear profile data sets with number of samples $m=20$ or 60. In some performance comparisons considered with $m=20$, the fixed

X -values were used twice within each sample to give a linear profile model with $n=20$. Also, in some performance comparisons considered with $m=20$, the fixed X -values of $-30, -23, -12, -4, 0, 3, 10, 20, 25,$ and 35 were used. The decision rule of each method was set to produce an overall probability of a Type I error of $\alpha = 0.04$. The different false alarm probabilities, percentiles, and control limits used for Method C and Method D are shown in Table 3.9 in Chapter 3. In Method LRT, for the case of $m=20$ and $X=0(0.2)1.8$ the lrt_{m_1} statistics in Equation (4.2) were divided by the simulated expected values $E(lrt_{m_1})$ in Table 4.2 to give the $lrtc_{m_1}$ statistics. In this case, a probability of a Type I error of approximately 0.04 corresponds to a threshold of 4.56. For the case of $m=60$ and $X=0(0.2)1.8$, the lrt_{m_1} statistics were divided by $E(lrt_{m_1})$ in Table 4.3, to give the $lrtc_{m_1}$ statistics. A probability of a Type I error of approximately 0.04 corresponds to a threshold of 4.94 in this case. Also for the case of $m=20$ and the values of $X=0(0.2)1.8$ were used twice within each profile, the lrt_{m_1} statistics were divided by $E(lrt_{m_1})$ in Table 4.4 to obtain the $lrtc_{m_1}$ statistics. A threshold of 4.52 produced a probability of a Type I error of approximately 0.04 in this case. Finally, for the case of $m=20$ and the fixed X -values of $-30, -23, -12, -4, 0, 3, 10, 20, 25,$ and 35 were used, the lrt_{m_1} statistics were divided by $E(lrt_{m_1})$ in Table 4.5 to obtain the $lrtc_{m_1}$ statistics. The threshold that corresponds to a probability of a Type I error of approximately 0.04 is approximately 4.55. Each threshold was estimated independently using 100,000 simulations.

The types of shifts investigated in this simulation are sustained step shifts taking place after sample k ($k < m$) for $k = 10, 15, 18$ and 19 if $m=20$ or $k = 40, 45, 57$ and 59 if $m=60$. Figures 4.1-4.4 show the simulated overall probabilities of an out-of-control signal for shifts in the Y -intercept, slope under the model in Equation (2.1), slope under the model in Equation (2.11), and process standard deviation, respectively, when $m=20$ and $X=0(0.2)1.8$. Figures 4.5-4.8 illustrate these probabilities when $m=60$ and $X=0(0.2)1.8$. Also Figures 4.9-4.12 present these probabilities when $m=20$ and $X=0(0.2)1.8$ were used twice within each profile. Finally, Figures 4.13-4.16 show these probabilities when $m=20$ and $X= -30, -23, -12, -4, 0, 3, 10, 20, 25,$ and 35 were used.

As shown in Figures 4.1-4.16, Method LRT has uniformly much better performance than the competing methods for shifts in the Y -intercept, slopes, or process standard deviation, when $k=10, 15, \text{ or } 18$ and $m=20$. Similar conclusion was obtained when $k=40, 45, \text{ or } 57$ and $m=60$. If the shift affects only the last profile, Method LRT and Method C have very similar performance, with Method C performs slightly better for very large shifts in the Y -intercept or slope under the model in Equation (2.11). For shifts in the process standard deviation affect the last sample, the three methods have very similar performance.

The out-of-control situations considered in these simulations are sustained step shifts taking place after k out of m samples. In practice, however, another out-of-control situation can occur, in which k unsustained shifts are scattered randomly among the m samples. It is known that the statistical approaches used for detecting parameter changes differ in reacting to different out-of-control situations. To investigate the performance of Method LRT under randomly occurring unsustained shifts in a process parameter, the underlying in-control linear profile model $Y_{ij} = X_i + \varepsilon_{ij}$, $i = 1, 2, \dots, n_j$, $j=1, 2, \dots, m$, was considered. The ε_{ij} 's were assumed to be i.i.d. $N(0, 1)$ random variables. The number of samples $m=20$ and the fixed X -values of $0(0.2)1.8$ were used in this simulation. The number of randomly occurring unsustained shifts of $k=1$ or 2 was considered.

Figures 4.17-4.20 show the simulated overall probabilities of an out-of-control signal when there are k ($k=1$ or 2) randomly occurring unsustained shifts in the Y -intercept, slope under the model in Equation (2.1), slope under the model in Equation (2.11), and process standard deviation, respectively. As shown in Figures 4.17-4.20, contrary to its performance in detecting sustained shifts in a process parameter, Method LRT has very poor performance in detecting isolated, temporary shifts.

Figure 4.1: Probability of out-of-control signal under intercept shifts from A_0 to $A_0 + \lambda \sigma / \sqrt{n}$ ($m=20$ and $X=0(0.2)1.8$).

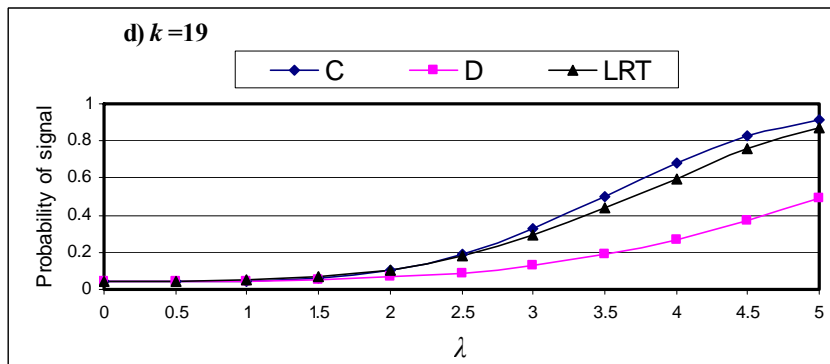
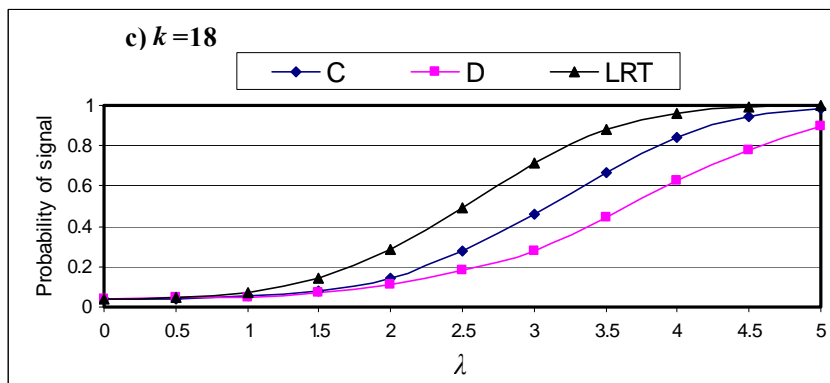
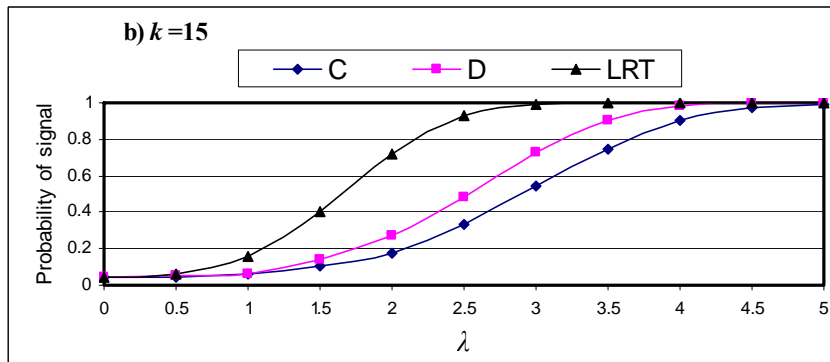
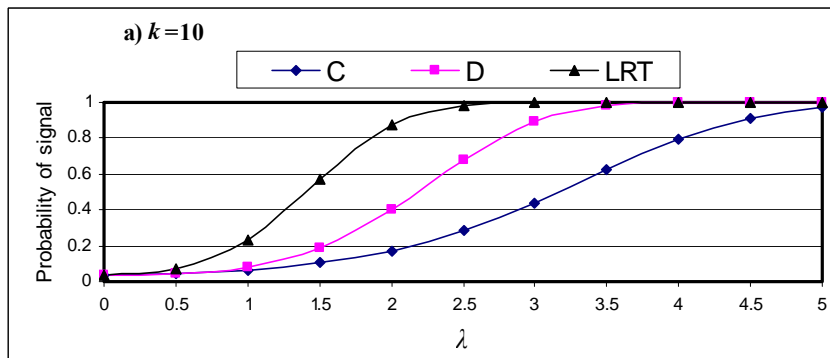


Figure 4.2: Probability of out-of-control signal under slope shifts from A_1 to $A_1 + \beta \sigma / \sqrt{S_{xx}}$ ($m=20$ and $X=0(0.2)1.8$).

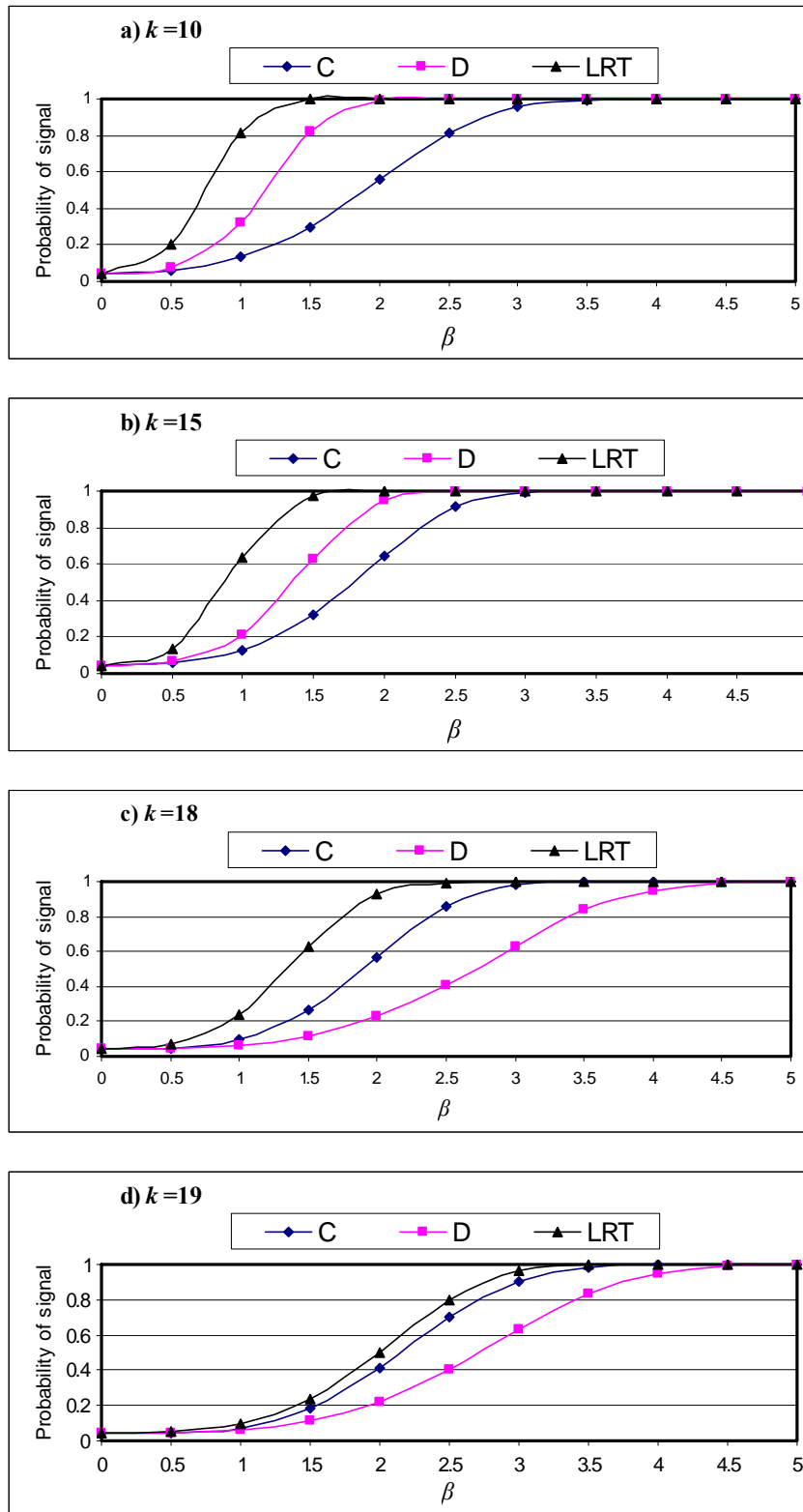


Figure 4.3: Probability of out-of-control signal under slope shifts from B_1 to $B_1 + \delta \sigma / \sqrt{S_{xx}}$ ($m=20$ and $X=0(0.2)1.8$).

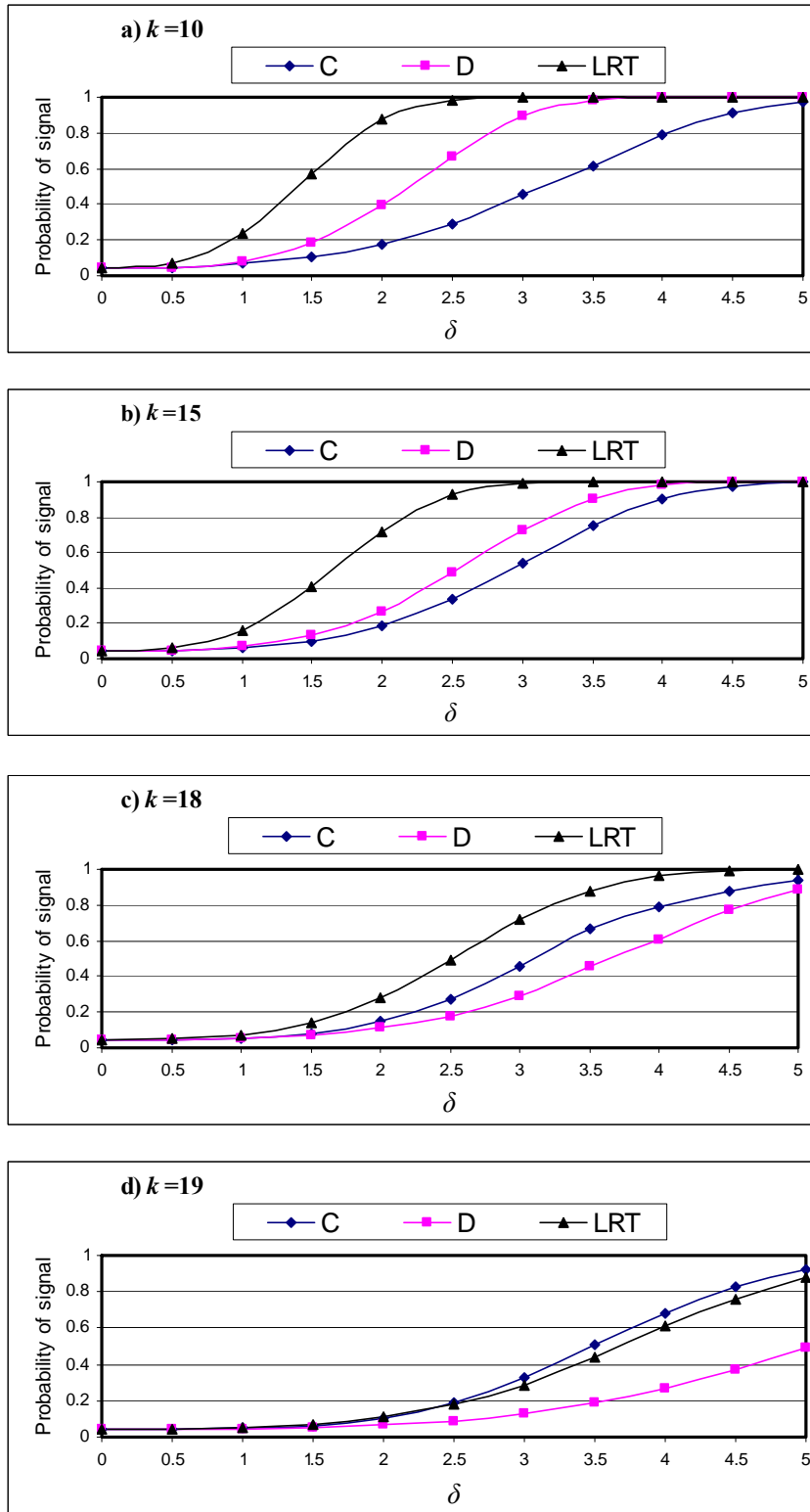


Figure 4.4: Probability of out-of-control signal under standard deviation shifts from σ to $\gamma\sigma$ ($m=20$ and $X=0(0.2)1.8$).

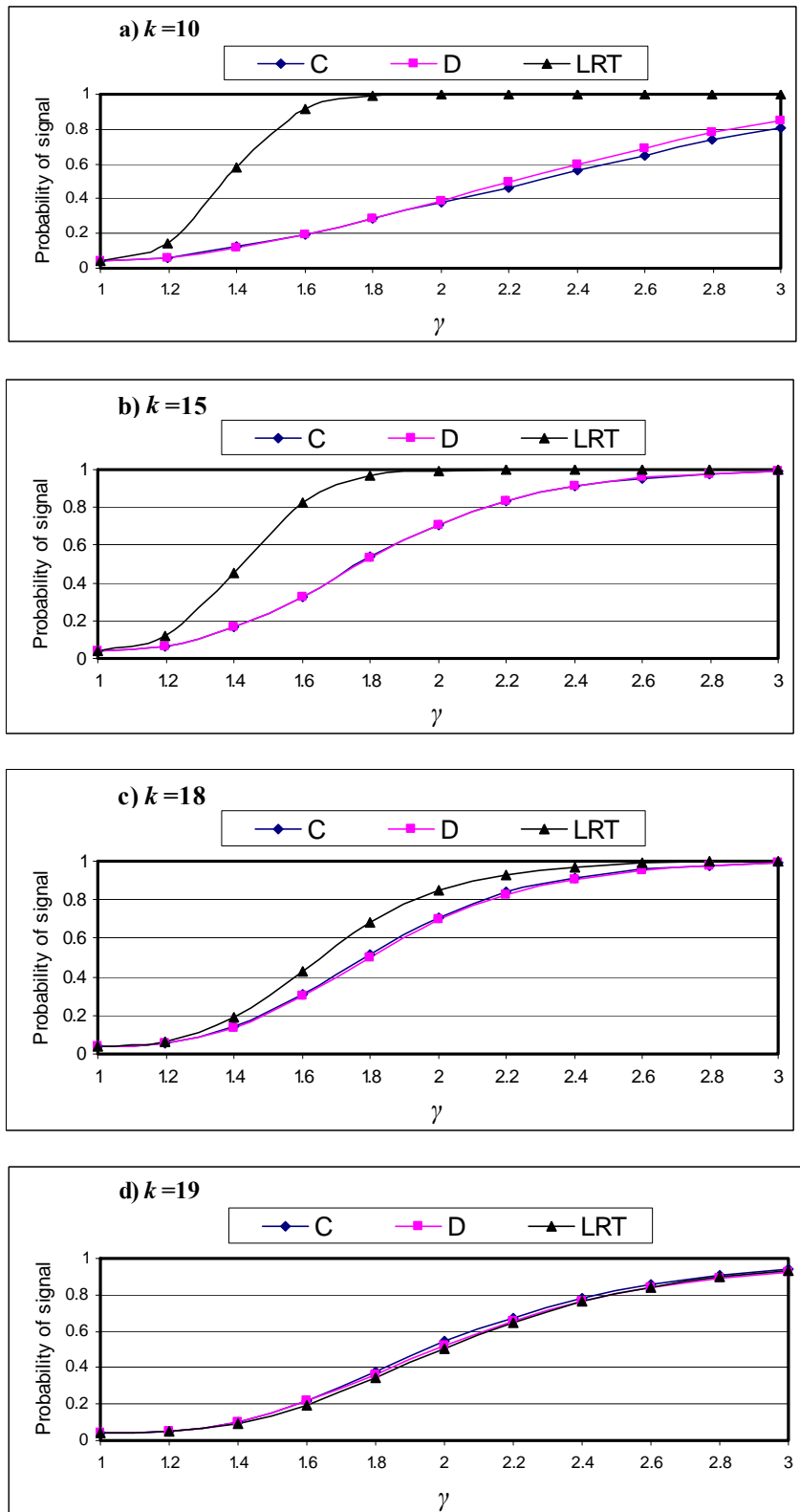


Figure 4.5: Probability of out-of-control signal under intercept shifts from A_0 to $A_0 + \lambda \sigma / \sqrt{n}$ ($m=60$ and $X=0(0.2)1.8$).

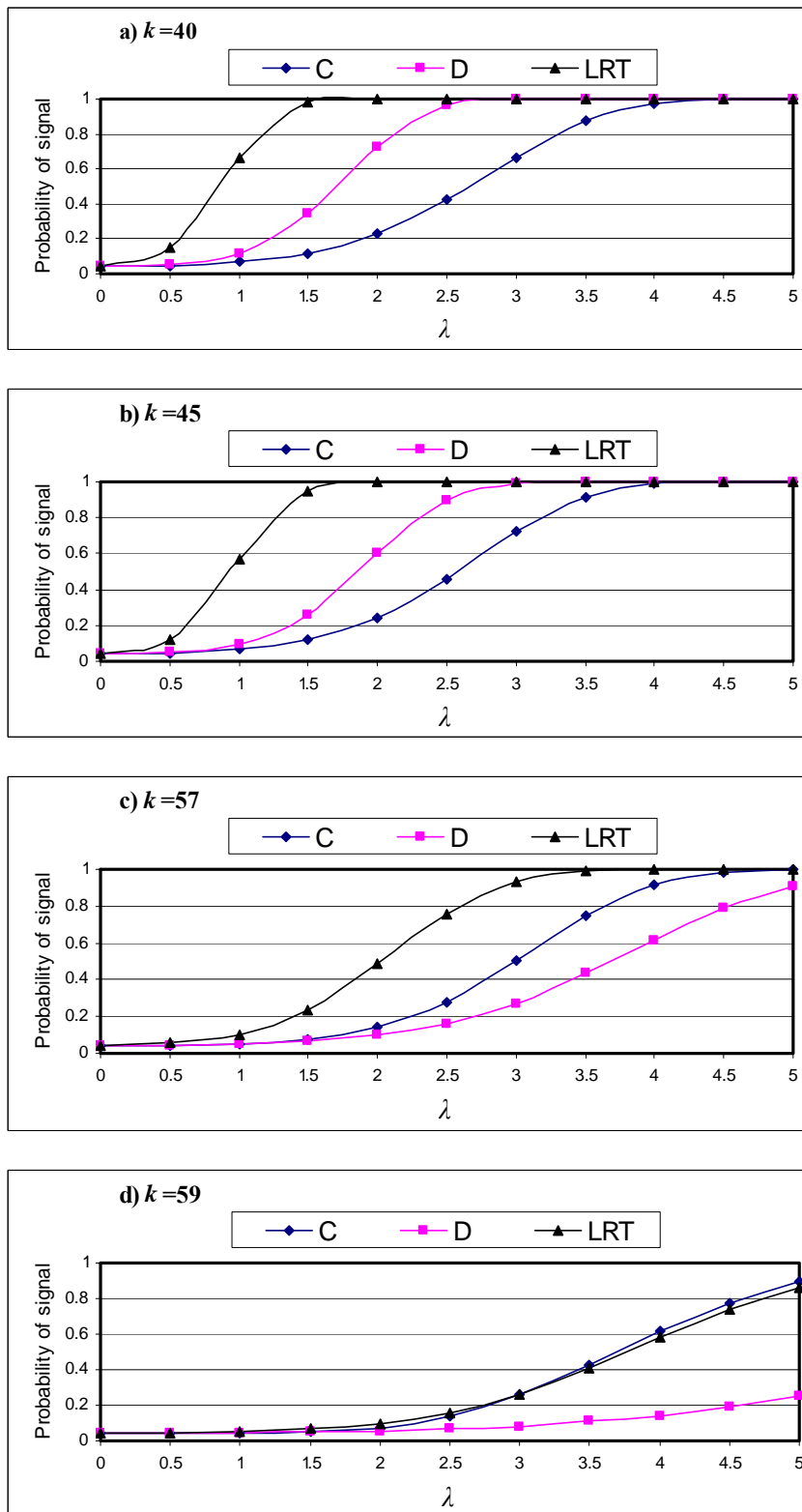


Figure 4.6: Probability of out-of-control signal under slope shifts from A_1 to $A_1 + \beta \sigma / \sqrt{S_{xx}}$ ($m=60$ and $X=0(0.2)1.8$).

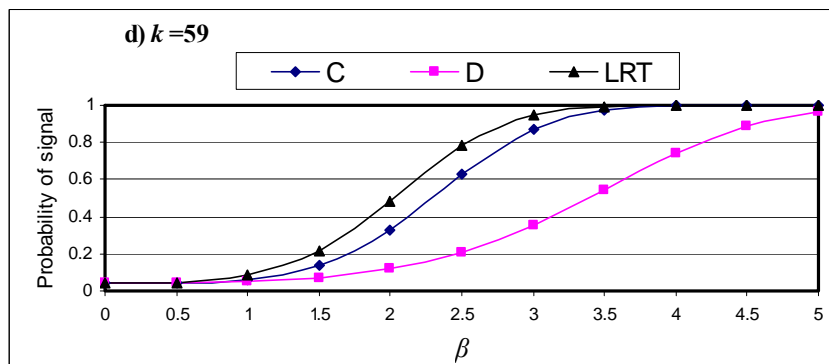
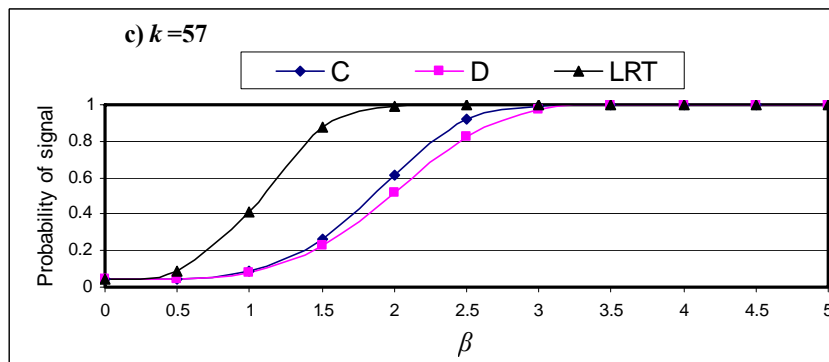
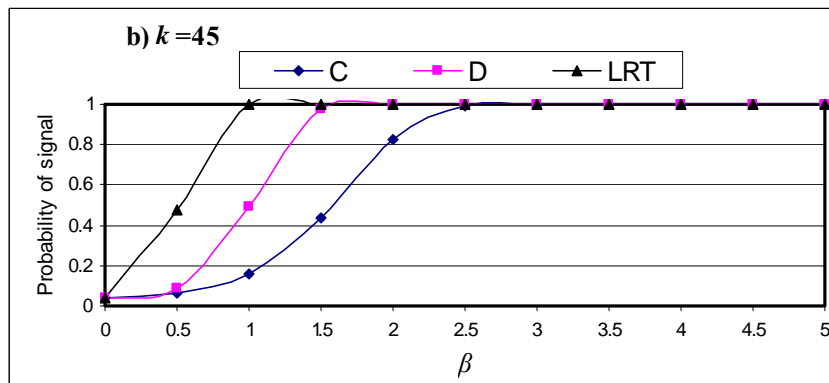
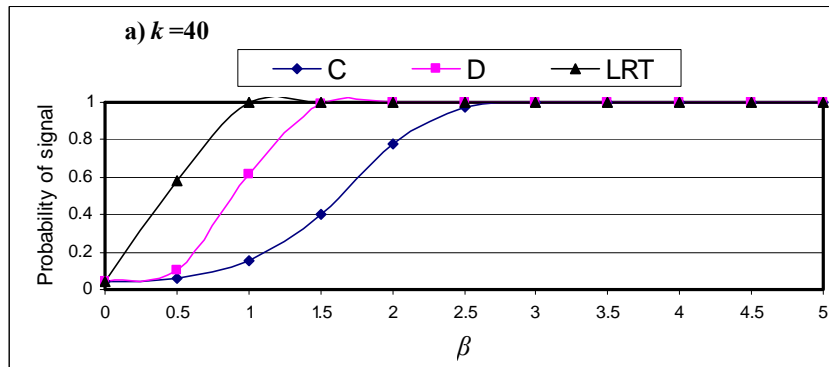


Figure 4.7: Probability of out-of-control signal under slope shifts from B_1 to $B_1 + \delta \sigma / \sqrt{S_{xx}}$ ($m=60$ and $X=0(0.2)1.8$).

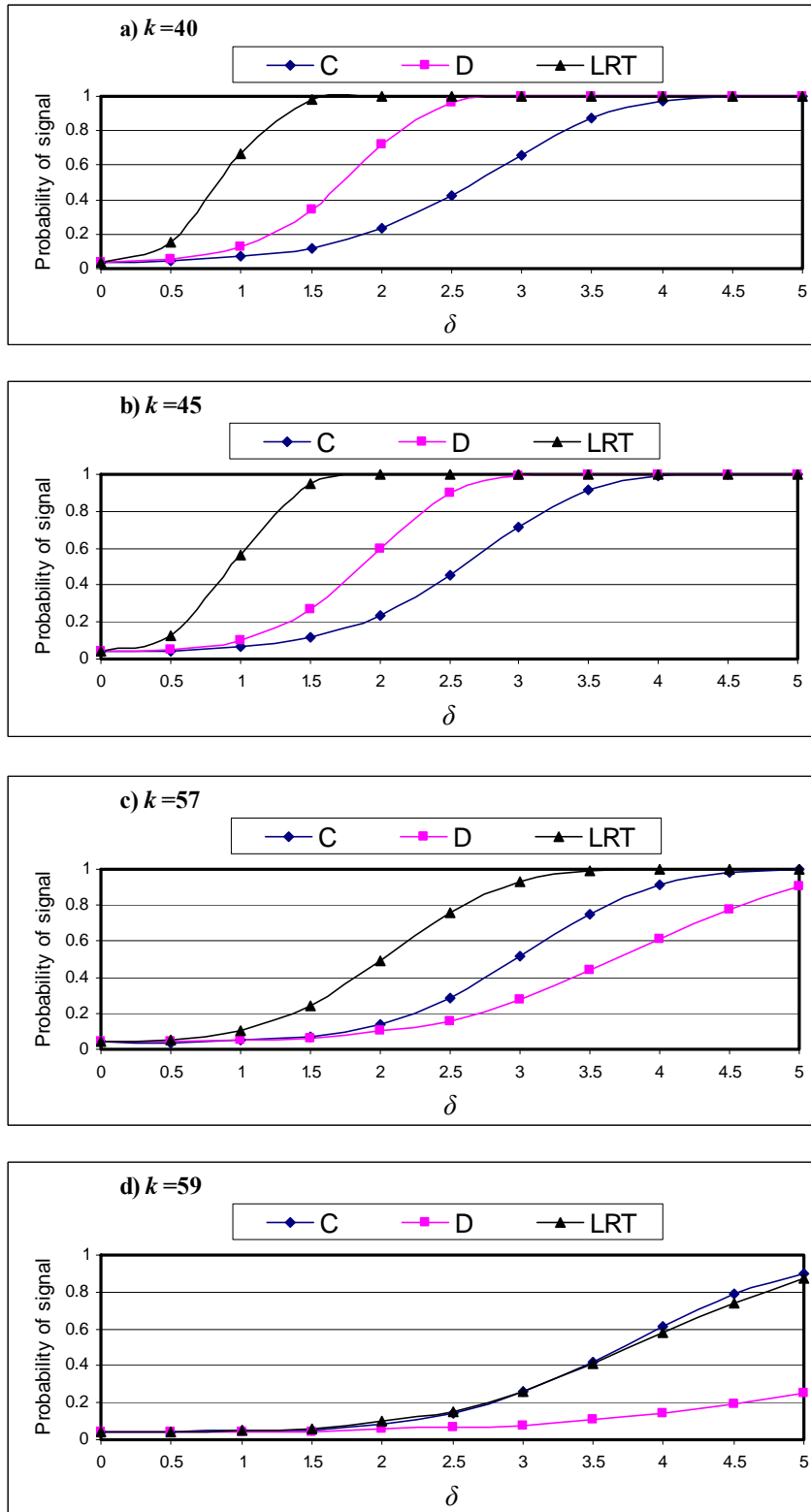


Figure 4.8: Probability of out-of-control signal under standard deviation shifts from σ to $\gamma\sigma$ ($m=60$ and $X=0(0.2)1.8$).

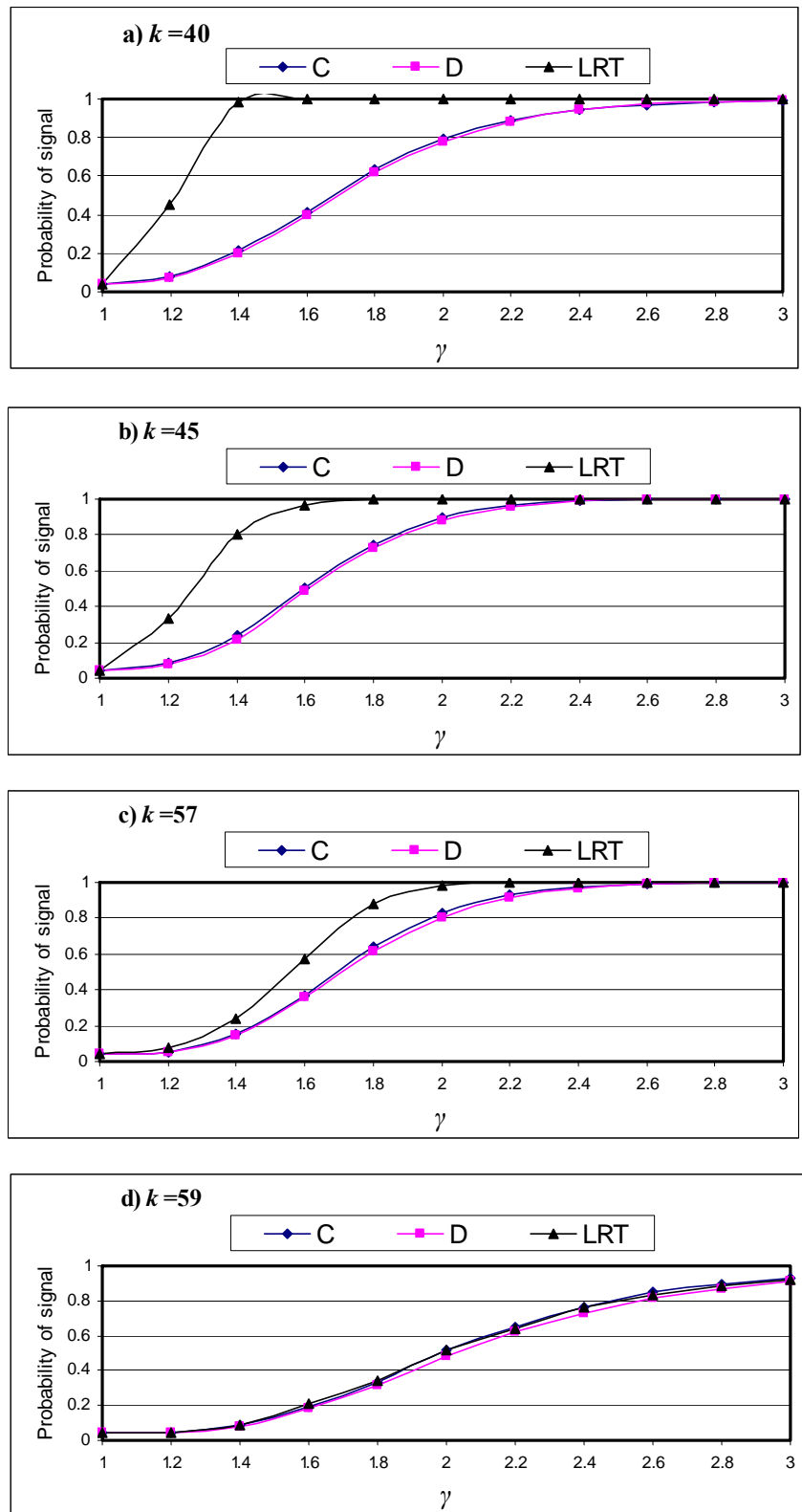


Figure 4.9: Probability of out-of-control signal under intercept shifts from A_0 to $A_0 + \lambda \sigma / \sqrt{n}$ ($m=20$ and the values of $X=0(0.2)1.8$ are used twice).

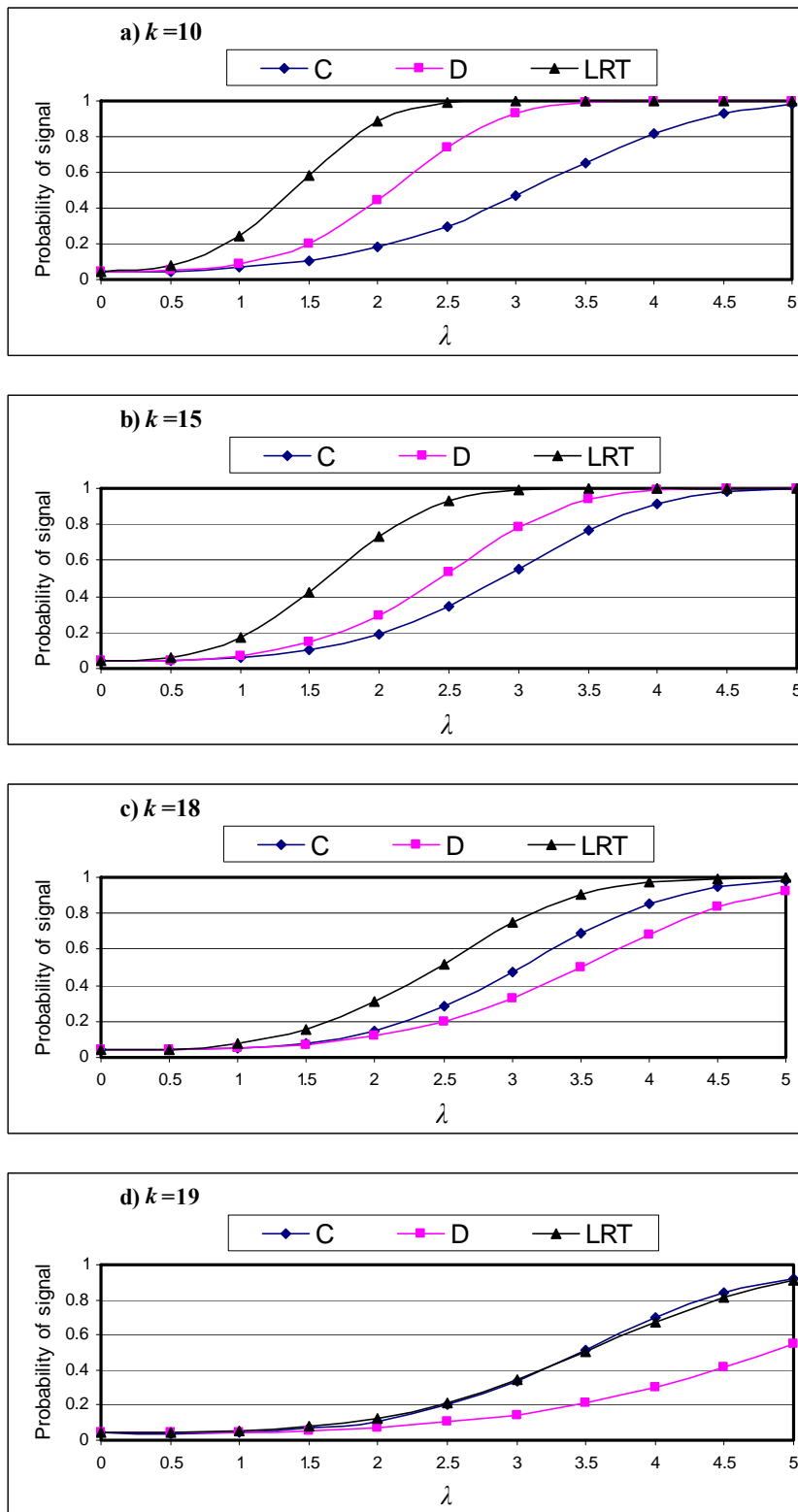


Figure 4.10: Probability of out-of-control signal under slope shifts from A_1 to $A_1 + \beta \sigma / \sqrt{S_{xx}}$ ($m=20$ and the values of $X=0(0.2)1.8$ are used twice).

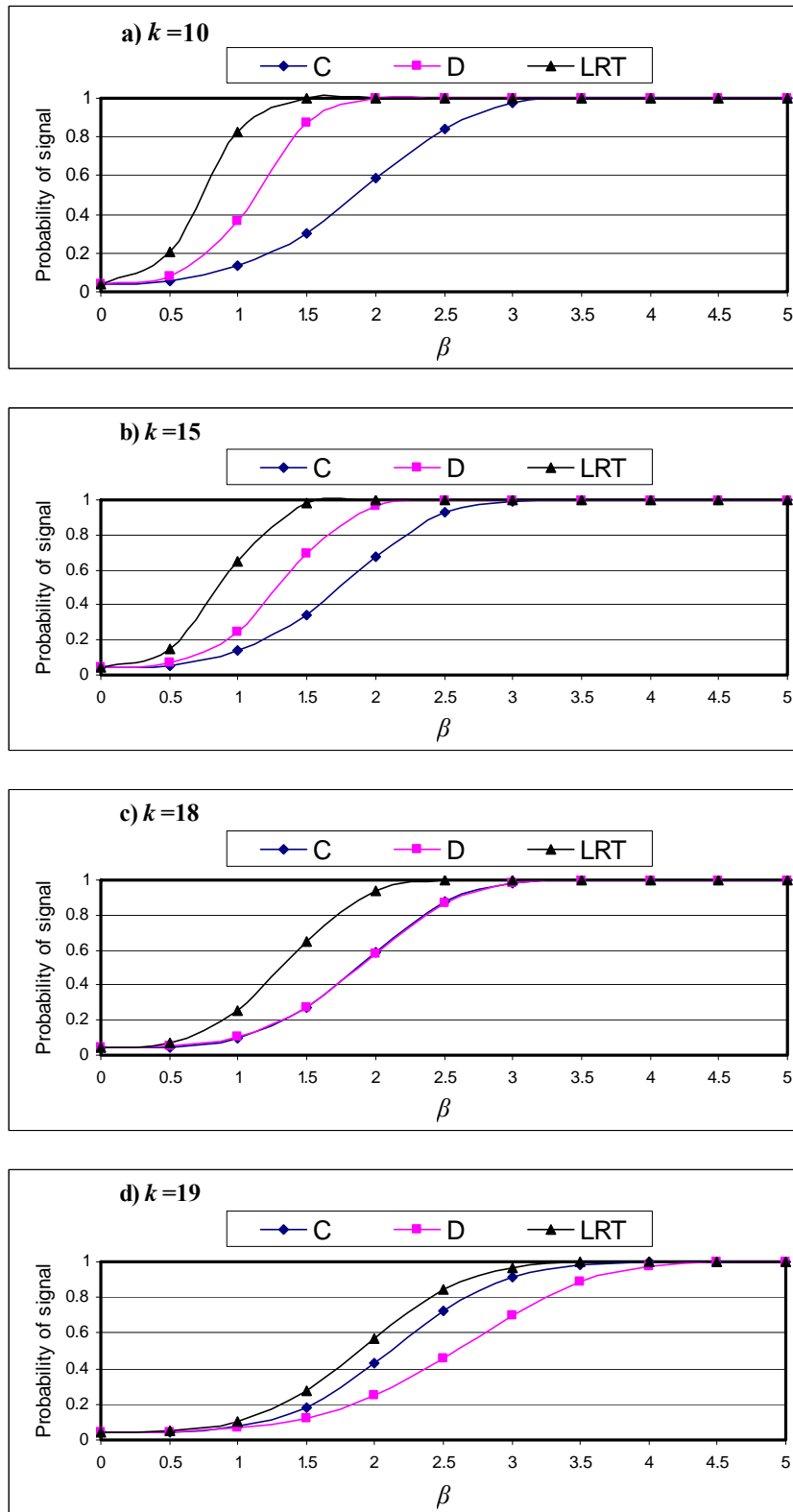


Figure 4.11: Probability of out-of-control signal under slope shifts from B_1 to $B_1 + \delta \sigma / \sqrt{S_{xx}}$ ($m=20$ and the values of $X=0(0.2)1.8$ are used twice).

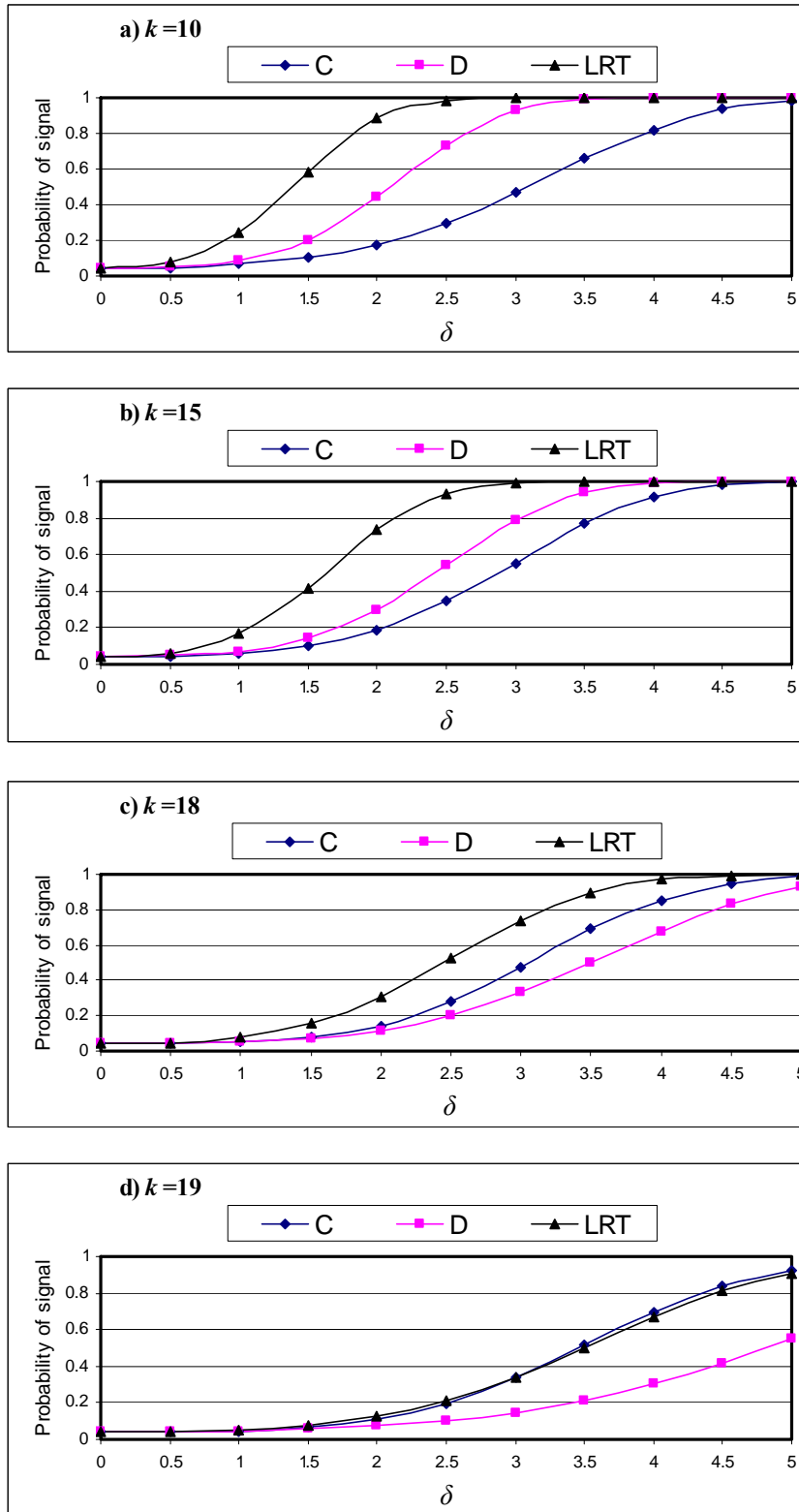


Figure 4.12: Probability of out-of-control signal under standard deviation shifts from σ to $\gamma\sigma$ ($m=20$ and the values of $X=0(0.2)1.8$ are used twice).

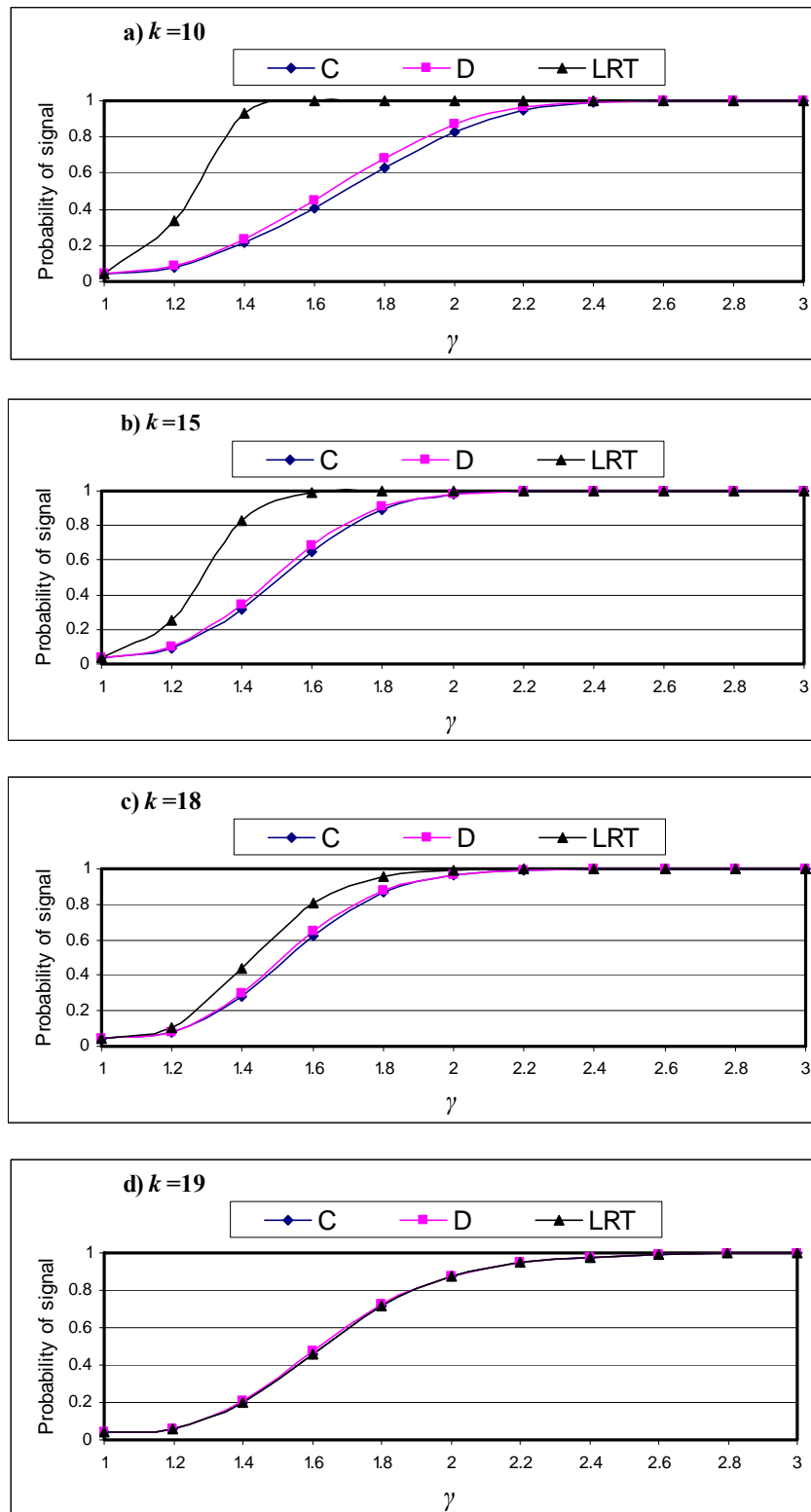


Figure 4.13: Probability of out-of-control signal under intercept shifts from A_0 to $A_0 + \lambda \sigma / \sqrt{n}$ ($m=20$ and $X = -30, -23, -12, -4, 0, 3, 10, 20, 25,$ and 35).

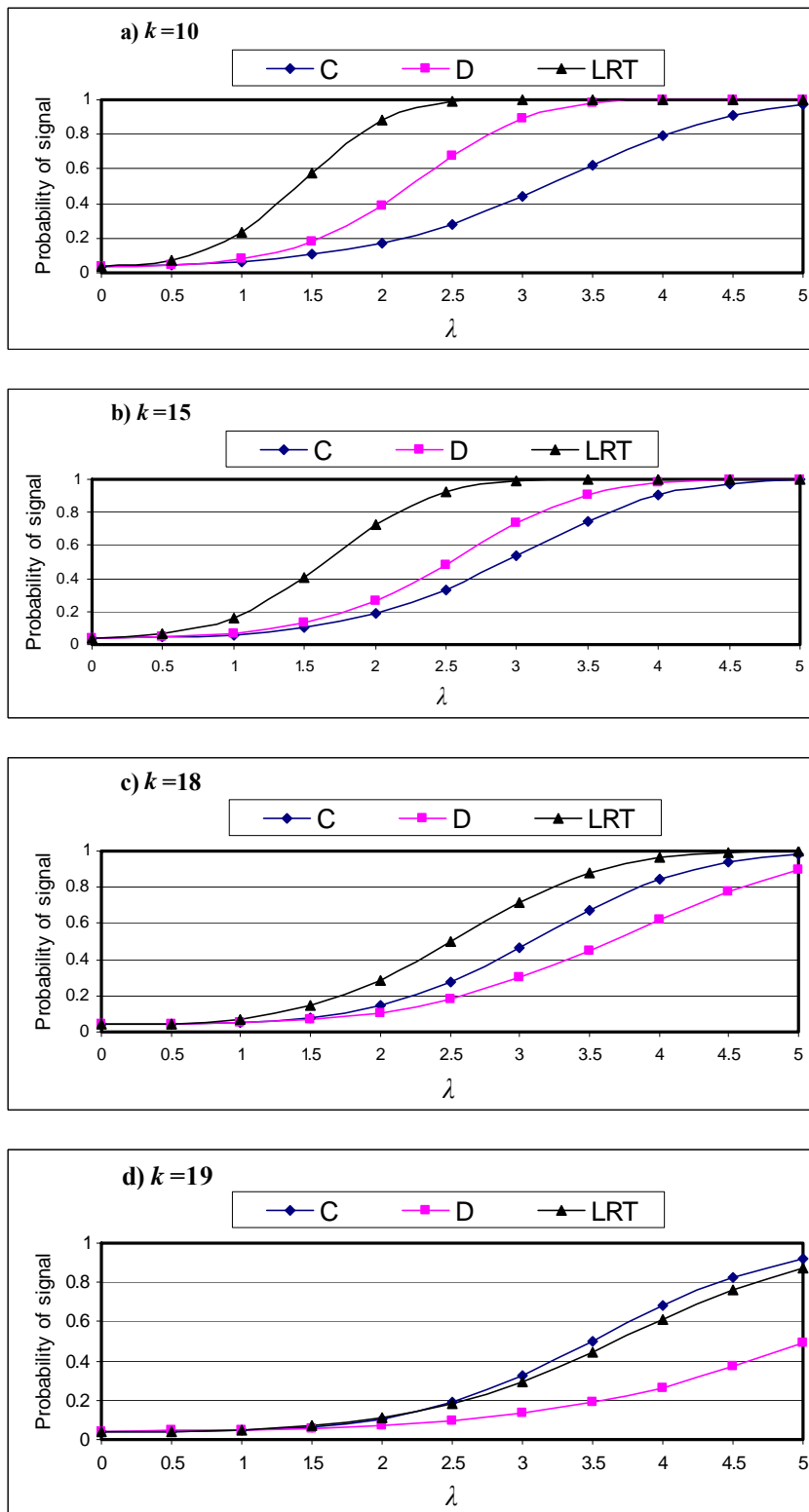


Figure 4.14: Probability of out-of-control signal under slope shifts from A_1 to $A_1 + \beta \sigma / \sqrt{S_{xx}}$ ($m=20$ and $X=-30, -23, -12, -4, 0, 3, 10, 20, 25,$ and 35).

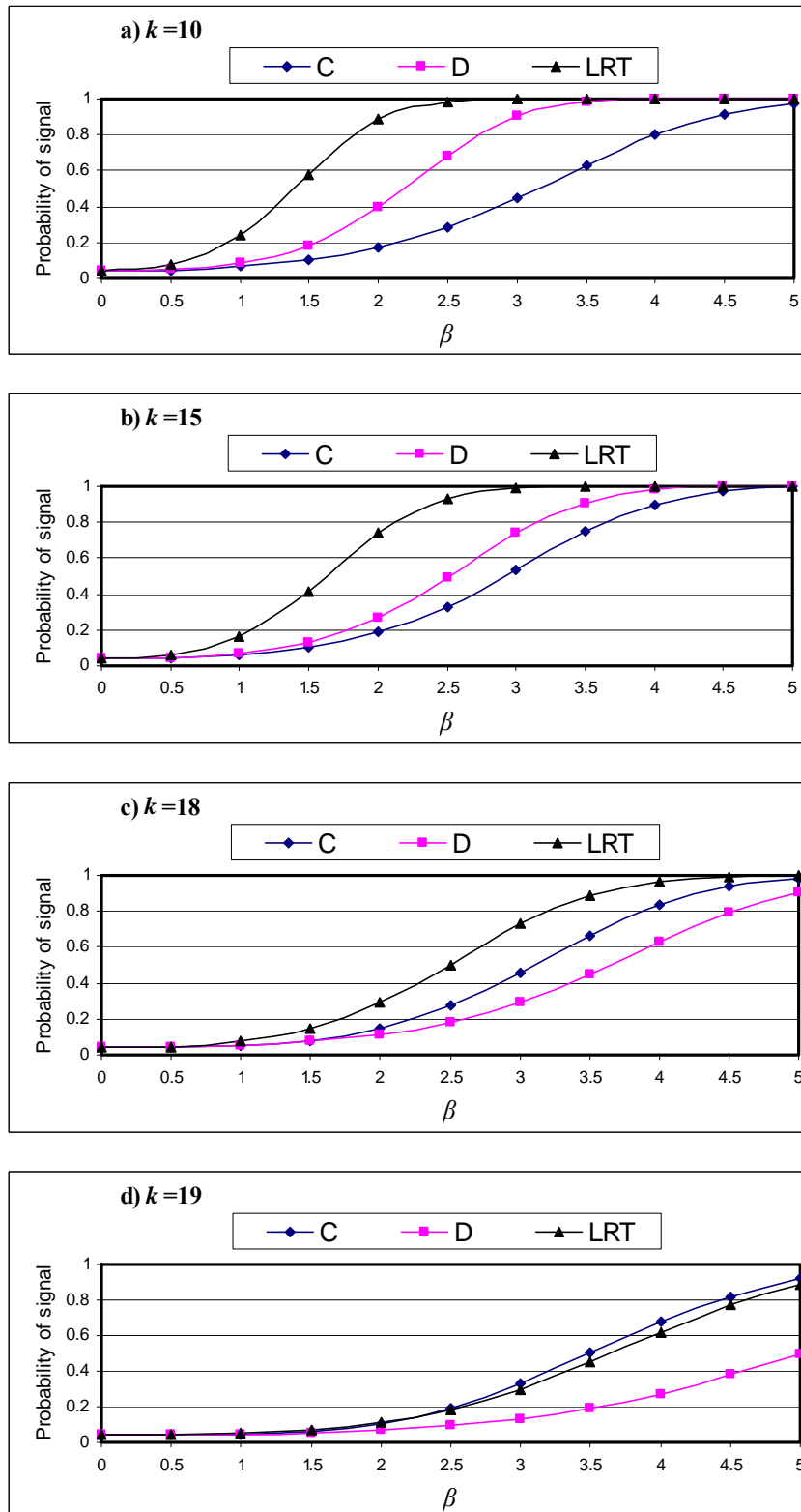


Figure 4.15: Probability of out-of-control signal under slope shifts from B_1 to $B_1 + \delta \sigma / \sqrt{S_{xx}}$ ($m=20$ and $X = -30, -23, -12, -4, 0, 3, 10, 20, 25,$ and 35).

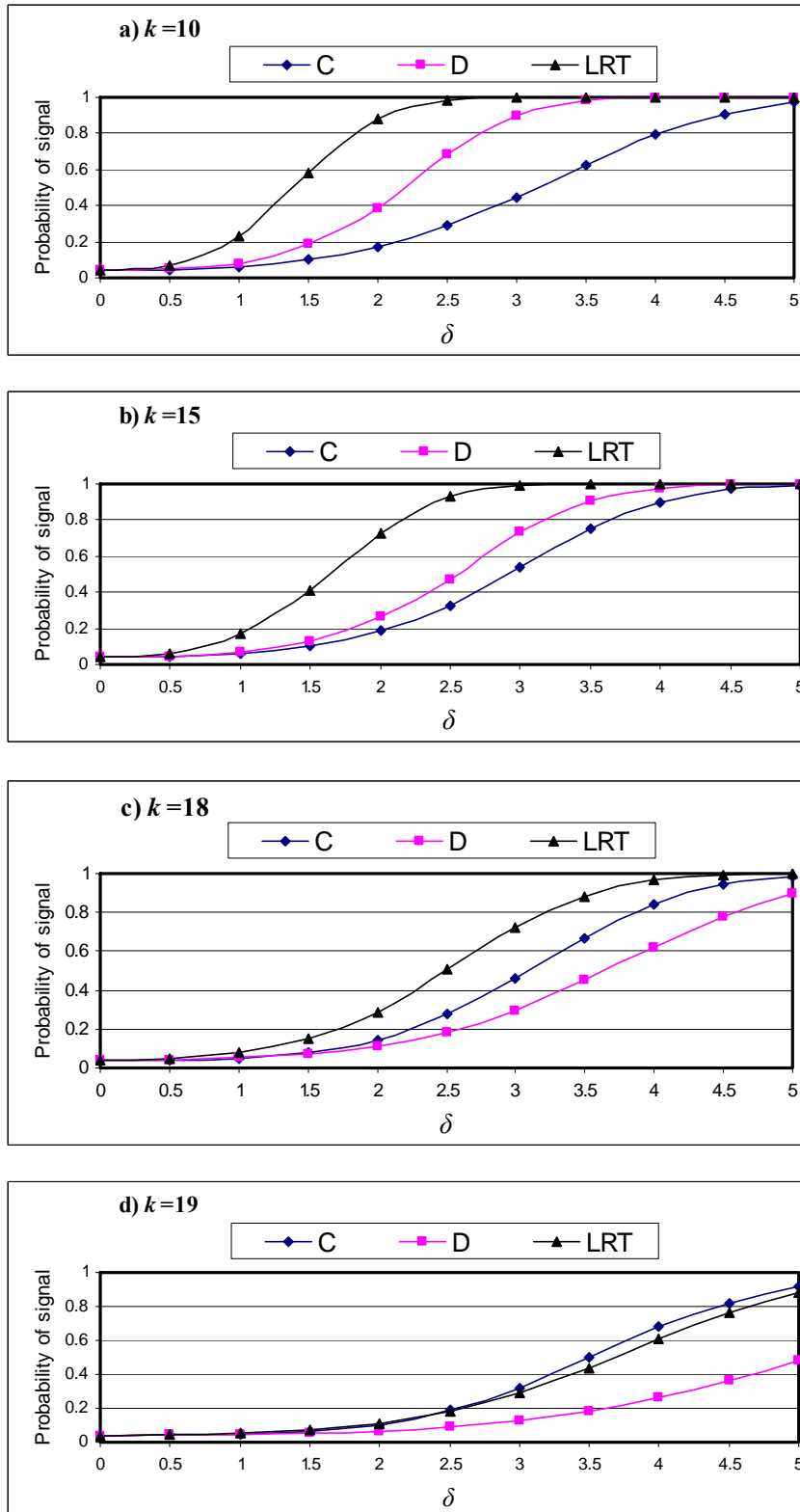


Figure 4.16: Probability of out-of-control signal under standard deviation shifts from σ to $\gamma\sigma$ ($m=20$ and $X=-30, -23, -12, -4, 0, 3, 10, 20, 25,$ and 35).

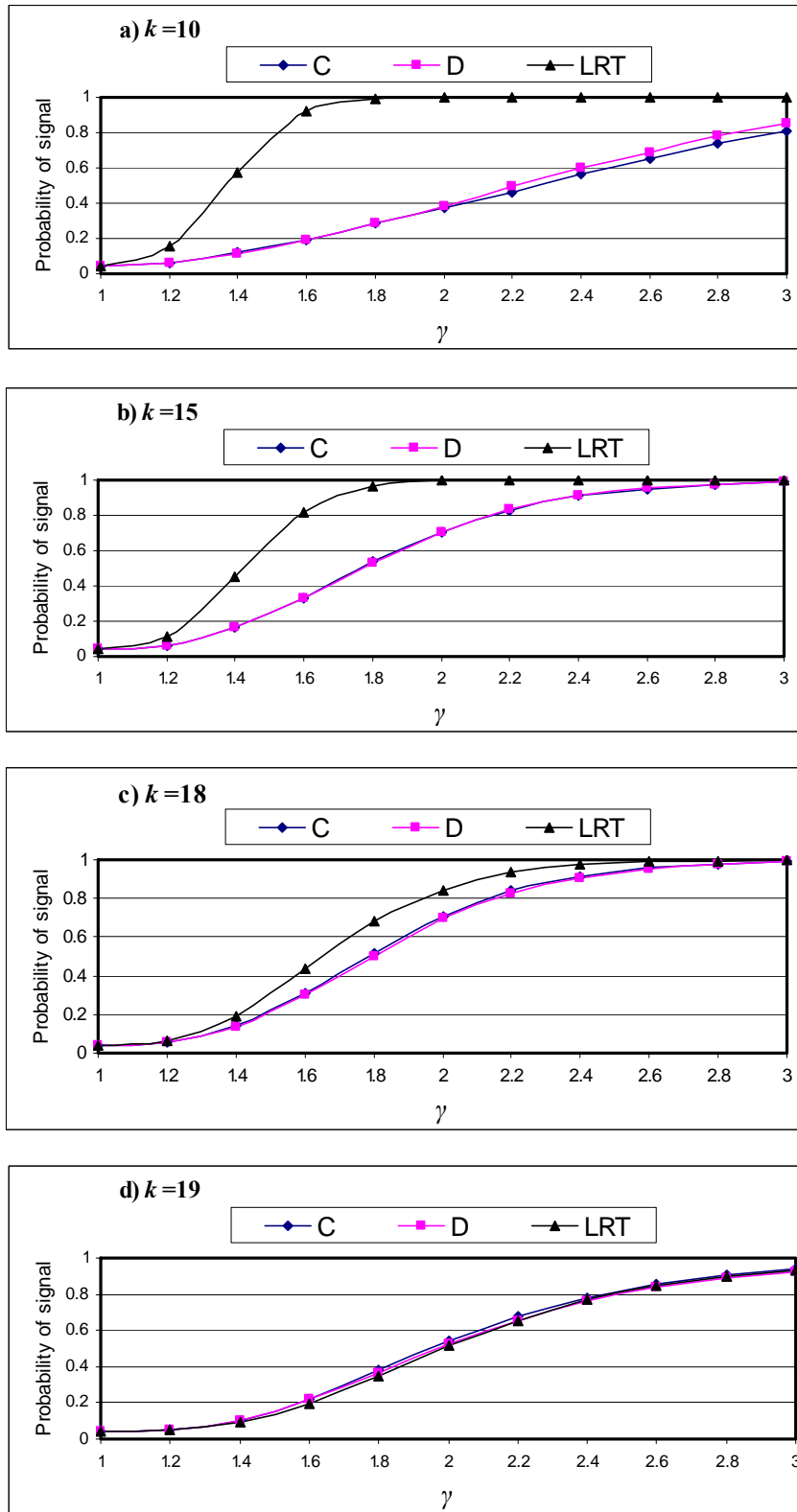


Figure 4.17: Probability of out-of-control signal under randomly occurring unsustained intercept shifts from A_0 to $A_0 + \lambda \sigma / \sqrt{n}$.

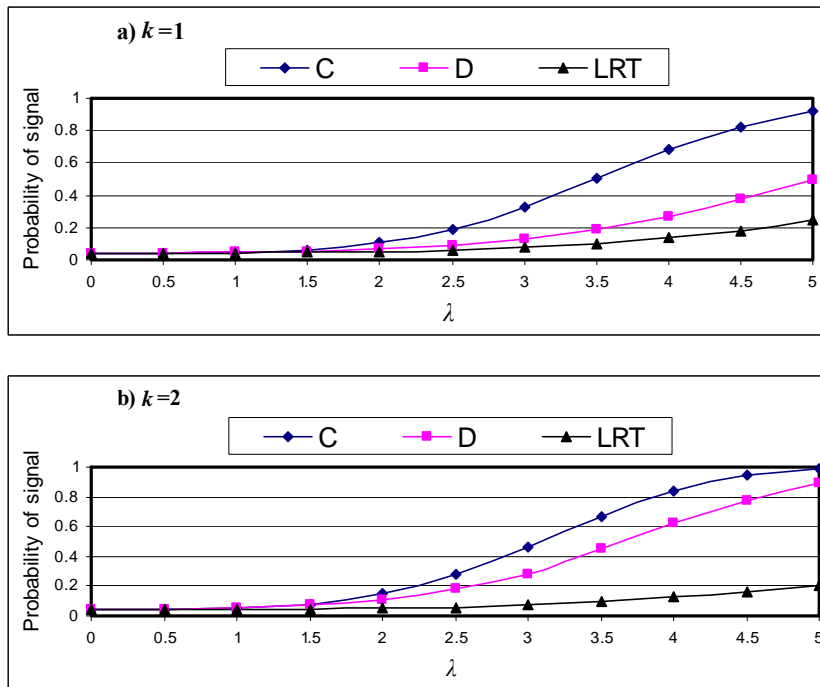


Figure 4.18: Probability of out-of-control signal under randomly occurring unsustained slope shifts from A_1 to $A_1 + \beta \sigma / \sqrt{S_{xx}}$.

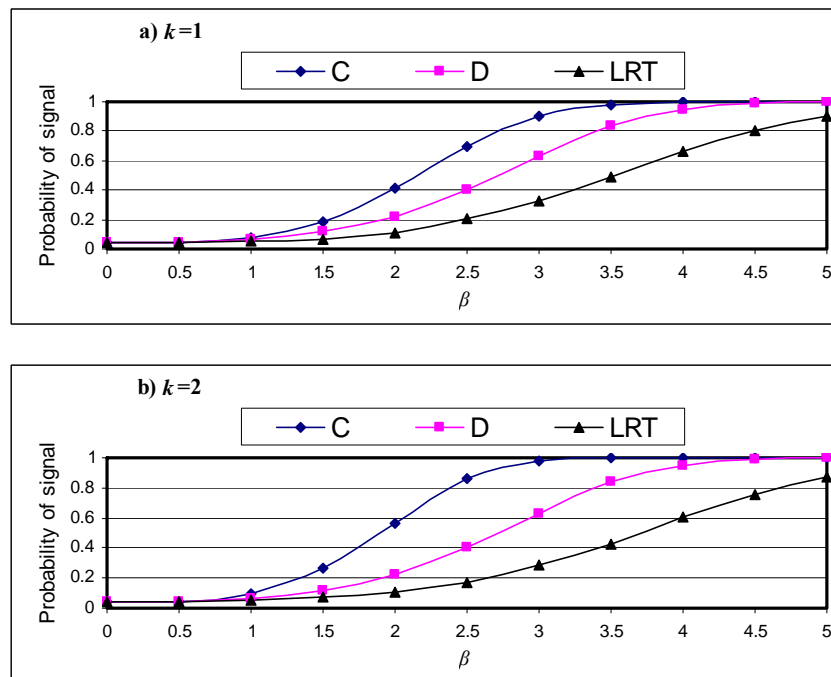


Figure 4.19: Probability of out-of-control signal under randomly occurring unsustained slope shifts from B_1 to $B_1 + \delta \sigma / \sqrt{S_{xx}}$.

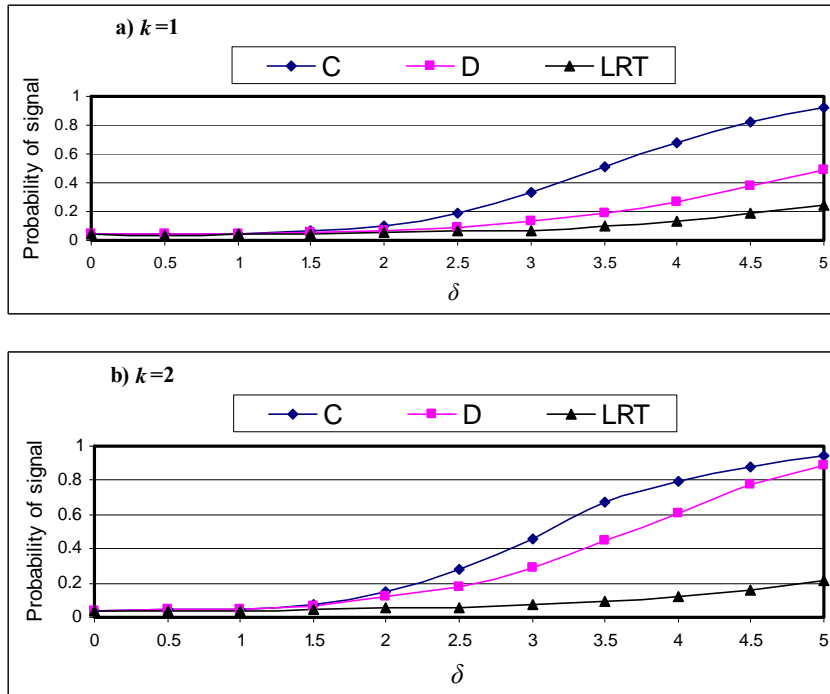
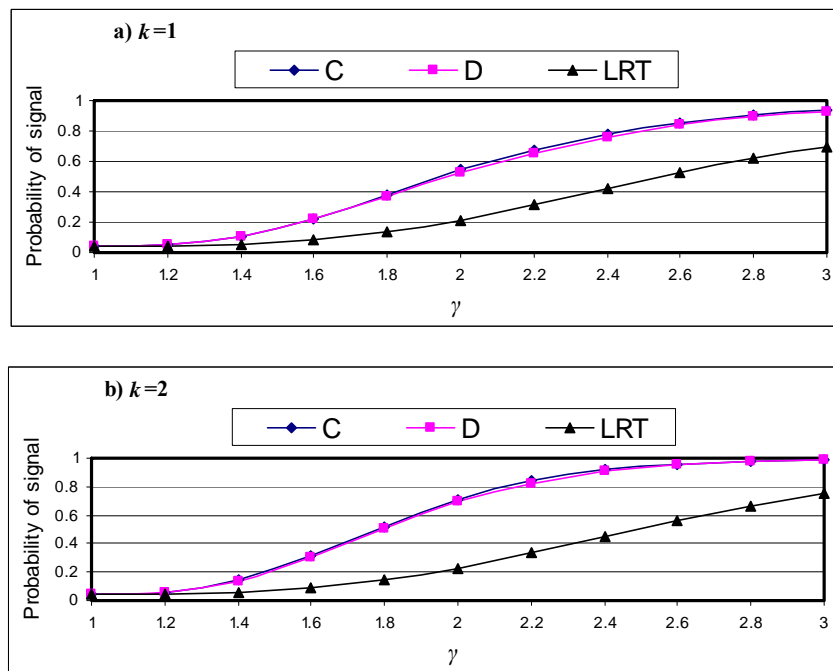


Figure 4.20: Probability of out-of-control signal under randomly occurring unsustained standard deviation shifts from σ to $\gamma\sigma$.



In general, Method LRT performs uniformly better than the competing control chart methods under sustained parameter shifts. On the other hand, both Method C and Method D have much better performance than Method LRT in detecting some other types of shifts in a process parameter. To protect against both kind of changes, sustained and randomly occurring unsustained shifts, one can employ Method LRT in conjunction with either Method C or Method D.

4.C Approximate Test Statistics

As mentioned in Section 4.A.2, the expected values of the lrt_{m_1} statistics in Equation (4.2) depend on the value of m_1 . An additional improvement to the performance of Method LRT was obtained by dividing each lrt_{m_1} statistic by its expected value $E(lrt_{m_1})$ to give the $lrtc_{m_1}$ statistics. Also, it is clear that the $m-1$ statistics, $lrtc_{m_1}$, $m_1=1, 2, \dots, m-1$, are correlated. The distribution of the maximum of the $lrtc_{m_1}$ [$\max(lrtc_{m_1})$] is intractable; hence thresholds that correspond to a specific probability of a Type I error cannot be exactly determined. In most applications, however, it is sufficient to find easily calculated thresholds that produce approximately the desired probability of a Type I error.

4.C.1 Approximate Thresholds

It can be shown that the probability of $\max(lrtc_{m_1})$ exceeding a threshold T is equal to the probability of the union of the $m-1$ $lrtc_{m_1}$ statistics exceeding T . The upper bound for the probability of the union of a sequence of LRT statistics can be determined based on the Bonferroni's inequality. The upper bound of the probability of the $\max(lrtc_{m_1})$ statistic under the null hypothesis of no change can be calculated using

$$\Pr(\max(lrtc_{m_1}) > T) \leq (m - 1) \Pr(lrt_{m_1} > T / 3). \quad (4.4)$$

The value of 3 in the right hand side of Equation (4.4) represents the asymptotic expected

value of the LRT statistic in Equation (4.2). Previous studies and our simulation studies show that the upper bound in Equation (4.4) is very conservative, unless m and α are very small. Table 4.6 shows the simulated overall probabilities of a Type I error produced using the conservative Bonferroni's inequality in Equation (4.4). In this simulation, the underlying in-control model with $A_0=0$ and $A_1=1$ and the fixed X -values of $0(0.2)1.8$ were used. As shown in Table 4.6, the conservative Bonferroni's inequality does not give accurate bound for the null probability distribution of the test statistics except for very small values of m and α .

Table 4.6: The overall probabilities of a Type I error using the conservative Bonferroni's inequality.

Nominal	Simulated						
	$m=5$	$m=10$	$m=15$	$m=20$	$m=30$	$m=40$	$m=60$
0.01	0.0098	0.0088	0.0084	0.0082	0.0072	0.0058	0.0038
0.02	0.0205	0.0176	0.0159	0.0135	0.0123	0.0114	0.0092
0.05	0.0469	0.0383	0.0343	0.0316	0.0276	0.0237	0.0214
0.10	0.0893	0.0764	0.0645	0.0602	0.0513	0.0444	0.0375
0.20	0.1620	0.1375	0.1232	0.1104	0.0911	0.0812	0.0660

Worsley (1983) proposed an improved Bonferroni's inequality for the two-segment multiple regression model. The improved Bonferroni's inequality, however, does not give accurate bound for the null probability distribution of the test statistics, as shown by Worsley (1983), if the sample size and/or α is large.

A valid alternative approach is a Bonferroni-like inequality

$$\Pr(\max(lrtc_{m_1}) > T) \leq r(m) \Pr(lrt_{m_1} > T/3), \quad (4.5)$$

where $r(m)$ is a function of m to give the most accurate bound for the Type I error probability. Using 20,000 simulated sets of samples, the author estimated the values of r corresponding to different values of m that minimized the maximum difference between the simulated CDF and the approximated CDF of $\max(lrtc_{m_1})$,

$$F_{\max}(x) = 1 - r(m)[1 - F(3x)],$$

at the 95th percentile of the distribution, where $F(\cdot)$ is the CDF of the chi-squared distribution with 3 degrees of freedom. The values of 5(5)90 for m were considered. In these simulations, the underlying in-control linear profile model with $A_0=0$ and $A_1=1$ and the fixed X -values of 0(0.2)1.8 were used.

The best values of r corresponding to different values of m are given in Table 4.7. Different simulations using different values for the variable X and for the sample size n gave approximately the same estimates for r as reported in Table 4.7. A least squares estimate for the best values of r using the logarithm of m as the independent variable in a simple linear regression model gave the following approximation for r

$$r^*(m) = -11.5 + 8.05 \log m. \quad (4.6)$$

Table 4.7: Best and approximate values of r .

m	Best r	r^*	m	Best r	r^*	m	Best r	r^*
5	3.72	1.455975	35	16.67	17.12055	65	21.89	22.10382
10	7.1	7.03581	40	18.2	18.19548	70	22.65	22.70039
15	9.3	10.2998	45	19.17	19.14363	75	23.58	23.25578
20	11.2	12.61565	50	19.95	19.99179	80	24.45	23.77531
25	13.12	14.41195	55	20.63	20.75903	85	24.71	24.26334
30	14.88	15.87964	60	21.3	21.45947	90	26.07	24.72347

Using r^* in Equation (4.6), the maximum difference between the simulated and approximated CDF for $\max(lrtc_{m_1})$ at the 95th percentile of the distribution was less than 0.001 for all values of $m > 6$. For very small values of m , the difference was appreciably larger. A better approximation for the upper bound of the probability of the $\max(lrtc_{m_1})$ statistic when $m \leq 6$ was obtained using the conservative Bonferroni's inequality in Equation (4.4). Therefore a threshold for the $\max(lrtc_{m_1})$ statistic that corresponds to a probability of a Type I error of α can be approximated using

$$T = \begin{cases} \chi_{3,1-\alpha/(m-1)}^2 / 3 & \text{if } m \leq 6 \\ \chi_{3,1-\alpha/r^*}^2 / 3 & \text{if } m > 6 \end{cases}, \quad (4.7)$$

where $\chi_{3,1-\alpha/(m-1)}^2$ is the $100(1-\alpha/(m-1))$ percentile of the chi-squared distribution with 3 degrees of freedom.

4.C.2 Approximate Normalizing Factor

The normalizing factor C_{m_1} used to obtain the $lrtc_{m_1}$ statistics can be determined by simulation as in Section 4.A.2. Alternatively, approximations of $E(lrtc_{m_1})$ can be obtained by using the following formula:

$$e_{m_1} \approx 2 - 2\left(\frac{1}{N} - \frac{1}{N_1} - \frac{1}{N_2}\right) - \left(\frac{N}{N-2} - \frac{N_1}{N_1-2} - \frac{N_2}{N_2-2}\right) - \frac{1}{3}\left(\frac{N}{(N-2)^2} - \frac{N_1}{(N_1-2)^2} - \frac{N_2}{(N_2-2)^2}\right). \quad (4.8)$$

The proof is given in Appendix 4.B. The columns in Tables 4.1-4.5 labeled as e_{m_1} give the approximate expected values for the $lrtc_{m_1}$ statistics using Equation (4.8) for the different cases considered in these tables. As shown in Tables 4.1-4.5, for each case considered, the simulated and approximate expected values are very close. Therefore, it is recommended that one use e_{m_1} in Equation (4.8) for the normalizing factor C_{m_1} .

4.C.3 Using Approximate Statistics to Estimate Probabilities of Type I Error

Table 4.8 presents the estimated probabilities of a Type I error produced by Method LRT when using the normalizing factor in Equation (4.8) to calculate the $lrtc_{m_1}$ statistics, with a threshold T calculated using Equation (4.7). The first column of Table 4.8 gives the desired nominal overall probabilities of a Type I error and the following columns give the estimated probabilities of a Type I error corresponding to

different values of m and n . Each of these estimates was obtained from simulating 100,000 Phase I data sets using the in-control model $Y_{ij} = X_i + \varepsilon_{ij}$, $i = 1, 2, \dots, n_j, j=1, 2, \dots, m$, and the fixed X -values of $0(0.2)1.8$. As shown in Table 4.8, the nominal and estimated probabilities of a Type I error are very close in each case considered. For some cases considered in these simulations the fixed X -values were used twice within each sample to give a linear profile model with $n=20$, and in another case they were used three times to give a linear profile model with $n=30$. Also, in the columns labeled as “*Different X values*”, the fixed X -values of $-30, -23, -12, -4, 0, 3, 10, 20, 25$, and 35 were used. In the column labeled as “*Varying X values*”, the number of samples $m=20$ was used and $X=0(0.2)1.8$ were used in samples 1 to 8, $X=0, 0.1, 0.5, 0.8, 1.8$ were used in samples 9 to 13, and $X=0.6, 0.8, 1.1, 1.2, 1.5, 1.6, 1.8$ were used in samples 14 to 20.

Table 4.8: Overall probabilities of a Type I error: nominal vs. simulated.

Nominal	Simulated						
	n=10				n=20		
	m=5	m=20	m=40	m=70	m=10	m=20	m=30
0.01	0.0101	0.0107	0.0112	0.0135	0.0093	0.0098	0.0111
0.02	0.0193	0.0189	0.0218	0.0227	0.0195	0.0199	0.0199
0.03	0.0291	0.0296	0.0304	0.0309	0.0291	0.0284	0.0273
0.05	0.0465	0.0482	0.0483	0.0495	0.047	0.0459	0.0464
0.10	0.0856	0.0858	0.0860	0.0915	0.0863	0.0854	0.0842
Nominal	Simulated						
	n=30				Different X values		Varying X Values
	m=5	m=10	m=20	m=30	m=20	m=30	m=20
0.01	0.0987	0.0951	0.0993	0.0108	0.0101	0.0102	0.0115
0.02	0.0191	0.0189	0.0192	0.0190	0.0193	0.0186	0.0184
0.03	0.0302	0.0291	0.0306	0.0309	0.0291	0.0281	0.0281
0.05	0.0465	0.0485	0.0474	0.0444	0.0489	0.0447	0.0512
0.10	0.0855	0.0846	0.0841	0.0836	0.0871	0.0821	0.0831

In general, the use of e_{m_1} in Equation (4.8) to calculate the $lrtc_{m_1}$ statistics and T in Equation (4.7) as a threshold for the $\max(lrtc_{m_1})$ statistic gave very close approximations to the probabilities of a Type I error for each case considered.

Generally speaking, the configurations of the explanatory variable X in the profile samples have very little impact on the approximation in Equation (4.7). Each of the LRT statistics has the same approximate chi-squared distribution, regardless of the values of the X variable. The distribution of $\max (Irtc_{m_i})$ depends on the individual profile samples only through their effect on the covariance structure of the LRT statistics. This distribution is affected by the individual profiles only if the X -values of the very first or the very last profile are much different than those of the other profiles, because this is where the co-variation between the LRT statistics is the smallest. Differences in the middle of the sequence of profiles should not have any perceptible effect on the approximation. In many of the linear profile applications, however, the X -values take the same values in all samples or change slightly from sample to sample.

As an alternative, one can consider the asymptotic distribution for the square root of the maximum LRT statistic derived by Csörgő and Horvath (1997, pp. 21-27). Table 4.9 gives the simulated overall probabilities of a Type I error produced using their approximation. Again, in this simulation the underlying in-control model with $A_0=0$ and $A_1=1$ and the fixed X -values of 0(0.2)1.8 were used. This table shows that the Csörgő and Horvath's (1997) approximation gives very liberal bounds unless m is considerably large. The asymptotic threshold given by Csörgő and Horvath (1997) is computationally demanding. The easy-to-calculate threshold in Equation (4.7) was shown to be much more accurate in these simulations.

Table 4.9: The overall probabilities of a Type I error using the approximation of Csörgő and Horvath (1997)

Nominal	Simulated						
	$m=5$	$m=10$	$m=15$	$m=20$	$m=30$	$m=40$	$m=60$
0.01	0.0160	0.0144	0.0153	0.0144	0.0136	0.0130	0.0139
0.02	0.0294	0.0230	0.0300	0.0265	0.0261	0.0268	0.0228
0.05	0.0719	0.0761	0.0733	0.0683	0.0661	0.0654	0.0629
0.10	0.1404	0.1538	0.1461	0.1385	0.1339	0.1280	0.1279

Appendix 4.A: Factoring the lrt_{m_1} Statistic into the Three Different Sources of Variability

The lrt_{m_1} statistic in Equation (4.2) can be written as

$$lrt_{m_1} = N \log[\hat{\sigma}^2 (\hat{\sigma}_1^2)^{-N_1/N} (\hat{\sigma}_2^2)^{-N_2/N}]. \quad (A1)$$

If we code the X -values so that the average coded value is zero, then $\hat{\sigma}^2$ can be written as

$$\hat{\sigma}^2 = \sum_{i=1}^N (y_i - b_0 - b_1 x'_i)^2 / N,$$

where $x'_i = X_i - \bar{x}$, (x'_i, y_i) , $i=1, 2, \dots, N$, are N bivariate observations resulting from pooling the m samples into one sample of size N , and b_0 and b_1 are the least squares estimates of the Y -intercept and slope of the simple linear regression model fitted for this pooled sample. Similarly $\hat{\sigma}_1^2$ and $\hat{\sigma}_2^2$ can be written as

$$\hat{\sigma}_1^2 = \sum_{i=1}^{N_1} (y_i - b_{0(1)} - b_{1(1)} x'_{1i})^2 / N_1 \quad \text{and} \quad \hat{\sigma}_2^2 = \sum_{i=N_1+1}^N (y_i - b_{0(2)} - b_{1(2)} x'_{2i})^2 / N_2,$$

where $x'_{1i} = X_i - \bar{x}_1$, $x'_{2i} = X_i - \bar{x}_2$, and $b_{0(1)}$ and $b_{1(1)}$ are the least squares estimates of the Y -intercept and slope of the simple linear regression model fitted for all the samples prior to m_1 pooled in one sample of size N_1 , and $b_{0(2)}$ and $b_{1(2)}$ are the least squares estimates of the Y -intercept and slope of the simple linear regression model fitted for all the samples following m_1 pooled in one sample of size N_2 .

$$\begin{aligned} \text{Now } \hat{\sigma}^2 &= \sum_{i=1}^{N_1} [y_i - b_{0(1)} - b_{1(1)} x'_{1i} + b_{0(1)} + b_{1(1)} x'_{1i} - b_0 - b_1 x'_i + b_1(\bar{x} - \bar{x}_1)]^2 / N + \\ &\quad \sum_{i=N_1+1}^N [y_i - b_{0(2)} - b_{1(2)} x'_{2i} + b_{0(2)} + b_{1(2)} x'_{2i} - b_0 - b_1 x'_i + b_1(\bar{x} - \bar{x}_2)]^2 / N \\ &= [(N_1 \hat{\sigma}_1^2 + N_2 \hat{\sigma}_2^2) + N_1 (b_0 - b_{0(1)})^2 + N_2 (b_0 - b_{0(2)})^2 + (b_1 - b_{1(1)})^2 S_{xx1} + (b_1 - b_{1(2)})^2 S_{xx2}] / N \\ &\quad + [N_1 b_1^2 (\bar{x} - \bar{x}_1)^2 + N_2 b_1^2 (\bar{x} - \bar{x}_2)^2 - 2N_1 b_1 (\bar{x} - \bar{x}_1)(\bar{y} - \bar{y}_1) - 2N_2 b_1 (\bar{x} - \bar{x}_2)(\bar{y} - \bar{y}_2)] / N. \end{aligned}$$

Defining $d_{B_0} = b_{0(2)} - b_{0(1)} = \bar{y}_2 - \bar{y}_1$, $d_{B_1} = b_{1(2)} - b_{1(1)} = (S_{xy2} / S_{xx2}) - (S_{xy1} / S_{xx1})$, $c_1 = N_1 \hat{\sigma}_1^2 + N_2 \hat{\sigma}_2^2$,

$c_2 = S_{xx1} S_{xx2} / S_{xx}$, $c_3 = N_1 N_2 / N$, and

$$\begin{aligned} c_4 &= \{ [N_1 N_2 (\bar{x}_2 - \bar{x}_1)^2 (S_{xx2} S_{xy1}^2 + S_{xx1} S_{xy2}^2) / N S_{xx} S_{xx1} S_{xx2}] \\ &\quad - [2N_1 N_2 (\bar{x}_2 - \bar{x}_1) (S_{xy1} + S_{xy2}) d_{B_0} / N S_{xx}] - [N_1^2 N_2^2 (\bar{x}_2 - \bar{x}_1)^2 d_{B_0}^2 / N^2 S_{xx}] \} \end{aligned}$$

then we have

$$\hat{\sigma}^2 = (c_1 + c_2 d_{B_1}^2 + c_3 d_{B_0}^2 + c_4) / N = c_1 [1 + c_2 d_{B_1}^2 / c_1 + (c_3 d_{B_0}^2 + c_4) / c_1] / N =$$

$$(c_1 / N)[1 + (c_2 d_{B_1}^2 / c_1)][1 + (c_4 + c_3 d_{B_0}^2) / (c_1 + c_2 d_{B_1}^2)]. \quad (\text{A2})$$

(Notice that the term c_4 is equal to zero in the special case when the X -values are the same for all samples). Also, we have

$$c_1 (\hat{\sigma}_1^2)^{-N_1/N} (\hat{\sigma}_2^2)^{-N_2/N} / N = (N_1 r^{2N_2/N} + N_2 r^{-2N_1/N}) / N, \quad (\text{A3})$$

where $r = \hat{\sigma}_1 / \hat{\sigma}_2$. Substituting Equations (A2) and (A3) into Equation (A1) we obtain

$$\begin{aligned} lrt_{m_1} &= N \log \{(N_1 r^{2N_2/N} + N_2 r^{-2N_1/N}) / N\} + N \log \{1 + (c_2 d_{B_1}^2 / c_1)\} \\ &\quad + N \log \{1 + [(c_4 + c_3 d_{B_0}^2) / (c_1 + c_2 d_{B_1}^2)]\}, \\ &= VAR_{\sigma^2} + VAR_{B_1} + VAR_{B_0}. \end{aligned}$$

Appendix 4.B: Derivation of the Approximate Expected Value of the lrt_{m_1} Statistic

The expected value of the lrt_{m_1} statistic is

$$E(lrt_{m_1}) = N E(\log \hat{\sigma}^2) - N_1 E(\log \hat{\sigma}_1^2) - N_2 E(\log \hat{\sigma}_2^2). \quad (\text{B1})$$

It can be shown that the quantity $N\hat{\sigma}^2 / 2\sigma^2$ has a gamma distribution with parameters $(N-2)/2$ and 1. For a random variable X having a gamma distribution with parameters p and 1, [see Kendall and Stuart (1977, p. 251)], we have

$$E \log(aX) = \log a + \log p - 1/2p - 1/12p^2 + O(1/p^3). \quad (\text{B2})$$

Hence, using Equation (B2) we can show that

$$E(\log \hat{\sigma}^2) = \log(2\sigma^2 / N) + \log \{(N-2)/2\} - 1/(N-2) - 1/3(N-2)^2 + O(1/N^3). \quad (\text{B3})$$

Similarly,

$$E(\log \hat{\sigma}_1^2) = \log(2\sigma^2 / N_1) + \log \{(N_1-2)/2\} - 1/(N_1-2) - 1/3(N_1-2)^2 + O(1/N_1^3), \quad (\text{B4})$$

and

$$E(\log \hat{\sigma}_2^2) = \log(2\sigma^2 / N_2) + \log \{(N_2-2)/2\} - 1/(N_2-2) - 1/3(N_2-2)^2 + O(1/N_2^3). \quad (\text{B5})$$

One can substitute Equations (B3-B5) into Equation (B1) to obtain

$$\begin{aligned} E(lrt_{m_1}) &\approx N \log \{(N-2)/2N\} - N_1 \log \{(N_1-2)/2N_1\} - N_2 \log \{(N_2-2)/2N_2\} - \\ &\quad [N/(N-2) - N_1/(N_1-2) - N_2/(N_2-2)] - [(N/(N-2)^2 - N_1/(N_1-2)^2 - N_2/(N_2-2)^2)], \end{aligned} \quad (\text{B6})$$

Moreover, using the Taylor expansion for the log function, we can show that

$$\log \{(N-2)/2N\} = \log \{0.5(1 - 2/N)\} = \log 0.5 - 2/N - 2/N^2 + O(1/N^3). \quad (\text{B7})$$

Similarly, we have

$$\log\{(N_1 - 2)/2N_1\} = \log\{0.5(1 - 2/N_1)\} = \log 0.5 - 2/N_1 - 2/N_1^2 + O(1/N_1^3)$$

and

$$\log\{(N_2 - 2)/2N_2\} = \log\{0.5(1 - 2/N_2)\} = \log 0.5 - 2/N_2 - 2/N_2^2 + O(1/N_2^3). \quad (\text{B8})$$

Substituting Equations (B7-B8) into Equation (B6), we obtain

$$e_{m_1} \approx 2 - 2\left(\frac{1}{N} - \frac{1}{N_1} - \frac{1}{N_2}\right) - \left(\frac{N}{N-2} - \frac{N_1}{N_1-2} - \frac{N_2}{N_2-2}\right) - \frac{1}{3}\left(\frac{N}{(N-2)^2} - \frac{N_1}{(N_1-2)^2} - \frac{N_2}{(N_2-2)^2}\right).$$

Chapter 5: Examples

This chapter presents three examples to illustrate the use of the proposed change point method described in Chapter 4 and compares its performance to that of Methods C and D. In the first two examples, simulated linear profile data sets were used in the analyses. The data sets for these examples are available at

<http://filebox.vt.edu/users/mamahmou/data%20for%20example%201-3.xls>.

In the last example the proposed change point method was applied to a real data set from a calibration application at NASA.

For the examples with simulated data sets, each method was applied based on a nominal overall false alarm probability of $\alpha = 0.05$. The fixed X -values of 0(0.2)1.8 were used in these examples. The simulated data set in each example consists of 30 samples of linear profiles; thus $m=30$ and $n=10$.

For Method C, each set of control limits of the three control charts for the Y -intercept, slope, and variance, were calculated using Equations (2.12), (2.13), and (2.16), respectively. Each set of chart limits were set based on a false alarm probability of $\alpha_2 = 0.00057$ to produce a nominal overall false alarm probability of $\alpha = 0.05$. In Method D, the F -test was performed based on the statistic in Equation (2.19) at the significance level $\alpha_3 = 0.02532$. Also, the control limits for the process variance control chart were determined based on $\alpha_4 = 0.000855$, so that the nominal overall false alarm probability produced by Method D was also $\alpha = 0.05$.

For Method LRT, the $lrtc_{m_i}$ statistics were calculated with a normalizing factor given by Equation (4.8). The threshold for the $\max(lrtc_{m_i})$ statistic was determined by Equation (4.7) at a significance level of $\alpha = 0.05$.

5.A Examples with Simulated Data Sets

In Example 1, a single step shift in the Y -intercept after sample 25 was considered. The data for this example were generated as follows. Given the fixed X -values, the underlying linear profile model was

$$Y_{ij} = 2 + 3X_i + \varepsilon_{ij}, \quad i=1, 2, \dots, 10, \quad j=1, 2, \dots, 25,$$

$$Y_{ij} = 3 + 3X_i + \varepsilon_{ij}, \quad i=1, 2, \dots, 10, \quad j=26, 27, \dots, 30,$$

where the ε_{ij} 's are i.i.d $N(0, 1)$ random variables.

Figures 5.1-5.3 give control charts for the variance, Y -intercept, and slope, respectively, using Method C. According to the chart in Figure 5.1, the variance is stable. Also, as shown in Figures 5.2 and 5.3, both the Y -intercept and slope appear stable. Hence, according to Method C, the process is in-control.

For Method D, the control limits for the process variance control chart are $LCL=0.0968$ and $UCL=3.7912$. All the variance estimates are within these control limits, indicating that the variance is stable. Also, the F -value calculated using Equation (2.19) for testing the equality of all the regression lines is $F=1.05873$ with a p -value=0.3749, which indicates that the process is in-control.

In Method LRT, the threshold T for the $\max(lrtc_{m_1})$ statistic calculated using Equation (4.7) is 4.6094. The value of $\max(lrtc_{m_1})$ statistic is 9.041, corresponding to $m_1=25$, signaling the presence of a change point and indicating that 25 is the MLE of the location of this change point. In this example, the proposed change point method correctly estimated the location of the change point. Also, for $m_1=25$, the three factors VAR_{B_0}/e_{m_1} , VAR_{B_1}/e_{m_1} and VAR_{σ^2}/e_{m_1} are 8.423, 0.169, and 0.449, respectively. As mentioned in Chapter 4, these factors represent to a large extent the relative contributions of the regression parameter shifts to an out-of-control signal. Thus, this out-of-control

situation is highly attributable to a shift in the Y -intercept, as the relative contribution of the Y -intercept is $8.423/9.041 \approx 93\%$. Applying Method LRT on the samples prior to the change point $m_1=25$ and samples following it gave no evidence of the presence of an additional change point at $\alpha = 0.025$. Notice that a Bonferroni-corrected significance level of $\alpha = 0.025$ was used here due to the fact that each segment (subset) represents another opportunity for a Type I erroneous split. Hence, using Method LRT one concludes that the process is out-of-control due to a Y -intercept shift that occurred at $m_1 = 25$.

Figure 5.1: Control chart for the variance (Example 1).

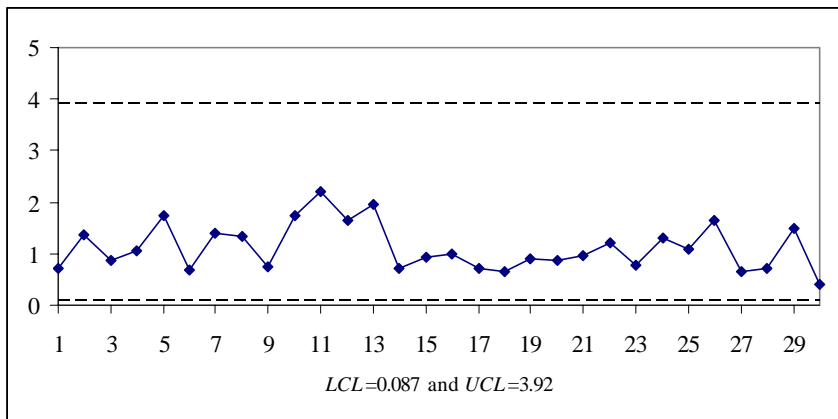


Figure 5.2: Control chart for the intercept (Example 1).

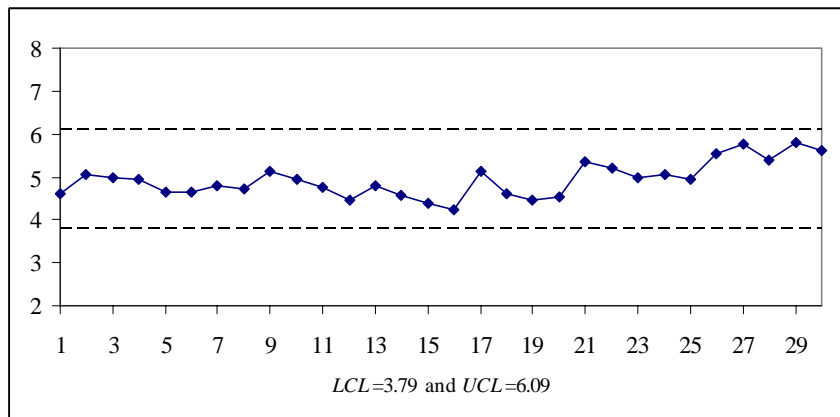
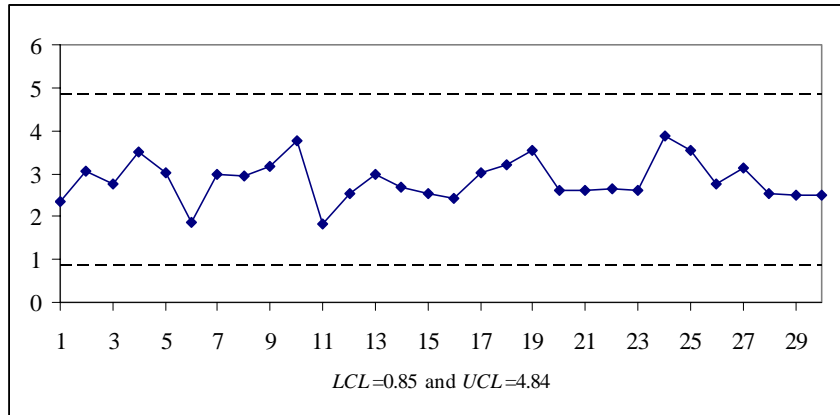


Figure 5.3: Control chart for the slope (Example 1).



In Example 2 a single step shift in the process variance after sample 20 was considered. The underlying linear profile model used in this example was

$$Y_{ij} = 2 + 3X_i + \varepsilon_{ij}, \quad i=1, 2, \dots, 10, j=1, 2, \dots, 20,$$

$$Y_{ij} = 2 + 3X_i + \varepsilon'_{ij}, \quad i=1, 2, \dots, 10, j=21, 22, \dots, 30.$$

Here the ε_{ij} 's are i.i.d $N(0, 1)$ random variables, while the ε'_{ij} 's are i.i.d $N(0, 2)$ random variables. Figures 5.4-5.6 present the three control charts for the variance, Y -intercept, and slope, respectively, using Method C. As shown in these figures, all the Y -intercept, slope, and variance estimates are within the corresponding control limits. Hence, the conclusion obtained from applying Method C on the data set of Example 2 is that the process is in-control.

For Method D, the control limits for the variance chart are (0.1173, 4.5926). Again, all the variance estimates are within these limits. Moreover, the F -value for testing the equality of all the regression lines is 1.0434 with p -value= 0.402. Therefore, according to Method D, the process is in-control.

For Method LRT, the value of the $\max(lrtc_{m_1})$ statistic is 10.781, corresponding to $m_1=20$. Method LRT signals the presence of a change point, since this value is greater

than $T=4.6094$. The MLE of the location of this change point is 20. Also the values of VAR_{B_0} / e_{m_1} , VAR_{B_1} / e_{m_1} and VAR_{σ^2} / e_{m_1} at $m_1=20$ are 0.202, 1.648, and 8.931, respectively. Therefore, this out-of-control situation is primarily attributable to a shift in the process variance, as the relative contribution of the variance shift to this out-of-control situation is $8.931/10.781 \approx 83\%$. Repeating Method LRT on the samples prior to $m_1=20$ and the samples following it did not give evidence of any additional change points with $\alpha=0.025$. Thus, using Method LRT, we conclude that there was a shift in the process variance after sample 20.

Figure 5.4: Control chart for the variance (Example 2).

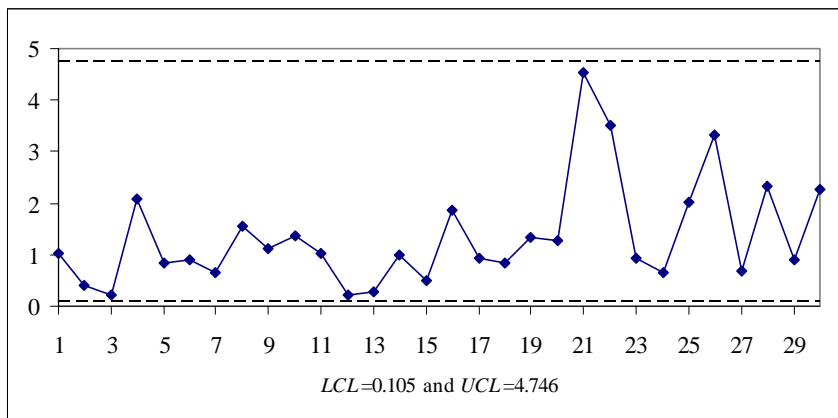


Figure 5.5: Control chart for the intercept (Example 2).

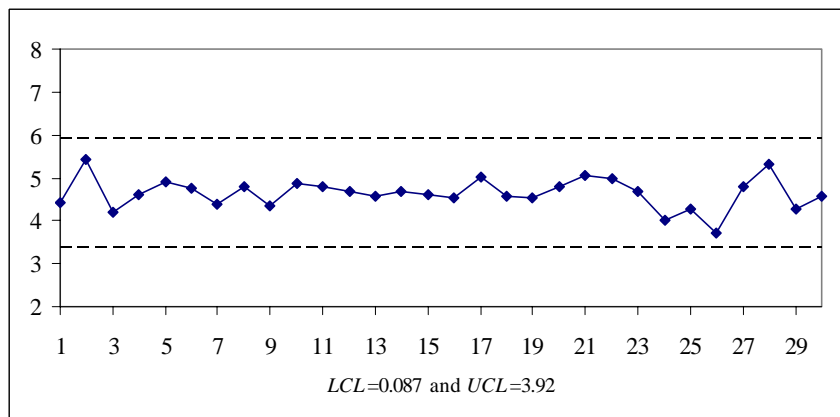
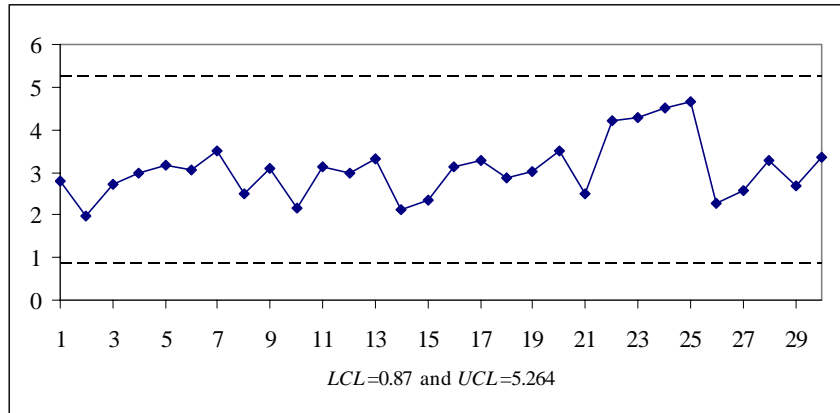


Figure 5.6: Control chart for the slope (Example 2).



5.B A Calibration Application at NASA¹

In this section, the proposed change point method is applied to a real data set from a calibration application. The purpose is to investigate replicated calibrations of a force balance used in wind tunnel experiments at NASA Langley Research Center. A force balance is a multiple-axis load cell that provides simultaneous measurement of three orthogonal components of aerodynamic force (normal, axial, and side force) and three orthogonal components of aerodynamic torque (rolling, pitching, and yawing moments) exerted on a scaled aircraft test article. The relative importance of each of these measurements depends on the nature of the aerodynamic investigation. However, in most investigations, the axial force component is of primary interest, and therefore it is considered in this example.

A force balance consists of a structural spring element instrumented with a network of strain gauges and is designed to elastically deform under the application of external forces and moments. This deformation results in differential strain across the

¹ The data set of this example was provided and described by Peter A. Parker; a Research Scientist, Advanced Model and Sensor Systems Branch, NASA Langley Research Center, Hampton, VA 23681-2199. Peter A. Parker is also a Ph. D. student in the Department of Statistics, Virginia Tech, Blacksburg, VA 24061-0439.

structure that is sensed by the strain gauges. Six electrical responses are produced by the strain gauges that are proportional to the magnitude and direction of their respective aerodynamic components. A calibration experiment was performed to model the relationship between the applied forces and moments (explanatory variables) and the electrical responses. See Parker et al. (2001) for a complete description of the calibration process. There are six prime sensitivities in the model that represent the dominant effect of each electrical response due to the level of one explanatory variable. To isolate the simple linear relationship of the axial force prime sensitivity and account for the influence of the other explanatory variables, a partial regression approach was used in this example [see Myers (1990)]. The partial regression adjusted axial response and axial force data set is available at

<http://filebox.vt.edu/users/mamahmou/Axial%20Force%20and%20Response.xls>.

Periodic calibrations provide information about the stability of the force balance, which is directly related to its performance in wind tunnel research. The data set used in this example consists of 11 samples of a linear profile each with 64, 73, or 74 data points; thus $m=11$ and $n=64, 73, \text{ or } 74$. These samples were collected over sixteen months, which has been traditionally considered a reasonable calibration interval. Applying a change-point method to historical data gives an indication about the calibration stability within this time interval. In addition, the ability to detect and diagnosis a step shift in one or more of the model parameters enables a classification of the nature and severity of the shift. For example, a shift in the slope or variance affects the bias and precision of the predicted forces and moments. Alternatively, small shifts in the Y -intercept are less important due to an offset correction procedure employed during wind tunnel operations. However, a large shift in the intercept may indicate that the structural frame of the balance has been damaged due to an overload condition or that one or more of the strain gauges has sustained physical or electrical damage. Therefore, it is not only necessary to detect a shift, but also to attribute the shift to a specific model parameter.

Some diagnostic statistics were obtained to check for the appropriateness of the model assumptions for each sample before applying the proposed change point method

on this data set. The results suggested that there is no significant evidence of departure from normality and linearity for each sample. Then, the Jones and Rice (1992) principal component approach was applied to the data set as a pre-analysis to understand and identify the pattern of variation among the 11 calibration curves. Since the X -values in this data set are not equal equally-spaced for each profile, a regression model for each sample was fitted and fitted responses for $X=-50(20)50$ were obtained. The first principal component accounts for approximately 81% of the total variability among the calibration curves. The three fitted calibration curves corresponding to the minimum, median, and maximum first principal component scores are plotted in Figure 5.7. These correspond to the calibration lines of samples 5, 8, and 9, respectively. As shown in Figure 5.7, these calibration lines differ primarily in the Y -intercept. Thus, using the Jones and Rice (1992) method, one concludes that 81% of the total variability is attributable to the variability in the Y -intercept.

Method LRT was applied to this data set based on a nominal false alarm probability of $\alpha = 0.05$. The value of the $\max(lrtc_{m_1})$ statistic is 7.776, corresponding to $m_1 = 8$. Method LRT signals the presence of a change point, since this value is greater than $T=4.2616$ (the threshold at $\alpha = 0.05$). Also the values of VAR_{B_0}/e_{m_1} , VAR_{B_1}/e_{m_1} and VAR_{σ^2}/e_{m_1} at $m_1=8$ are 7.281, 0.00009 and 0.495, respectively. Therefore, this out-of-control situation is primarily attributable to a shift in the intercept, as the relative contribution of the intercept shift to this out-of-control situation is $7.281/7.776 \approx 93.63\%$. Repeating Method LRT on the subset of samples following $m_1=8$ and prior to it gave no evidence of the presence of an additional change point at $\alpha = 0.025$.

A plot of the intercept estimates in Figure 5.8 indicates that the change is a shift in the level of the Y -intercept. This change is on the order of less than 10 microvolts per volt, which is approximately 1% of the maximum response of the axial force channel. Therefore, this small shift would not have a significant impact on the performance of the force balance, and furthermore it would not warrant re-calibration. It should be noted

that in the application of a change point method to calibration data, a result of not detecting a change point is equally as informative as detection.

Figure 5.7: Calibration curves corresponding to the minimum, median, and maximum first principal component scores.

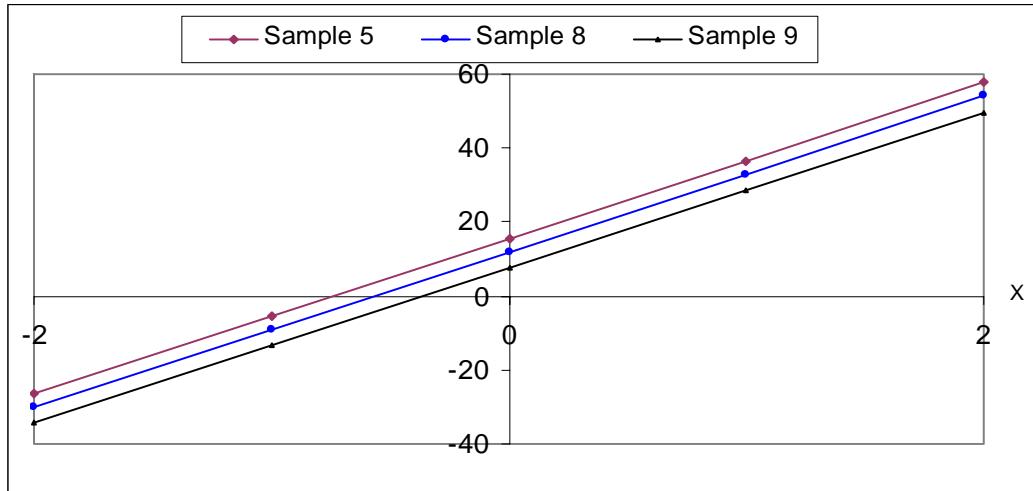
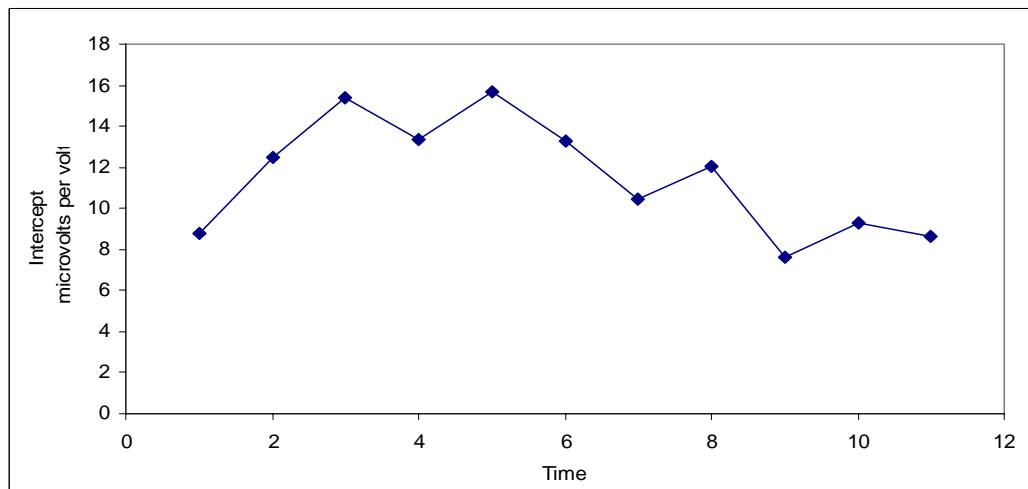


Figure 5.8: A chart for the intercept estimates for the NASA data set.



There are two primary conclusions that can be drawn from this example. First, Method LRT gave evidence of a shift in the axial force sensitivity during this set of replicated calibrations. The ability to attribute the shift to the *Y*-intercept and interpret its magnitude supports the validity of wind tunnel measurements obtained during this time interval. Second, based on this historical data set, it provides some initial evidence to suggest that the force balance calibration interval of sixteen months may be reasonable. An overall assessment of calibration stability would require an analysis of the other five responses.

Chapter 6: The Inertial Properties of Quality Control Charts

Any control chart that combines sample information over time, e.g., the CUSUM chart and the EWMA chart, has an ability to detect process changes that varies over time depending on the past data observed. The chart statistics, however, can take values such that some shifts in the parameters of the underlying probability distribution of the quality characteristic are more difficult to detect. For instance, a trend may occur in one direction of the target parameter value when a shift occurs in the opposite direction, and as a result the chart becomes less effective in reacting to this shift. This is referred to as the “inertia problem” in the literature.

This study shows under realistic assumptions that the worst-case run length performance of control charts is as informative as the steady-state performance. Also, this study introduces a simple new measure of the inertial properties of control charts, the signal resistance.

6.A Some Control Charting Methods for Monitoring the Process Mean

In this study, only control charts for monitoring the process mean or mean vector are considered, although the ideas can be easily extended to other types of charts. For a univariate quality characteristic X , it is assumed that the observed data $(x_{1i}, x_{2i}, \dots, x_{ni})$, $i=1, 2, \dots$, are samples of size n taken at regular time intervals on X . For each sample, it is assumed that $x_{1i}, x_{2i}, \dots, x_{ni}$ are i.i.d. normal random variables with mean μ and variance σ^2 . This study considers methods for detecting changes in μ from a target value μ_0 . Without loss of generality, it is assumed that $\mu_0 = 0$ and $\sigma / \sqrt{n} = 1$. Thus, this chapter considers the Phase II application of control charts with the in-control values of the parameters assumed to be known. The multivariate quality characteristic case is discussed in Section 6.D.

The well-known Shewhart control chart (\bar{X} -chart) signals that the process mean is off target if the i^{th} sample mean, \bar{X}_i , falls outside the control limits $\pm L_1$, where $L_1 > 0$ can be chosen to obtain a specified in-control ARL .

The two-sided CUSUM chart signals a shift in the process mean if

$$S_i \geq h_1 \text{ or } T_i \leq -h_1,$$

where $h_1 > 0$ is chosen to give a specified in-control ARL and the cumulative sum statistics S_i and $T_i, i = 1, 2, \dots$, are defined as

$$S_i = \max(0, S_{i-1} + \bar{X}_i - k) \text{ and } T_i = \min(0, T_{i-1} + \bar{X}_i + k), \quad (6.1)$$

where $S_0 = T_0 = 0, k = d/2 > 0$, and d is the smallest shift in the process mean, measured in units of the standard error, considered important enough to be detected quickly.

The EWMA control chart is based on the statistics

$$Y_i = \lambda \bar{X}_i + (1 - \lambda)Y_{i-1}, i=1, 2, \dots, \quad (6.2)$$

where $Y_0 = 0$ and λ ($0 < \lambda \leq 1$), usually called the smoothing parameter, determines the weighting of past data. To quickly detect small shifts in the process mean, it is usually recommended that one choose a small value of λ . It is well-known that the in-control expected value and variance of Y_i are

$$E(Y_i) = 0 \text{ and } Var(Y_i) = \lambda[1 - (1 - \lambda)^{2i}]/(2 - \lambda), \quad (6.3)$$

respectively. The EWMA control chart signals an out-of-control condition in the process mean if the i^{th} EWMA chart statistic Y_i falls outside the control limits

$$\pm L_2 \sqrt{Var(Y_i)}, \quad (6.4)$$

where $L_2 > 0$ can be chosen to give a specified in-control ARL . The control limits in Equation (6.4) vary from sample to sample. It is common to use the asymptotic variance

in calculating the control limits. The asymptotic control limits for the EWMA chart are $\pm h_2$, where

$$h_2 = L_2 \sqrt{\lambda / (2 - \lambda)}. \quad (6.5)$$

6.B Limitations of Steady-State Analysis

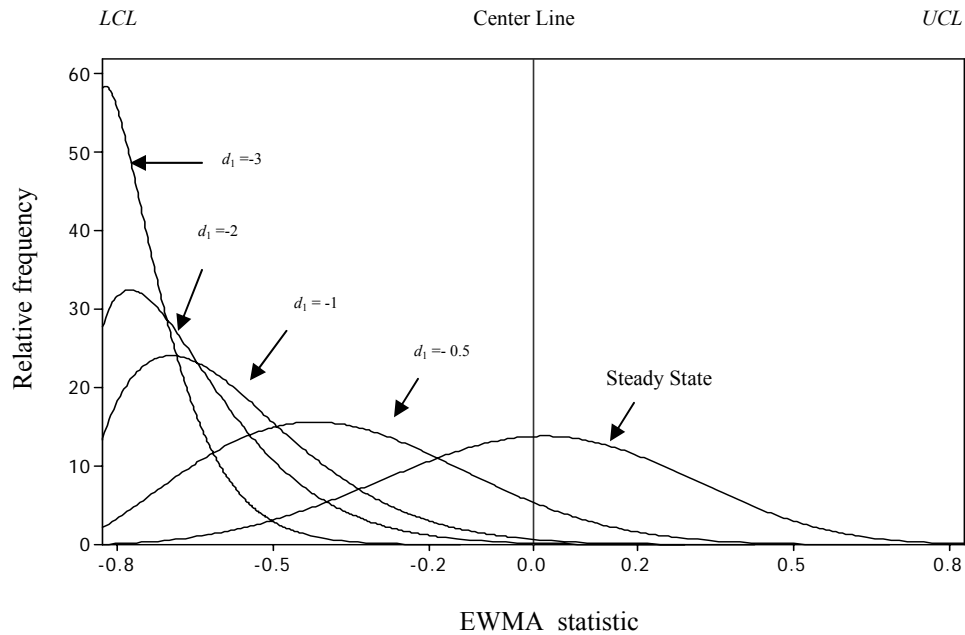
Ryan (2000, p. 247) pointed out that the EWMA chart has been shown to have more of an inertia problem than the CUSUM chart, but stated that it is arguable about how often the problem is likely to occur in practice. To consider how often the inertia problem might have a practical impact, we can examine the steady-state distribution of the control chart statistic first assuming that the process stays on target and that there is no signal given. The steady-state distribution for the commonly used EWMA chart with $\lambda = .15$ and $L_2 = 3.0$ is illustrated in Figure 6.1. This distribution was approximated using the Markov chain approach described in Lucas and Saccucci (1990) with 501 transient states. The in-control *ARL* of this EWMA chart was estimated to be approximately 655 using this Markov chain approach.

It can be seen from Figure 6.1 that it is somewhat unusual to have the EWMA statistic wander relatively far from the centerline when the process is in-control. The EWMA statistic crosses a control limit on average only every 655 samples when the process is in control.

One important limitation of the studies of steady-state properties is that it is assumed that the process mean stays on target until the specified shift in the mean occurs. This assumption may not hold in practice. There could be, for example, an undetected sustained shift in the mean of size d_1 when the specified shift of size d occurs. The estimated distributions for the EWMA chart statistic with $\lambda = 0.15$ and $L_2 = 3.0$ are shown in Figure 6.1 for undetected sustained decreases in the mean of size $d_1 = -0.5, -1.0, -2.0,$ and -3.0 . Each of these distributions was estimated using 50,000 simulations. For each simulation a sequence of 100 in-control samples from the normal distribution

with $\mu_0 = 0$ and $\sigma = 1$ were generated before the shift was introduced. Then five more samples from the normal distribution with $\mu = d_1$ and $\sigma = 1$ were generated. If an EWMA chart produced an out-of-control signal in the sequence of 105 observations, this chart was discarded. Figure 6.1 illustrates the distributions of the EWMA values after the 105th sample. Under these conditions the worst-case performance of the charts becomes more meaningful than the usual steady-state performance based on the assumption of no prior shift in the mean.

Figure 6.1: The steady state distribution and the distributions of the EWMA statistic when there is an undetected sustained shift with size d_1 for $\lambda = 0.15$ and $L_2 = 3.0$.



Under this framework, the shift in the mean that could be delayed due to the presence of inertia is $d - d_1$, obviously greater in absolute value than d if d and d_1 are of opposite signs. Without a more elaborate model, we cannot evaluate the probability of an undetected shift in the mean at the time of another mean shift. If a practitioner believes, however, that this situation is realistic, then more emphasis on worst-case analysis seems appropriate.

6.C Signal Resistance of Univariate Control Charts

This section evaluates the signal resistance of several recommended univariate control chart approaches. In the case of monitoring the mean in the univariate case we refer to the largest standardized deviation of the sample mean from the target value not leading to an immediate out-of-control signal as the *signal resistance* of a chart. This measure is most relevant when there is an interest in detecting assignable causes that affect the distribution of only one sample mean, although it does give some indication regarding chart performance in detecting sustained shifts in the mean. Run length performance is not relevant when an assignable cause affects only a single sample. Note that determining the value of the signal resistance does not require any distributional assumptions, although if one makes a distributional assumption it would be straightforward to calculate the probability of an immediate signal for a particular value of the control chart statistic and an assumed process mean shift.

The signal resistance of a basic Shewhart chart is simply the multiplier L_1 used to obtain the control limits, i.e., a constant. In general, the signal resistance for the CUSUM chart is

$$SR(\text{CUSUM})=(h_1 - w + k),$$

where w is the upper CUSUM statistic value. For the EWMA chart, the signal resistance is

$$SR(\text{EWMA})=[h_2 - (1 - \lambda)w]/\lambda,$$

where w is the value of the EWMA statistic. For the CUSUM chart the maximum signal resistance, over all possible values of the CUSUM statistic, is $(h_1 + k)$ standard errors. For the EWMA chart with asymptotic control limits, the corresponding value is $L_2\sqrt{(2 - \lambda)/\lambda} = h_2(2 - \lambda)/\lambda$ standard errors. These results are based on shifts measured in units of the standard error, so they apply for any value of the sample size n .

It is commonly recommended that one use a Shewhart limit in conjunction with other types of charts. Lucas and Saccucci (1990) and others have recommended that a Shewhart limit be used in conjunction with the EWMA chart, in part to alleviate the inertia problem. Lucas (1982) proposed a Shewhart limit in conjunction with the CUSUM chart. Box and Luceño (1997, p. 232) and Hawkins and Zamba (2003-04) have also recommended that if CUSUM or EWMA charts are used, then it is advisable to use a Shewhart chart as well. Note that if one uses a Shewhart limit in conjunction with another chart, then the control limits of the other chart must be widened slightly to maintain the same in-control run length properties unless the Shewhart limits are sufficiently wide to have no noticeable effect on these properties.

Woodall and Maragah (1990) and Yashchin (1993) held that the basic inertia deficiency of the EWMA chart can only partially be alleviated by the incorporation of a Shewhart limit, with Yashchin (1993) arguing, “long sequences of data corresponding to unacceptable process levels (but not violating the Shewhart limit) can still remain undetected for a long time.”

The signal resistance for an EWMA control chart in conjunction with Shewhart control limits is

$$SR(\text{EWMA}+\text{Shewhart})=\begin{cases} L_1, & \text{if } -h_2 \leq w < (h_2 - \lambda L_1)/(1 - \lambda) \\ [h_2 - (1-\lambda)w]/\lambda, & \text{if } (h_2 - \lambda L_1)/(1 - \lambda) \leq w \leq h_2, \end{cases}$$

where L_1 is the value of the multiplier used to obtain the Shewhart limit and w is the value of the EWMA statistic. Obviously, in this case, the signal resistance cannot exceed the value of the multiplier used to obtain the Shewhart limit, i.e., L_1 .

Capizzi and Masarotto (2003) proposed an adaptive EWMA (AEWMA) approach for detecting shifts in the process mean. One of their purposes was to overcome the inertia problems of the EWMA chart. Their approach combined the EWMA and the Shewhart approaches in a smoother way than use of an EWMA chart in conjunction with Shewhart limits described above. The idea behind their method was to adjust the value of

λ according to the magnitude of the difference (called the error) between the current sample mean and the previous AEWMA statistic. This AEWMA control chart is based on the statistics

$$Y_i = \omega(e_i)\bar{X}_i + [1 - \omega(e_i)]Y_{i-1}, i=1, 2, \dots, \quad (6.6)$$

where $\omega(e_i) = \phi(e_i)/e_i$ and e_i the i^{th} error is defined as $e_i = \bar{X}_i - Y_{i-1}$. The score function $\phi(e_i)$ is defined as

$$\phi(e_i) = \begin{cases} e_i + (1 - \lambda)k, & \text{if } e_i < -k \\ \lambda e_i, & \text{if } -k \leq e_i \leq k \\ e_i - (1 - \lambda)k, & \text{if } e_i > k. \end{cases} \quad (6.7)$$

The AEWMA control chart signals an out-of-control condition in the process mean if $|Y_i| > h_3$, where Y_i is as defined in Equation (6.6) and h_3 is a suitable threshold.

Capizzi and Masarotto (2003) also used two other formulas for the score function $\phi(e_i)$, but they compared their AEWMA approach to some other control chart approaches using only the score function defined in Equation (6.7). They found that their AEWMA approach has better performance than the competing methods in terms of the *ARL* and the worst-case *ARL*.

It can be shown that the signal resistance of the Capizzi and Masarotto's (2003) AEWMA using the score function in Equation (6.7) is equal to

$$SR(\text{AEWMA}) = \begin{cases} \{h_3 - (1 - \lambda)w\} / \lambda, & \text{if } h_3 - \lambda k \leq w \leq h_3 \\ h_3 + (1 - \lambda)k, & \text{if } -h_3 \leq w < h_3 - \lambda k, \end{cases} \quad (6.8)$$

where w is the AEWMA chart statistic.

Domangue and Patch (1991) proposed an EWMA control chart for detecting simultaneously shifts in both the process mean and standard deviation, referred to as the omnibus EWMA chart. This EWMA control chart is based on the statistics

$$Y_i = \lambda|Z_i|^\alpha + (1-\lambda)Y_{i-1}, \quad i=1, 2, \dots, \quad (6.9)$$

for some specified constant α , where $Z_i = \sqrt{n}(\bar{X}_i - \mu_0)/\sigma_0$ and $Y_0 = E(Y_i)$. The asymptotic in-control expected value and variance of the EWMA statistic in Equation (6.9) are

$$E(Y_i) = \sqrt{\left(\frac{2^\alpha}{\pi}\right)\Gamma[(1+\alpha)/2]} \quad \text{and} \quad \text{var}(Y_i) = \frac{2^\alpha \lambda}{(2-\lambda)\pi} [\sqrt{\pi}\Gamma(0.5+\alpha) - (\Gamma[(1+\alpha)/2])^2],$$

respectively. Domangue and Patch (1991) investigated the performance of their proposed EWMA chart for $\alpha=0.5$ and $\alpha=2$. The chart signals an out-of-control condition in the process mean or standard deviation, or both, if $Y_i \geq h_4 = E(Y_i) + L_4 \sqrt{\text{var}(Y_i)}$, where L_4 is chosen to obtain a specified in-control *ARL*. It can be shown that the signal resistance of this control chart is

$$SR(\text{omnibus EWMA}) = [(h_4 - (1-\lambda)w) / \lambda]^{1/\alpha}, \quad (6.10)$$

where w is the value of their EWMA chart statistic.

Domangue and Patch (1991) compared their EWMA approach to several other procedures, including a CUSUM chart based on the statistic $|Z_i|^\alpha$, where Z_i is as defined in Equation (6.9). They referred to this CUSUM chart as the omnibus CUSUM. They noted that, for $n=1$ and $\alpha=0.5$ the omnibus CUSUM chart is equivalent to the CUSUM chart proposed by Hawkins (1981) for controlling a scale parameter. For $n=1$ and $\alpha=2$, on the other hand, the omnibus CUSUM chart is a univariate version of the CUSUM chart proposed by Healy (1987) for monitoring the covariance matrix of a multivariate normal process. It can be shown that the signal resistance of the omnibus CUSUM chart is

$$SR(\text{omnibus CUSUM}) = [h_H + k_H - w]^{1/\alpha},$$

where h_H and k_H are the chart control limit and reference parameter, respectively, and w is the omnibus CUSUM chart statistic.

It should also be mentioned that the signal resistance of some of the proposed charts based solely on run rules can be unbounded. For example, the synthetic control chart, proposed by Wu and Spedding (2000) and evaluated by Davis and Woodall (2002), signals if the sample mean falls outside the Shewhart limits $\pm L_1$ only if the conforming run length (CRL) is less than or equal to K , where $K > 0$. The CRL is the number of samples since the most recent violation of the Shewhart limits or since sampling began if there has been no previous violation. The signal resistance of this chart is

$$SR(\text{synthetic}) = \begin{cases} L_1, & \text{if CRL} < K \\ \infty, & \text{otherwise.} \end{cases}$$

The same property applies to the control charts proposed by Klein (2000).

It is somewhat more difficult to evaluate the signal resistance of charting methods for monitoring the process mean that are based on statistics other than simply the sample mean, e.g., the methods by Amin et al. (1999) and Reynolds and Stoumbos (2004). In these cases it is necessary to make simplifying assumptions or to use computer simulation.

6.D Signal Resistance of Multivariate Control Charts

This section extends the study of the inertial properties of control charts to the multivariate case. Suppose that $\mathbf{x}_1, \mathbf{x}_2, \dots$ is a sequence of $p \times 1$ random vectors taken at regular time intervals, each representing the p quality characteristics to be monitored. Without loss of generality, it is assumed that the random vector \mathbf{x}_i represents the sample mean vector at time i , $i=1, 2, \dots$. Also, it is assumed that \mathbf{x}_i , $i=1, 2, \dots$, are i.i.d. multivariate normal random vectors with mean vector $\boldsymbol{\mu}$ and known constant covariance matrix $\boldsymbol{\Sigma}$. The main concern in this case is to detect shifts in the mean vector $\boldsymbol{\mu}$ from a target vector $\boldsymbol{\mu}_0$. Without loss of generality, the target vector is assumed to be $\boldsymbol{\mu}_0 = \mathbf{0}$.

We refer to the largest standardized distance of the sample mean vector from the target vector in any direction not leading to an immediate out-of-control signal as the signal resistance of a multivariate control chart, i.e., the signal resistance of a multivariate chart is equal to $\max_{\mathbf{x}_i} \sqrt{\mathbf{x}_i^T \boldsymbol{\Sigma}^{-1} \mathbf{x}_i}$ subject to the resulting chart statistic not exceeding the control limit. This definition is a straightforward extension of the univariate signal resistance measure presented in Section 6.C.

The multivariate control charts that are considered in this chapter are all directionally invariant. The *ARL* performance of a directionally invariant control chart can be determined solely by the non-centrality parameter D , where

$$D^2 = \boldsymbol{\mu}^T \boldsymbol{\Sigma}^{-1} \boldsymbol{\mu}. \quad (6.11)$$

In other words, the *ARL* will be the same if the process mean vector $\boldsymbol{\mu}$ shifts to $\boldsymbol{\mu}_1$ or $\boldsymbol{\mu}_2$ as long as $\boldsymbol{\mu}_1^T \boldsymbol{\Sigma}^{-1} \boldsymbol{\mu}_1 = \boldsymbol{\mu}_2^T \boldsymbol{\Sigma}^{-1} \boldsymbol{\mu}_2$.

The traditional Shewhart-type χ^2 -chart, a natural multivariate extension of the \bar{X} -chart, signals that the process mean vector is off target at the sampling time i , $i=1, 2, \dots$, if the i^{th} charted statistic

$$\chi_i^2 = \mathbf{x}_i^T \boldsymbol{\Sigma}^{-1} \mathbf{x}_i$$

exceeds the control limit h_5 , where $h_5 > 0$ can be chosen to obtain a specified in-control *ARL*. The signal resistance of a χ^2 -chart is equal to the square root of its control limit, i.e., $\sqrt{h_5}$.

The multivariate EWMA (MEWMA) control chart for monitoring the process mean vector proposed by Lowry et al. (1992) is a straightforward extension of the univariate EWMA chart. The MEWMA chart is based on the statistic

$$T_i^2 = \mathbf{z}_i^T \boldsymbol{\Sigma}_{z_i}^{-1} \mathbf{z}_i, \quad i=1, 2, \dots,$$

where the MEWMA vectors \mathbf{z}_i are calculated using

$$\mathbf{z}_i = \mathbf{R} \mathbf{x}_i + (\mathbf{I} - \mathbf{R}) \mathbf{z}_{i-1}, \quad (6.12)$$

where $\mathbf{z}_0 = \mathbf{0}$, $\mathbf{R} = \text{diag}(\lambda_1, \lambda_2, \dots, \lambda_p)$, $0 < \lambda_j \leq 1$, $j=1, 2, \dots, p$, and Σ_{z_i} is the covariance matrix of \mathbf{z}_i . Lowry et al. (1992) considered only the case of equal smoothing parameters, i.e., $\lambda_1 = \lambda_2 = \dots = \lambda_p = \lambda$. The MEWMA chart statistic is usually constructed in terms of the asymptotic covariance matrix

$$\Sigma_{z_i} = \{\lambda/(2 - \lambda)\} \Sigma. \quad (6.13)$$

The MEWMA chart signals that the process mean vector is off target as soon as $T_i^2 > h_6$, where $h_6 > 0$ can be chosen to achieve a specified in-control *ARL*.

It can be shown that the signal resistance of the MEWMA control chart is

$$SR(\text{MEWMA}) = \sqrt{\lambda/(2 - \lambda)} [\sqrt{h_6} + (1 - \lambda)w] / \lambda, \quad (6.14)$$

where $w = \sqrt{T_i^2}$, and T_i^2 is the MEWMA statistic. The proof is in Appendix 6.A.

In general, if the MEWMA vector $\mathbf{z}_i \neq \mathbf{0}$ then the sample mean vector corresponding to the signal resistance is in the form $\mathbf{x} = (c_1, c_2, \dots, c_p)^T$, where

$$c_j = -z_{ji} [\sqrt{h_6/T_i^2} + (1 - \lambda)] / \lambda, \quad j=1, 2, \dots, p,$$

where z_{ji} is the j^{th} element of the MEWMA vector \mathbf{z}_i . Notice that if $\mathbf{z}_i = \mathbf{0}$, then the solution for \mathbf{x} is not unique; a possible solution in this case is the $p \times 1$ vector

$$(\sqrt{h_6}/[\lambda(2 - \lambda)a_{11}], 0, \dots, 0)^T, \quad (6.15)$$

where a_{11} is the first diagonal element of the matrix Σ^{-1} .

In order to alleviate the inertia problem to a considerable extent, Lowry et al. (1992) recommended a Shewhart-type limit be used with the MEWMA chart. It can be shown that the signal resistance of the MEWMA chart used with a Shewhart χ^2 -limit is

$$SR(\text{MEWMA}+\text{Shewhart})=\min [\sqrt{h_5}, SR(\text{MEWMA})]$$

where h_5 is the control limit of the χ^2 -chart and $SR(\text{MEWMA})$ is as defined in Equation (6.14). In this case, the signal resistance cannot exceed the square root of the χ^2 -limit.

Crosier (1988) proposed two multivariate CUSUM control charts, MCUSUM and COT. He showed that the MCUSUM chart has much better *ARL* performance than the COT chart. The MCUSUM chart is based on the statistics

$$C_i = \sqrt{(\mathbf{s}_{i-1} + \mathbf{x}_i)^T \boldsymbol{\Sigma}^{-1} (\mathbf{s}_{i-1} + \mathbf{x}_i)}$$

and

$$\mathbf{s}_i = \begin{cases} \mathbf{0}, & \text{if } C_i \leq k_1 \\ (\mathbf{s}_{i-1} + \mathbf{x}_i)(1 - k_1/C_i), & \text{if } C_i > k_1 \end{cases}, \quad i=1, 2, \dots,$$

where $\mathbf{s}_0 = \mathbf{0}$, $k_1=D_1/2 >0$, and D_1 is the smallest shift in the process mean vector considered important enough to be detected quickly, as measured by the non-centrality parameter defined in Equation (6.11). This chart signals that the process mean vector is off target if

$$Y_i = \sqrt{\mathbf{s}_i^T \boldsymbol{\Sigma}^{-1} \mathbf{s}_i} > h_7, \quad (6.16)$$

where $h_7 > 0$ is the control limit.

The COT chart is based on the CUSUM statistics

$$S_i = \max(0, S_{i-1} + \sqrt{\mathbf{x}_i^T \boldsymbol{\Sigma}^{-1} \mathbf{x}_i} - k_2), \quad i=1, 2, \dots, \quad (6.17)$$

where $S_0=0$, and $k_2 > 0$ is a constant. The COT chart gives an out-of-control signal as soon as $S_i > h_8$, where $h_8 > 0$ is a suitable threshold. Crosier (1988) noted that to detect a shift in

the process mean vector of size D_1 , the reference parameter should be chosen to be $k_2 = \sqrt{p}$.

It can be shown that the signal resistance of the MCUSUM chart is

$$SR(\text{MCUSUM}) = k_1 + h_7 + w, \quad (6.18)$$

where $w = Y_i$ and k_1 , h_7 , and Y_i are as defined in Equation (6.16). For this chart, if $\mathbf{s}_i \neq \mathbf{0}$ then the sample mean vector yielding the signal resistance is in the form $\mathbf{x} = (c_1, c_2, \dots, c_p)^T$, where

$$c_j = -s_{ji} [1 + (k_1 + h_7)/Y_i], \quad j=1, 2, \dots, p,$$

where s_{ji} is the j^{th} element of the vector \mathbf{s}_i . Again, the solution for \mathbf{x} is not unique if $\mathbf{s}_i = \mathbf{0}$; a possible solution in this case is the $p \times 1$ vector $((k_1 + h_7)/\sqrt{a_{11}}, 0, \dots, 0)^T$, where a_{11} is the first diagonal element of the matrix Σ^{-1} .

It can be shown that the signal resistance of the worst-case scenario for the COT chart is $(h_8 + k_2)$. The COT chart involves reducing each \mathbf{x} vector to a scalar then applying a one-sided CUSUM chart to the scalars. (This was not the case for the MEWMA and MCUSUM charts that involve accumulating the \mathbf{x} vectors before calculating the chart statistic). Thus, the signal resistance of the COT chart cannot exceed $(h_8 + k_2)$. The COT chart compares favorably to the MCUSUM chart with respect to the signal resistance measure as shown later in Section 6.E. The MCUSUM chart, however, has been shown to have much superior *ARL* performance.

Pignatiello and Runger (1990) also proposed two multivariate CUSUM charts, MC1 and MC2. The MC1 chart, the one with better *ARL* performance, is based on the chart statistics

$$MC1_i = \max \{0, \sqrt{\mathbf{d}_i^T \Sigma^{-1} \mathbf{d}_i} - k_3 l_i\},$$

where the cumulative sum vector

$$\mathbf{d}_i = \sum_{j=i-l_i+1}^i \mathbf{x}_j,$$

$k_3=D_1/2>0$, and

$$l_i = \begin{cases} l_{i-1} + 1, & \text{if } MC1_{i-1} > 0 \\ 1, & \text{otherwise} \end{cases}, i=1, 2, \dots \quad (6.19)$$

The MC1 chart gives an out-of-control signal as soon as $MC1_i > h_9$, where $h_9 > 0$ is a threshold.

It can be shown that the signal resistance of the MC1 chart is

$$SR(MC1) = k_3 + h_9 + w,$$

where

$$w = (MC1_i + l_i). \quad (6.20)$$

If $MC1_i > 0$, then the $p \times 1$ vector \mathbf{x} yielding this signal resistance is in the form $\mathbf{x} = (c_1, c_2, \dots, c_p)^T$, where

$$c_j = -d_{ji} [1 + \{(k_3(1 + l_i) + h_9) / \sqrt{\mathbf{d}_i^T \boldsymbol{\Sigma}^{-1} \mathbf{d}_i}\}], \quad j=1, 2, \dots, p,$$

where d_{ji} is the j^{th} element of the vector \mathbf{d}_i . If $MC1_i = 0$, then a possible solution for \mathbf{x} is the $p \times 1$ vector $((k_3 + h_9) / \sqrt{a_{11}}, 0, \dots, 0)^T$. Lowry et al. (1992) pointed out that the MC1 chart can, at least theoretically, build up an arbitrarily large amount of inertia. The results of this study support this conclusion. Observe that the signal resistance of the worst-case scenario of the MC1 chart depends on the value of the counter l_i . If a sequence of relatively large shifts from the target vector does not trigger the MC1 chart and the chart statistic stays greater than 0 for a long time, the value of l_i can become quite large. Consequently, the signal resistance can be very large, resulting in a chart with very poor worst-case performance. Section 6.E shows using an example with simulated data set that the MC1 chart can build up an exceedingly large amount of inertia.

As recommended by Lowry et al. (1992), one may use a χ^2 -limit in conjunction with the MC1 chart to alleviate, in part, potential problems with inertia. It can be shown that the signal resistance of the MC1 chart used with a Shewhart χ^2 -limit is

$$SR(\text{MC1}+\text{Shewhart})=\min[\sqrt{h_5}, SR(\text{MC1})].$$

The MC2 chart is based on the statistics

$$MC2_i = \max(0, MC2_{i-1} + \mathbf{x}_i^T \boldsymbol{\Sigma}^{-1} \mathbf{x}_i - k_4), i=1, 2, \dots,$$

where $MC2_0=0$. The reference parameter should be $k_4=p + D_1^2/2$ if a shift in the process mean vector of size D_1 is considered important enough to be detected quickly. This chart signals as soon as $MC2_i>h_{10}$, where $h_{10}>0$.

As was the case for the COT chart, the MC2 chart operates by reducing each \mathbf{x} vector to a scalar and then applying a one-sided CUSUM chart to the scalars. The signal resistance of the worst-case scenario for the MC2 chart is $\sqrt{h_{10} + k_4}$. Obviously, the MC2 chart has better performance than the MC1 chart with respect to the signal resistance measure, but the latter was shown to have much superior *ARL* performance.

Unlike the MEWMA chart, none of the above-mentioned multivariate CUSUM procedures is a natural multivariate extension of its univariate version. Ngai and Zhang (2001) developed, via projection pursuit, a multivariate extension of the CUSUM chart, namely PPCUSUM. The PPCUSUM procedure signals as soon as $C_i > h_{11}$, where h_{11} is the control limit and C_i is the chart statistic, where

$$C_i = \max_{1 \leq q \leq i} \{0, C_{iq}\},$$

and

$$C_{iq} = \sqrt{(\sum_{r=q}^i \mathbf{x}_r)^T \boldsymbol{\Sigma}^{-1} (\sum_{r=q}^i \mathbf{x}_r) - (i - q + 1)k_5}, \quad 1 \leq q \leq i, \quad i = 1, 2, \dots, \quad (6.21)$$

where $k_5=D_1/2$ and, again, D_1 is the smallest shift in the process mean vector to be detected quickly, as measured by the non-centrality parameter defined in Equation (6.11). Ngai and Zhang (2001) stated that their approach is more effective than the other multivariate control charts in coping with the inertia problem. They also showed that their chart reduces to the two-sided CUSUM chart when $p=1$. Moreover, they showed using simulation that the PPCUSUM chart has better worst-case and steady-state *ARL* performance than the competing multivariate control charts.

It can be shown that the signal resistance of the worst-case scenario for the PPCUSUM chart is $(h_{11} + k_5)$. For $p=1$, the signal resistance of this chart is equivalent to that of the univariate two-sided CUSUM chart. While the PPCUSUM chart is more effective than the competing multivariate charts in terms of inertia, determining its chart statistic is more computationally demanding.

6.E Performance Comparisons

This section compares the worst-case performance of some of the recommended univariate and multivariate control charts using the signal resistance measure. All the control charts considered in this section except those compared in Figures 6.7, 6.10, and 6.11 were set so that the in-control *ARL* is approximately 370. Each control chart limit (s) was (were) estimated independently from 50,000 Phase II simulations.

6.E.1 Univariate Control Charts

Figure 6.2 and Figure 6.3 show the signal resistance plotted against the value of the control chart statistic for the EWMA chart (with $\lambda=0.15$ and $L_2 =2.801$) and the two-sided CUSUM chart (with $k= 0.5$ and $h_1 =4.775$), respectively. It can be seen from Figures 6.2 and 6.3 that the EWMA chart has worse inertial properties than the CUSUM chart in the sense that the signal resistance values can be considerably higher. A sample mean can be more than 9.8 standard errors from the target without necessarily leading to an immediate out-of-control signal.

Figure 6.2: The signal resistance for the EWMA control chart with $\lambda = .15$ and $L_2 = 2.801$. (The signal resistance for the worst-case scenario is 9.837 corresponding to $w = -0.798$. The signal resistance for the best-case scenario is 0.798 corresponding to $w = 0.798$.)

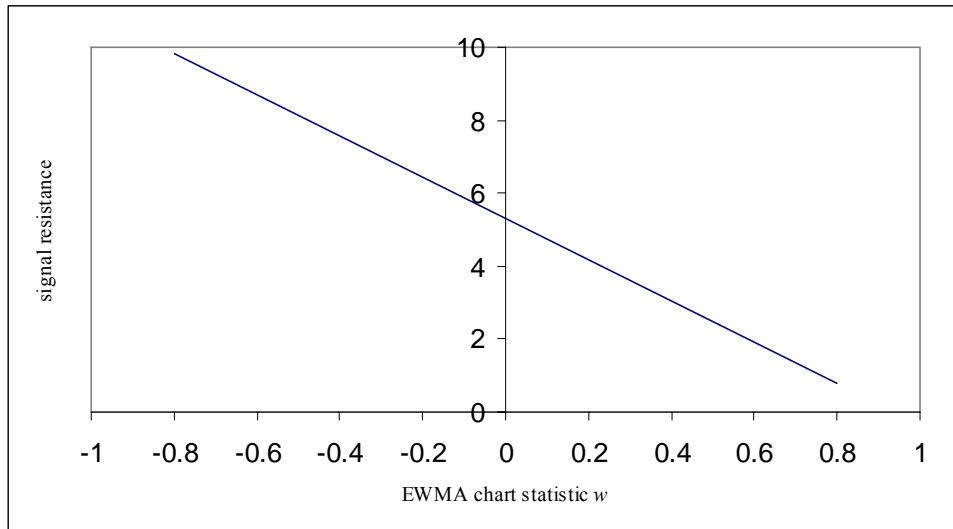
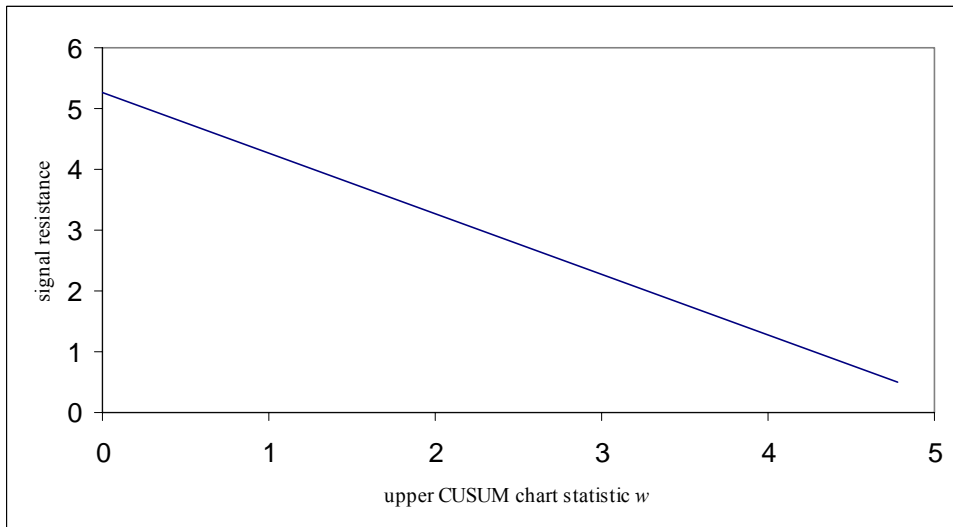


Figure 6.3: The signal resistance for the CUSUM control chart with $k = 0.5$ and $h_1 = 4.775$. (The signal resistance for the worst-case scenario is 5.275 corresponding to $w = 0$. The signal resistance for the best-case scenario is 0.5 corresponding to $w = 4.775$.)

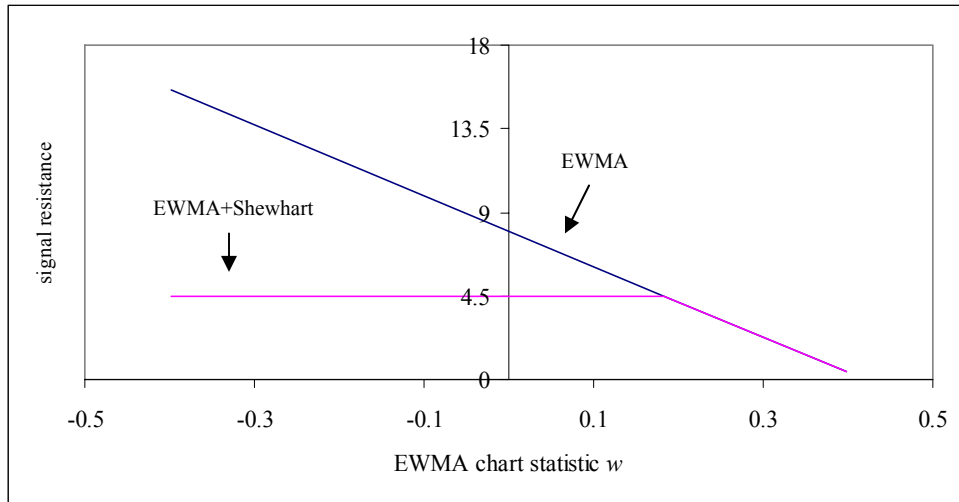


The maximum value of the signal resistance of an EWMA chart increases as the value of the smoothing constant λ decreases. A small value of λ means that the current observation receives a small weight, λ , and an observation very far from the target value may not result in an immediate out-of-control signal. Borror et al. (1999) recommended

a value of $\lambda = 0.05$ to achieve robustness of the performance of the EWMA chart to non-normality. A more comprehensive study of the robustness of the EWMA chart was given by Stoumbos and Reynolds (2000). Montgomery (2001) recommended values of λ between 0.05 and 0.20 and gave the values 0.05, 0.10, and 0.20 as popular choices.

The signal resistance values of the univariate EWMA chart recommended by Borror et al. (1999) with $\lambda = 0.05$ and $L_2 = 2.492$ are shown in Figure 6.4. The reader may be surprised to note that under a worst-case scenario a sample mean more than 15 standard errors from the target value does not lead to an immediate out-of-control signal.

Figure 6.4: The signal resistance values for the EWMA control chart with $\lambda = .05$ and $L_2 = 2.492$ used alone and used in conjunction with a 4.5-sigma Shewhart limit.



Also Figure 6.4 shows the signal resistance values for the EWMA chart with $\lambda = 0.05$ and $L_2 = 2.492$ used in conjunction with a 4.5-sigma Shewhart limit. It is clear from this figure that the adverse effect of inertia has been alleviated to a considerable extent with respect to the signal resistance measure.

Figure 6.5 shows the signal resistance for the AEWMA control chart with the parameters $\lambda = 0.1354$, $h_3 = 0.7615$, and $k = 3.2587$ studied by Capizzi and Masarotto (2003). As shown in Figure 6.5, the signal resistance of the AEWMA chart resembles that of the EWMA control chart in conjunction with Shewhart control limits shown in

Figure 6.4. However, as shown by Capizzi and Masarotto (2003), the AEWMA chart has somewhat better performance than the EWMA control chart used in conjunction with Shewhart control limits in terms of worst-case *ARL*.

Figure 6.5: The signal resistance for the AEWMA control chart with $\lambda = 0.1354$, $h_3 = 0.7615$, and $k=3.2587$. (The signal resistance for the worst-case scenario is 3.579 corresponding to $-0.7615 \leq w < 0.3203$. The signal resistance for the best-case scenario is 0.7615 corresponding to $w=0.7615$.)

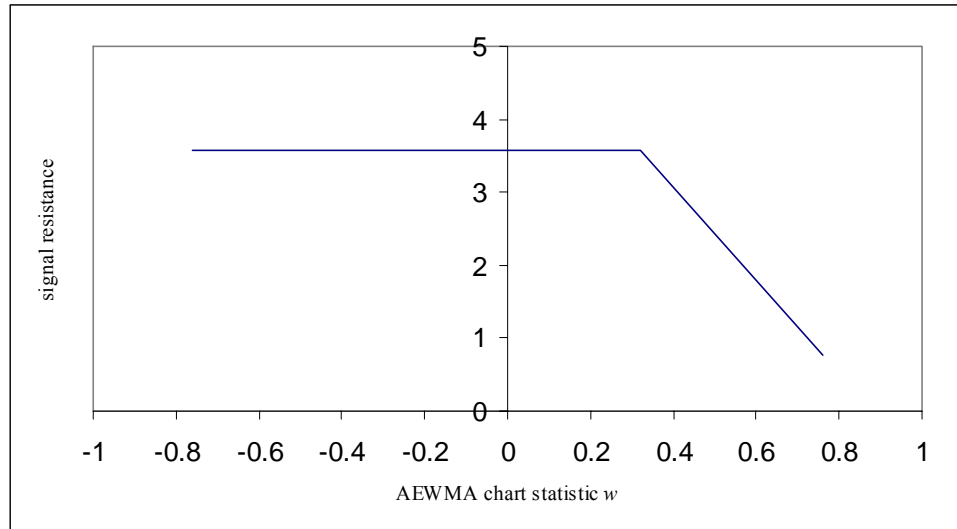
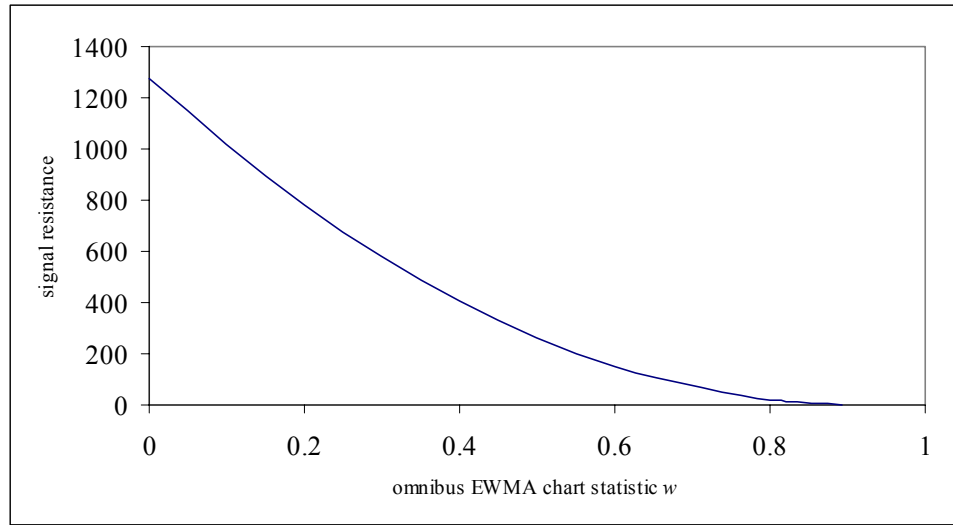


Figure 6.6 illustrates the signal resistance for the omnibus EWMA chart for $\alpha=0.5$ with parameters $\lambda = 0.025$ and $h_4=0.8935$ studied by Domangue and Patch (1991). The infimum of the omnibus EWMA chart statistic in Equation (6.9) is zero. If the sample means stay very close to target for a long time the chart statistic in Equation (6.9) tends to zero. As shown in Figure 6.6, the omnibus EWMA control chart of Domangue and Patch (1991) has very poor performance in terms of signal resistance as the control chart statistic wanders below its in-control mean. For this chart, under the worst-case scenario, a sample mean more than 1277 standard errors from target does not lead to an immediate out-of-control signal. On the other hand, the signal resistance under the worst-case scenario for the omnibus EWMA chart for $\alpha=2$ with parameters $\lambda = 0.025$ and $h_4=1.3115$ studied by Domangue and Patch (1991) is 7.243, corresponding to $w=0$, where w is the chart statistic. Obviously, the signal resistance values of the omnibus EWMA chart are much lower for $\alpha=2$ than for $\alpha=0.5$.

Figure 6.6: The signal resistance for the omnibus EWMA control chart for $\alpha=0.5$, with $\lambda = 0.025$ and $L_4=1.815$. (The signal resistance for the worst-case scenario is 1277.35 corresponding to $w=0$. The signal resistance for the best-case scenario is 0.7983 corresponding to $w=0.8935$.)



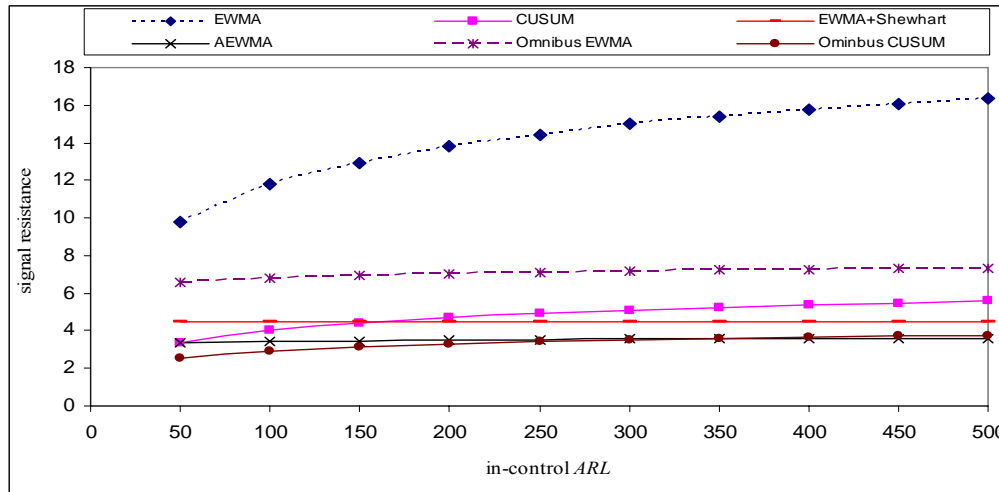
The signal resistance for the worst-case scenario of the omnibus CUSUM chart with $\alpha=0.5$, $k_H=1$, and $h_H=1.412$ studied by Domangue and Patch (1991) is 5.8177, corresponding to $w=0$, where w is the chart statistic. Also, the signal resistance for the worst-case scenario of the omnibus CUSUM chart with $\alpha=2$, $k_H=1.4$, and $h_H=11.69$ is 3.6197, corresponding to $w=0$. The signal resistance values are much lower for the omnibus CUSUM chart than for the omnibus EWMA chart, especially for $\alpha=0.5$. It is well-known, however, that the omnibus CUSUM chart is not effective in detecting decreases in the process variability.

Note that for the CUSUM chart, omnibus EWMA chart, and omnibus CUSUM chart, the combinations of values of past sample means that result in the maximum signal resistance include the case for which all the past sample means were exactly on target. This is not the case, for example, for the EWMA and AEWMA charts.

Figure 6.7 compares the worst-case signal resistance of some control chart approaches for different in-control ARL values. These charts compared are the EWMA with $\lambda=0.05$, the EWMA with $\lambda=0.05$ used in conjunction with a 4.5-sigma Shewhart

limit, the CUSUM with $k=0.5$, the AEWMA with $\lambda=0.1354$ and $k=3.2587$, the omnibus EWMA with $\lambda=0.025$ and $\alpha=2$, and the omnibus CUSUM with $\alpha=2$, $k_H=1.4$. For each ARL value considered in Figure 6.7, each control chart limit (s) was (were) estimated independently from 50,000 Phase II simulations. As shown in Figure 6.7, the EWMA chart with $\lambda=0.05$ has the highest worst-case signal resistance for all the in-control ARL values considered. For small in-control ARL values the omnibus CUSUM chart with $\alpha=2$, $k_H=1.4$ has the best worst-case performance, while for large in-control ARL values the AEWMA chart with $\lambda=0.1354$ and $k=3.2587$ has the best worst-case performance. Both charts, however, have very close worst-case signal resistance values, especially for large in-control ARL values.

Figure 6.7: The worst-case signal resistance values for some univariate control charts corresponding to different in-control ARL values.

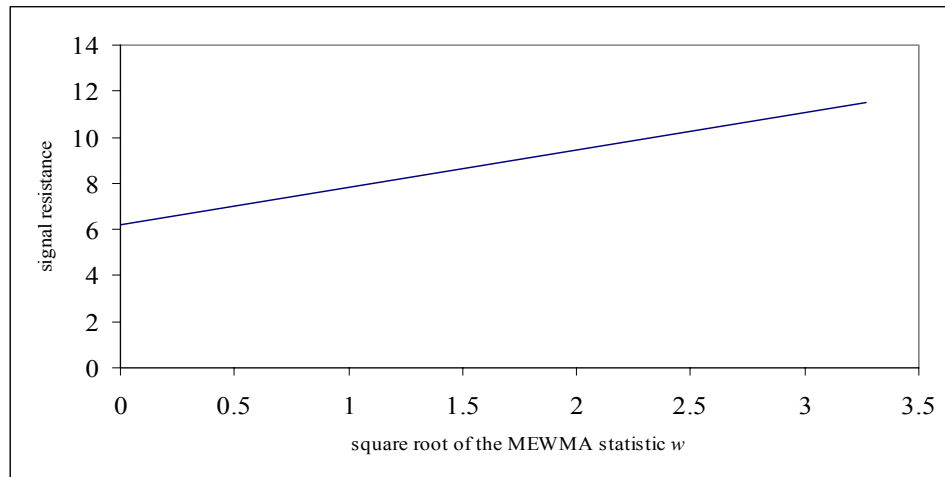


6.E.2 Multivariate Control Charts

Figure 6.8 shows the signal resistance of the MEWMA chart with $\lambda = 0.15$, $p=2$, and $h_6=10.7$ plotted against the value of w , where w is the square root of the MEWMA statistic. Note that for a MEWMA chart, the control chart statistic can be close to the upper control limit if the mean vector shifts in any direction. Thus, the worst-case scenario in this case is that the MEWMA chart statistic is at the control limit, while the

best-case scenario is that the chart statistic is equal to 0. (This was not the case for the univariate EWMA chart for example). This property applies to all the multivariate charts discussed in this paper.

Figure 6.8: The signal resistance for the MEWMA control chart with $\lambda = 0.15$, $p=2$, and $h_6 = 10.7$. (The signal resistance for the worst-case scenario is 11.4877 corresponding to $w=3.2711$. The signal resistance for the best-case scenario is 6.2096 corresponding to $w=0$).



The signal resistance of the worst-case scenario for the MEWMA chart increases as the number of quality characteristics p increases. This is because the control limit h_6 must be increased as p increases to maintain the same in-control ARL . For instance, if $p=3$ and $\lambda = 0.15$, the control limit h_6 should be 12.965 so that the in-control ARL is 370. In this case, the signal resistance of the worst-case scenario is 12.6452 corresponding to $w=3.6007$. If $p=5$ and $\lambda = 0.15$, the control limit h_6 should be 16.96, and in this case the signal resistance under the worst-case scenario is 14.4628 corresponding to $w=4.1183$.

It is well-known that quicker detection of small shifts in the process mean vector requires smaller values of the smoothing parameter λ . Stoumbos and Sullivan (2002) stated that the smoothing constant should not be lower than necessary, but recommended smoothing parameters in the range from 0.02 to 0.05, and sometimes lower, to achieve robustness to violations of the assumption of multivariate normality. As was the case for the EWMA chart, however, the signal resistance under the worst-case scenario for a MEWMA chart increases as the smoothing parameter λ decreases. For instance, the

signal resistance of the worst-case scenario for the MEWMA chart with $\lambda = 0.02$, $p = 2$, and $h_6 = 6.92$ is 26.174, corresponding to $w = 2.6306$.

Lowry et al. (1992) pointed out that if the Shewhart χ^2 -limit is used with the MEWMA chart then there is a trade-off between the quick detection of small shifts in the process mean and protection against building up a large amount of inertia. Figure 6.9 shows the signal resistance values for two different schemes plotted against w , where w is the square root of the MEWMA statistic. The first scheme is the MEWMA chart with $\lambda = 0.02$, $p = 2$, and $h_6 = 6.92$, while the second scheme is this MEWMA chart used in conjunction with a χ^2 -chart with control limit $h_5 = 20.25$. The signal resistance under the worst-case scenario for the second scheme is 4.5. As shown in Figure 6.9, adding a χ^2 -limit to the MEWMA chart substantially improves the signal resistance performance of the MEWMA chart with a small smoothing parameter value.

Figure 6.10 shows the worst-case signal resistance values for some multivariate control chart approaches corresponding to different in-control ARL values. These charts compared are the MEWMA with $\lambda = 0.02$, the MEWMA with $\lambda = 0.02$ combined with a χ^2 -chart with control limit $h_5 = 20.25$, the MCUSUM with $k_1 = 0.5$, the COT with $k_2 = 1.41$, the MC2 with $k_4 = 2.5$, and the PPCUSUM with $k_5 = 0.5$. The value of $p = 2$ dimensions was used for each of these charts. Again, for each ARL value considered in Figure 6.10, each control chart limit (s) was (were) estimated independently from 50,000 Phase II simulations. Inspection of this figure shows that the MEWMA chart combined with a χ^2 -limit, the MC2 chart, the PPCUSUM chart, and the COT chart have the best worst-case performance. These charts have much better worst-case performance than both the MCUSUM and the MEWMA charts. The COT chart and the MC2 chart, however, have very poor steady state performance. The MEWMA chart with $\lambda = 0.02$ has very poor performance with respect to inertial properties.

Figure 6.9: The signal resistance for the MEWMA chart with $\lambda = 0.02$, $p=2$, and $h_6=6.92$ used alone and used in conjunction with a χ^2 -chart with control limit $h_5=20.25$.

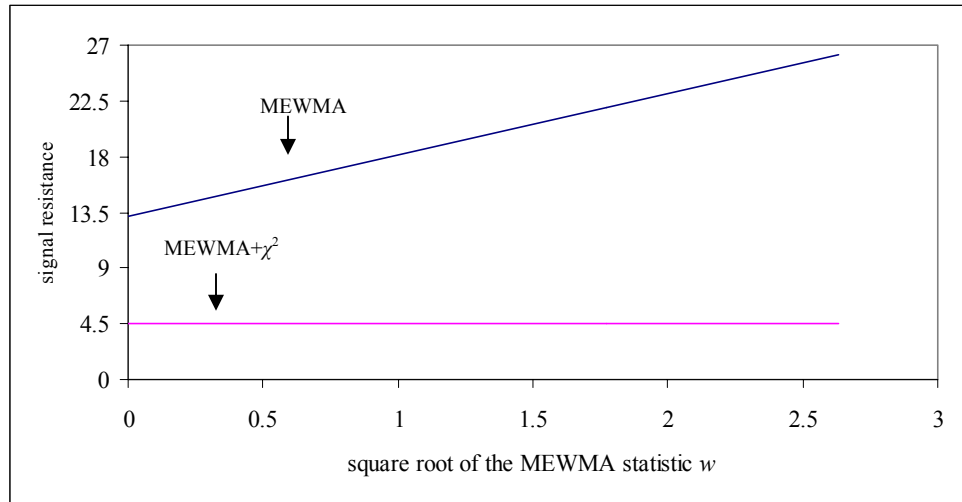
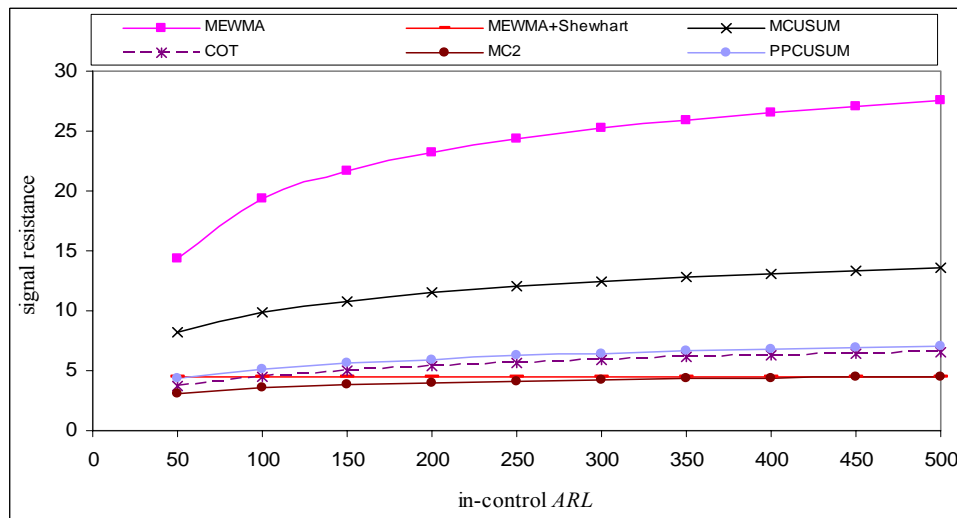


Figure 6.10: The worst-case signal resistance values for some multivariate control charts corresponding to different in-control ARL values.



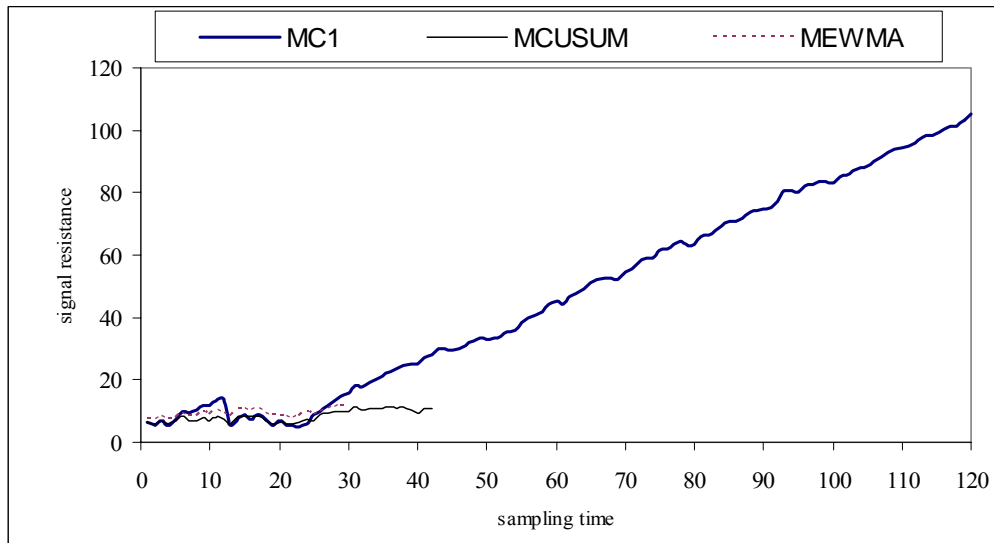
This section also presents an illustrative example with simulated data set in which some of the multivariate control charts presented in Section 6.D are compared. The purpose is to demonstrate how some of the recommended charts can build up an extremely large amount of inertia. The Phase II data set used in this example consists of 120 bivariate observations. The first 20 observations were generated from a bivariate normal distribution with $\mu=0$ and $\Sigma=I$, while the last 100 observations were generated

from a bivariate normal distribution with $\boldsymbol{\mu}=(-0.1, -0.1)^T$ and $\boldsymbol{\Sigma}=\mathbf{I}$. The data set of this example is available at:

<http://filebox.vt.edu/users/mamahmou/data%20set.xls>.

Three control chart procedures were applied on this data set; these are the MEWMA chart with $\lambda=0.1$ and $h_6=8.66$, the MCUSUM chart with $k_1=0.5$ and $h_7=5.5$, and the MC1 chart with $k_3=0.5$ and $h_9=4.75$. Using 50,000 simulations, the in-control *ARL* was estimated to be approximately 200 for each chart. The MEWMA chart signaled at sampling time 31 ($T_{31}^2=9.2778$), while the MCUSUM chart signaled at sampling time 43 ($Y_{43}=5.5943$). On the other hand, the MC1 chart did not detect the specified shift in the process mean vector. Figure 6.11 shows the signal resistance value for each chart plotted against the sampling time. As shown in this figure, the signal resistance of the MC1 chart can increase dramatically with time. As a consequence, the chart becomes substantially ineffective in reacting to some delayed shifts in the mean vector.

Figure 6.11: The signal resistance values for some multivariate control charts calculated for the example with simulated data.



Appendix 6.A: Derivation of Signal Resistance for MEWMA Chart

The following is an outline of the derivation of the signal resistance of the MEWMA chart. Our aim is to obtain the sample mean vector $\mathbf{x}=(c_1, c_2, \dots, c_p)^T$ that maximizes the quantity $\sqrt{\mathbf{x}^T \boldsymbol{\Sigma}^{-1} \mathbf{x}}$ subject to the chart statistic not exceeding the control limit. Any chart that is directionally invariant has control chart statistics that are invariant to any full rank linear transformation of the data. Thus, we can assume without loss of generality that $\boldsymbol{\Sigma}=\mathbf{I}$, where \mathbf{I} is the identity matrix.

Suppose that \mathbf{z}_i is the most recent MEWMA vector. Intuitively, the new observation vector \mathbf{x} that maximizes the quantity $\sqrt{\mathbf{x}^T \mathbf{x}}$ subject to the chart statistic not exceeding the control limit and given \mathbf{z}_i is in the form

$$\mathbf{x} = -a\mathbf{z}_i,$$

where $a > 0$. This can be also shown using a Lagrange differentiation approach.

Now the new MEWMA vector is

$$\tilde{\mathbf{z}} = \lambda(-a\mathbf{z}_i) + (1 - \lambda)\mathbf{z}_i = (1 - \lambda - a\lambda)\mathbf{z}_i$$

and the new MEWMA statistic is

$$\tilde{T}^2 = (2 - \lambda) \tilde{\mathbf{z}}^T \tilde{\mathbf{z}} / \lambda = (1 - \lambda - a\lambda)^2 w^2 \stackrel{\text{set}}{=} h_6, \quad (\text{A1})$$

where $w = \sqrt{T_i^2}$ and $T_i^2 = (2 - \lambda) \mathbf{z}_i^T \mathbf{z}_i / \lambda$ is the most recent MEWMA chart statistic.

Solving Equation (A1) for a we obtain

$$a = [(\sqrt{h_6} / w) + (1 - \lambda)] / \lambda.$$

Thus, the signal resistance of the MEWMA chart is

$$SR(\text{MEWMA}) = \sqrt{\mathbf{x}^T \mathbf{x}} = a \sqrt{\mathbf{z}_i^T \mathbf{z}_i} = aw \sqrt{\lambda / (2 - \lambda)} = \sqrt{\lambda / (2 - \lambda)} [\sqrt{h_6} + (1 - \lambda)w] / \lambda.$$

The signal resistance of the other multivariate control charts can be obtained similarly.

Chapter 7: Summary, Conclusions, and Future Work

In the first part of this dissertation, the author presented several control chart methods for monitoring a linear profile process in Phase I. The author also proposed a method based on using indicator variables in a multiple regression model. Through a simulation study, the author compared the performance of four methods of monitoring linear profiles in Phase I. These are the T^2 control chart proposed by Stover and Brill (1998) (Method A), the T^2 control chart proposed by Kang and Albin (2000) (Method B), the three Shewhart-type control charts proposed by Kim et al. (2003) (Method C), and the F -test method (Method D). Method D is much more effective than the other methods in detecting shifts affecting much of the Phase I data. On the other hand, for shifts for the slope and Y -intercept affecting only a few samples of the Phase I data, both the Kang and Albin (2000) method and the Kim et al. (2003) method gave much better results. However, the Kang and Albin (2000) method was shown to be ineffective in detecting shifts in the process standard deviation. The Kim et al. (2003) method is much more interpretable than the Kang and Albin (2000) method. Hence, it is recommended that either the F -test method or the Kim et al. (2003) method be used for monitoring linear profile processes in Phase I.

Both the simulation study and the calibration example presented in Chapter 3 show that the T^2 control chart proposed by Stover and Brill (1998) is ineffective in detecting shifts in the process parameters. As mentioned in Sullivan and Woodall (1996), the reason is that the population covariance matrix can be poorly estimated by the pooled sample covariance matrix when applying a T^2 control chart with individual vector observations. The same conclusion applies to the overparameterized T^2 control chart proposed by Mestek et al. (1994).

I believe that much more work is needed on this type of application. For instance, Sullivan and Woodall (1996) and Vargas (2003) proposed several alternative methods for estimating the covariance matrix for the T^2 control chart for individual multivariate observations. We might obtain better results when replacing the usual pooled sample

covariance matrix by one of these alternative estimators. This study could be extended to other types of shifts and out-of-control situations such as drifts in the process parameters. Since the simulation studies show that all of the Phase I methods are non-robust to violations of the normality assumption, there is a need to develop more robust linear profile methods.

Woodall et al. (2004) developed a general strategy for monitoring more complicated models than the simple linear regression model considered in this dissertation. These included applications of nonlinear models, wavelets, and splines. Readers are referred to this paper for an overall review of profile monitoring using control charts.

In the second part of this dissertation, the author proposed a change point method based on segmented regression technique to detect changes in a linear profile data set. This method, Method LRT, was applied to the analysis of Phase I linear profiles. Using simulations, the author compared the performance of Method LRT to that of Method C and Method D. The performance of Method LRT in terms of the probability of signal under an out-of-control sustained step shift in a regression parameter is much better than that of the competing methods. If the sustained shift affects only the last sample, Method C gave the best performance. On the other hand, the simulation study showed that Method LRT is insensitive to randomly scattered unsustained shifts in the parameters. Thus to protect against both types of shifts, one might apply Method LRT in conjunction with Method C or Method D.

Method LRT also provides diagnostic aids to help in understanding and interpreting out-of-control signals and in detecting accurately the location(s) of the shift(s). Exact thresholds for the maximum of the LRT statistics, $\max(lrtc_{m_1})$, cannot be determined. Chapter 4 gives approximate thresholds for the $\max(lrtc_{m_1})$ statistic that produce approximately the desired probabilities of a Type I error.

In Phase I simple linear profile applications, we usually are interested in detecting any parameter changes in the variance, slope, and intercept from their in-control values. For this reason, the heteroscedastic segmented regression model was used to detect changes in the three parameters. This is a generalization of the typical quality control problem in which one tests for changes in the mean and variance of a process characterized by the distribution of a univariate quality characteristic. However, if in a particular application the variance is not expected to change from sample to sample, one can use alternatively methods based on the homoscedastic segmented regression model to detect changes in the slope and intercept more powerfully.

Again, I believe that much more work needs to be done in this type of application. Methods that allow for in-control variation both within and between profiles are needed. In addition, the proposed change point method can be generalized to handle more complicated regression models such as multiple linear regression, polynomial regression, and multivariate multiple regression models. For example, as mentioned in the NASA calibration application presented in Chapter 5, an overall assessment of the calibration stability of the force balance would require an analysis of six responses with six explanatory variables. Method LRT could also be extended to the Phase II monitoring of linear profile applications as in Hawkins et al. (2003). In some calibration applications the explanatory variable is a random variable. Thus, I believe that more work is needed to address the problem of detecting change points in a linear profile data set with random explanatory variable(s).

In the last part of this dissertation, the author studied the inertial properties of control charts. The results of this study suggest that the inertial properties of control charts be considered as an important factor in control chart selection to complement the use of run length properties. This study showed that the current use of steady-state performance measures can be misleading when there is the possibility of an undetected sustained shift in the mean from the target when another shift in the mean occurs. The author proposed a simple, easy-to-calculate measure of inertia, the signal resistance, as

the largest standardized deviation (distance) from the target value (vector) not leading to an immediate out-of-control signal. Use of this measure further demonstrated that EWMA and MEWMA charts with small smoothing parameters have poor worst-case performance.

The results of this study suggest that EWMA and MEWMA charts be used only in conjunction with Shewhart limits, especially with low values of the smoothing parameter, so as to remove much of the adverse effect of inertia. Note that Borror et al. (1999) and Stoumbos and Sullivan (2002) recommended that one use small values of λ in designing the EWMA and MEWMA, respectively, to achieve robustness to violations of the normality assumptions. Neither of them, however, used Shewhart limits in conjunction with the recommended charts since this would lead to non-robust methods. This issue was studied in more detail by Stoumbos and Reynolds (2000).

This study showed that the omnibus EWMA method of Domangue and Patch (1991) with $\alpha = 0.5$ has worst-case performance so poor that it should not be used unless supplemented with Shewhart limits. In general, the omnibus CUSUM procedure, proposed by Hawkins (1981) and studied by Domangue and Patch (1991), has much better worst-case performance than the omnibus EWMA procedure, especially for $\alpha = 0.5$. Likewise, the AEWMA procedure proposed by Capizzi and Masarotto (2003) has much better worst-case performance compared to the omnibus EWMA chart.

The example with simulated data set presented in Chapter 6 illustrated that the MC1 chart of Pignatiello and Runger (1990) can build up an exceedingly large amount of inertia when used to monitor the process mean vector. Thus, to protect against inertia, it is recommended that the MC1 chart be used only with Shewhart limits.

The signal resistance can be calculated for other types of control charts, including control charts based on attribute data, in order to gain additional insight on their inertial properties.

References

- Ajmani, V. (2003), "Using EWMA Control Charts to Monitor Linear Relationships in Semiconductor Manufacturing," paper presented at the Joint Statistical Meetings, San Francisco.
- Amin, R. W., Wolff, H., Besenfelder, W., and Baxley, R., Jr. (1999), "EWMA Control Charts for the Smallest and Largest Observations," *Journal of Quality Technology*, 31, 189-206.
- Borrer, C. M.; Montgomery, D. C.; and Runger, G. C. (1999), "Robustness of the EWMA Control Chart to Non-normality," *Journal of Quality Technology*, 31, 309-316.
- Box, G. E. P. and Luceño, A. (1997), *Statistical Control By Monitoring and Feedback Adjustment*, John Wiley & Sons, Inc., New York, NY.
- Brown, R. L., Durbin, J., and Evans, J. M. (1975), "Techniques for Testing the Constancy of Regression Relationships Over Time (with discussion)," *Journal of the Royal Statistical Society*, B 37, 149-192.
- Burn, D. A., and Ryan, T.A., Jr. (1983), "A Diagnostic Test for Lack of Fit in Regression Models," *ASA Proceedings of the Statistical Computing Section*, 286-290.
- Capizzi, G. and Masarotto, G. (2003), "An Adaptive Exponentially Weighted Moving Average Control Chart," *Technometrics*, 45, 199-207.
- Chang, Y., and Huang, W. (1997), "Inferences for the Linear Errors-in-Variables with Change-point Models," *Journal of the American Statistical Association*, 92, 171-178.
- Chen, J. (1998), "Testing for a Change Point in Linear Regression Models," *Communications in Statistics, Part A -- Theory and Methods*, 27, 2481-2493.
- Crosier, R. B. (1988), "Multivariate Generalizations of Cumulative Sum Quality Control Schemes," *Technometrics*, 30, 291-303.
- Crowder, S. V. and Hamilton, M. D. (1992), "An EWMA for Monitoring a Process Standard Deviation," *Journal of Quality Technology*, 24, 12-21.
- Csörgő, M., and Horvath, L. (1997), *Limit Theorems in Change-Point Analysis*, John Wiley & Sons, New York, NY.

- Davis, R. B. and Woodall, W. H. (2002), "Evaluating and Improving the Synthetic Control Chart," *Journal of Quality Technology*, 34, 200-208.
- Domangue, R. and Patch, S. C. (1991), "Some Omnibus Exponentially Weighted Average Statistical Process Control Schemes," *Technometrics*, 33, 299-313.
- Emerson, J., and Kao, C. (2001), "Testing for Structural Change of a Time Trend Regression in Panel Data: Part I," *Journal of Propagations in Probability and Statistics* 1, 57 – 75.
- Emerson, J., and Kao, C. (2002), "Testing for Structural Change of a Time Trend Regression in Panel Data: Part II," *Journal of Propagations in Probability and Statistics* 2, 207-250.
- Esterby, S. R., and El-Shaarawi, A. H. (1981), "Inference about the Point of Change in a Regression Model," *Applied Statistics*, 30, 277-285.
- Farley, J. U., and Hinich, M. J. (1970), "A Test for a Shifting Slope Coefficient in a Linear Model," *Journal of the American Statistical Association*, 65, 1320-1329.
- Fatti, P. L., and Hawkins, D. M. (1986), "Variable Selection in Heteroscedastic Discriminant Analysis," *Journal of the American Statistical Association*, 81, 494-500.
- Gallant, A. R., and Fuller, W. A. (1973), "Fitting Segmented Polynomial Regression Models Whose Joint Points Have to be Estimated," *Journal of the American Statistical Association*, 69, 945-947.
- Gnanadesikan, R., and Kettenring, J. R. (1972), "Robust Estimates, Residuals, and Outlier Detection with Multiresponse Data," *Biometrics*, 28, 81-124.
- Gulliksen, H., and Wilks, S. S. (1950), "Regression Tests for Several Samples," *Psychometrika*, 15, 91-114.
- Han, A. K., and Park, D. (1989), "Testing for Structural Change in Panel Data: Application to a Study of U. S. Foreign Trade in Manufacturing Goods," *The Review of Economics and Statistics* 71, 135-142.
- Hansen, B. E. (1999), "Threshold Effects in Non-dynamic Panels: Estimation, Testing, and Inference," *Journal of Econometrics* 93, 345-368.
- Hawkins, D. M. (1976), "Point Estimation of the Parameters of Piecewise Regression Models," *Applied Statistics*, 25, 51-57.

- Hawkins, D. M. (1981), "A CUSUM for a Scale Parameter," *Journal of Quality Technology*, 13, 228-231.
- Hawkins, D. M. (2001), "Fitting Multiple Change-Point Models to Data," *Computational Statistics and Data Analysis*, 37, 323-341.
- Hawkins, D. M., Qiu, P., and Kang, C. W. (2003), "The Changepoint Model for Statistical Process Control," *Journal of Quality Technology*, 35, 355-366.
- Hawkins, D. M. and Zamba, K. D. (2003-04), "On Small Shifts in Quality Control," *Quality Engineering*, 16, 143-149.
- Healy, J. D. (1987), "A Note on Multivariate CUSUM Procedures," *Technometrics*, 29, 409-412.
- Jandhyala, V. K. , and Al-Saleh, J. A. (1999), "Parameter Changes at Unknown Times in Non-Linear Regression," *EnvironMetrics*, 10, 711-724.
- Jandhyala, V. K. , and MacNeill, I. B. (1991), "Tests for Parameter Changes at Unknown Times in Linear Regression Models," *Journal of Statistical Planning and Inference*, 27, 291-316.
- Jensen, D. R., Hui, Y. V., and Ghare, P.M. (1984), "Monitoring an Input-Output Model for Production. I. The Control Charts," *Management Science*, 30, 1197-1206.
- Jin, J., and Shi, J. (1999), "Feature-Preserving Data Compression of Stamping Tonnage Information Using Wavelets," *Technometrics*, 41, 327-339.
- Jones, M. C., and Rice, J. A. (1992), "Displaying the Important Features of Large Collections of Similar Curves," *The American Statistician*, 46, 140-145.
- Kang, L., and Albin, S. L. (2000), "On-Line Monitoring When the Process Yields a Linear Profile," *Journal of Quality Technology*, 32, 418-426.
- Kendall, M. , and Stuart, A. (1977), *The Advanced Theory of Statistics*, Vol. 2: Inference and Relationship, 4th edition, Charles Griffin & Co, London and High Wycombe, UK.
- Kim, H. (1994), "Likelihood Ratio and Cumulative Sum Tests for a Change-Point in Linear Regression," *Journal of Multivariate Analysis*, 51, 54-70.
- Kim, H. , and Cai, L. (1993), "Robustness of the Likelihood Ratio Test for a Change in Simple Linear Regression," *Journal of the American Statistical Association*, 88, 864-871.

- Kim, H., and Siegmund, D. (1989), "The Likelihood Ratio Test for a Change-Point in Simple Linear Regression," *Biometrika*, 76, 409-423.
- Kim, K., Mahmoud, M. A., and Woodall, W. H. (2003), "On the Monitoring of Linear Profiles," *Journal of Quality Technology*, 35, 317-328.
- Klein, M. (2000), "Two Alternatives to the Shewhart \bar{X} Control Chart," *Journal of Quality Technology*, 32, 427-432.
- Kleinbaum, D. G., and Kupper, L.L. (1978), *Applied Regression Analysis and Other Multivariate Methods*, Wadsworth Publishing Company, Inc., Belmont, CA.
- Krieger, A. M., Pollak, M., and Yakir, B. (2003), "Surveillance of a Simple Linear Regression," *Journal of the American Statistical Association*, 98, 456-469.
- Kulasekera, K. B. (1995), "Comparison of Regression Curves Using Quasi-Residuals," *Journal of the American Statistical Association*, 90, 1085-1093.
- Lawless, J. F., MacKay, R. J., and Robinson, J. A. (1999), "Analysis of Variation Transmission in Manufacturing Processes-Part I," *Journal of Quality Technology*, 31, 131-142.
- Lowry, C. A. and Montgomery, D. C. (1995), "A Review of Multivariate Control Charts," *IIE Transactions*, 27, 800-810.
- Lowry, C. A.; Woodall, W. H.; Champ, C. W.; and Rigdon, S. E. (1992), "A Multivariate Exponentially Weighted Moving Average Control Chart," *Technometrics*, 34, 46-53.
- Lucas, J. M. (1982), "Combined Shewhart-CUSUM Quality Control Schemes," *Journal of Quality Technology*, 14, 51-59.
- Lucas, J. M. and Saccucci, M.S. (1990), "Exponentially Weighted Moving Average Control Schemes: Properties and Enhancements," *Technometrics*, 32, 1-29.
- MacNeill, I. B. (1978), "Properties of Sequences of Partial Sums of Polynomial Regression Residuals with Applications to Tests for Change of Regression at Unknown Times," *The Annals of Statistics*, 6, 422-433.
- Mason, R. L., Chou, Y. M., and Young, J. C. (2001), "Applying Hotelling's T^2 Statistic to Batch Processes," *Journal of Quality Technology*, 33, 466-479.

- Mestek, O., Pavlik, J., and Suchánek, M. (1994), "Multivariate Control Charts: Control Charts for Calibration Curves," *Fresenius' Journal of Analytical Chemistry*, 350, 344-351.
- Montgomery, D. C. (2001), *Introduction to Statistical Quality Control*, 4th Edition, John Wiley & Sons, Inc., New York, NY.
- Moustakides, G. V. (1986), "Optimal Stopping for Detecting Changes in Distribution," *Annals of Statistics*, 14, 1379-1387.
- Myers, R. H. (1990), *Classical and Modern Regression with Applications*, 2nd Edition, PWS-Kent Publishing Company, Boston, MA.
- Nelson, P. R. (1982), "Exact Critical Points for the Analysis of Means," *Communications in Statistics – Theory and Methods*, 11, 699-709.
- Neter, J., Wasserman, W., and Kutner, M. H. (1990), *Applied Linear Statistical Models*, 3rd edition, Richard D. Irwin, Inc, Boston, MA.
- Ngai, H. and Zhang, J. (2001), "Multivariate Cumulative Sum Control Charts Based on Projection Pursuit," *Statistica Sinica*, 11, 747-766.
- Parker, P.A., Morton, M., Draper, N. R., Line, W. P. (2001), "A Single-Vector Force Calibration Method Featuring the Modern Design of Experiments," paper presented at the American Institute of Aeronautics and Astronautics 39th Aerospace Sciences Meeting & Exhibit, Reno, Nevada.
- Pignatiello, J. J., Jr., and Runger, G. C. (1990), "Comparisons of Multivariate CUSUM Charts," *Journal of Quality Technology*, 22, 173-186.
- Quandt, R. E. (1958), "The Estimation of the Parameter of a Linear Regression System Obeying Two Separate Regimes," *Journal of the American Statistical Association*, 53, 873-880
- Quandt, R. E. (1960), "Tests of the Hypothesis That a Linear Regression System Obeys Two Separate Regimes," *Journal of the American Statistical Association*, 55, 324-330
- Ramsay, J. O., and Silverman, B. W. (2002), *Applied Functional Data Analysis: Methods and Case Studies*, Springer: New York, NY.
- Reynolds, M. R., Jr., and Stoumbos, Z. G. (2004), "Control Charts and the Efficient Allocation of Sampling Resources," *Technometrics*, 46, 200-214.

- Ryan, T. P. (1997), *Modern Regression Methods*, John Wiley & Sons, New York, NY.
- Ryan, T. P. (2000), *Statistical Methods for Quality Improvement*, 2nd Edition, John Wiley & Sons, Inc., New York, NY.
- Stoumbos, Z. G. and Reynolds, M. R., Jr. (2000), "Robustness to Non-normality and Autocorrelation of Individuals Control Charts," *Journal of Statistical Computation and Simulation*, 66, 145-187.
- Stoumbos, Z. G. and Sullivan, J. H. (2002), "Robustness to Non-normality of the Multivariate EWMA Control Chart," *Journal of Quality Technology*, 34, 260-276.
- Stover, F. S., and Brill, R. V. (1998), "Statistical Quality Control Applied to Ion Chromatography Calibrations," *Journal of Chromatography*, A 804, 37-43.
- Sullivan, J. H., and Woodall, W. H. (1996a), "A Comparison of Multivariate Control Charts for Individual Observations," *Journal of Quality Technology*, 28, 398-408.
- Sullivan, J. H., and Woodall, W. H. (1996b), "A Control Chart for Preliminary Analysis of Individual Observations," *Journal of Quality Technology*, 28, 265-278.
- Tracy, N.D., Young, J. C., and Mason, R. L. (1992), "Multivariate Control Charts for Individual Observations," *Journal of Quality Technology*, 24, 88-95.
- Vargas N., J. A. (2003), "Robust Estimation in Multivariate Control Charts for Individual Observations," *Journal of Quality Technology*, 35, 367-376.
- Vostrikova, L. J. (1981), "Detecting "Disorder" in Multidimensional Random Processes," *Soviet Mathematics Doklady*, 24, 55-59.
- Walker, E., and Wright, S. P. (2002), "Comparing Curves Using Additive Models," *Journal of Quality Technology*, 34, 118-129.
- Williams, J. D., Woodall, W. H., and Birch, J. B. (2003), "Phase I Monitoring of Nonlinear Profiles," paper presented at the 2003 Quality and Productivity Research Conference, Yorktown Heights, New York.
- Wludyka, P. S., and Nelson, P. R. (1997), "Analysis of Means Types Test for Variances from Normal Populations," *Technometrics*, 39, 274-285.
- Woodall, W. H. and Adams, B. M. (1998), "Statistical Process Control," Chapter 7 in *Handbook of Statistical Methods for Engineers and Scientists* edited by H. M. Wadsworth, Jr., McGraw-Hill Companies, Inc., New York, NY.

- Woodall, W. H. and Maragah, H. D. (1990), Discussion of "Exponentially Weighted Moving Average Control Schemes - Properties and Enhancements," by J. M. Lucas and M. S. Saccucci, *Technometrics*, 32, 17-18.
- Woodall, W. H., Spitzner, D. J., Montgomery, D. C., and Gupta, S. (2004). "Using Control Charts to Monitor Process and Product Profiles", *Journal of Quality Technology*, 36, 309-320.
- Worsley, K. J. (1983), "Testing for a Two-Phase Multiple Regression," *Technometrics*, 25, 35-42.
- Wu, Z. and Spedding, T. A. (2000), "A Synthetic Control Chart for Detecting Small Shifts in the Process Mean," *Journal of Quality Technology*, 32, 32-38.
- Yakir, B. , Krieger, A. M., and Pollak, M. (1999), "Detecting a Change in Regression: First-Order Optimality," *The Annals of Statistics*, 27(6), 1896-1913.
- Yashchin, E. (1987), "Some Aspects of the Theory of Statistical Control Schemes," *IBM Journal of Research and Development*, 31, 199-205.
- Yashchin, E. (1993), "Statistical Control Schemes: Methods, Applications and Generalizations," *International Statistical Review*, 61, 41-66.

Vita

Mahmoud A. Mahmoud.

Mahmoud A. Mahmoud was born on August 14, 1970 in Alexandria, Egypt. He graduated from El Ramel High School, Alexandria, Egypt, in 1988. He graduated from Cairo University, Faculty of Economic and Political Sciences, Department of Statistics, with a B.Sc. in 1992. He worked as a Teaching Assistant after graduation in Cairo University, Faculty of Economic and Political Sciences, Department of Statistics. He received his M.Sc. in Statistics from Cairo University, Faculty of Economic and Political Sciences, Department of Statistics, in 1997.